

**Genetic Regulation of Dietary Restriction-Induced Longevity
in *Caenorhabditis elegans***

by

Nicholas A. Bishop

B.A. Biochemistry
Rice University


Submitted to the Department of Biology
in partial fulfillment of the requirements
for the degree of

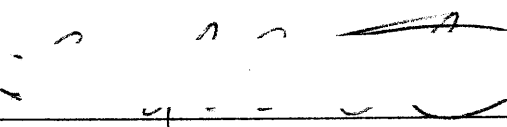
DOCTOR OF PHILOSOPHY IN BIOLOGY


at the
Massachusetts Institute of Technology
June, 2007

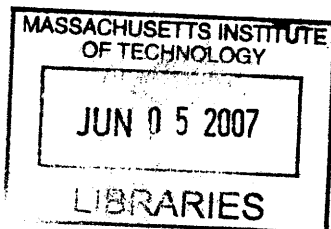
© 2007 by Nicholas A. Bishop. All rights reserved.

The author hereby grants to MIT permission to reproduce
and distribute publicly paper and electronic copies of this
thesis document in whole or in part.

Signature of Author  _____
Department of Biology

Certified by  _____
Leonard Guarente
Novartis Professor of Biology
Thesis Supervisor

Accepted by  _____
Stephen Bell
Chairman, Biology Graduate Committee



ARCHIVES

Genetic Regulation of Dietary Restriction-Induced Longevity in *Caenorhabditis elegans*

Nicholas A. Bishop

Submitted to the Department of Biology on May 4, 2007 in partial fulfillment of the requirements for the degree of Doctor of Philosophy in Biology at the Massachusetts Institute of Technology

ABSTRACT

Dietary restriction (DR), the limitation of food intake below the *ad libitum* (AL) level without malnutrition, extends mean and maximum lifespan in every organism in which it has been tested. Perhaps even more significantly, DR has also been shown in animal models to slow progression of, or even prevent entirely, an array of age-dependent pathologies, including cardiovascular disease, multiple types of cancer, several neurodegenerative disorders, and diabetes. Short-term DR also reduces the risk of coronary disease and stroke in humans. Clearly, identification of the genetic mechanisms underlying these protective effects of DR would have profound implications for the development of novel medical interventions affecting diseases of aging.

Recent studies of model organisms have revealed many genetic pathways that control the physiological rate of aging. However, advances in understanding DR longevity have lagged behind, especially in metazoans. Here, I use the roundworm *C. elegans* as a model of DR longevity and identify some of the underlying genetic mechanisms.

DR profoundly alters endocrine function in mammals, but no causal role of any hormonal signal in DR longevity has been demonstrated. I show that increased longevity of diet-restricted *C. elegans* requires the transcription factor *skn-1* acting specifically in the ASIs, a pair of neurons in the head. DR activates *skn-1* in the ASIs, which signals peripheral tissues to increase metabolic activity. These findings demonstrate that increased lifespan in a diet-restricted metazoan depends on cell-nonautonomous signaling from central neuronal cells to non-neuronal body tissues, and suggest that the ASIs mediate dietary restriction-induced longevity by an endocrine mechanism.

Next, I identify *sek-1*, a conserved stress-responsive MAPKK, as essential for DR-induced longevity and several other physiological responses to DR. I show that *sek-1* acts in the ASI neurons to maintain *skn-1* expression and mediate the DR longevity response. *sek-1* functions downstream of the MAPKKK *nsy-1* during DR. Thus, activation of a stress-sensitive MAPK pathway in the brain may be a crucial initial event in DR-induced longevity.

To summarize, I have established a three-member genetic pathway that mediates DR longevity by acting in the ASI neurons of *C. elegans*.

Thesis Supervisor: Leonard Guarente
Title: Novartis Professor of Biology

DEDICATION

This thesis is dedicated to my parents, Alan and Jennifer Bishop.

ACKNOWLEDGEMENTS

First and foremost, I thank my thesis advisor, Lenny Guarente, for giving me the great opportunity to pursue aging research, a truly fascinating area of scientific inquiry. You have always been there with crucial project insights and advice. I have learned a lot from you, and have been lucky to have you as a teacher.

Thanks also to Bob Horvitz, without whose generous sharing of time and equipment this work would never have been possible. Trial by fire in your group meetings has allowed me to become a far better and more rigorous scientist, and I thank you for the invaluable training.

I would also like to thank the members of my thesis committee: Bob Horvitz, Dennis Kim, Michael Yaffe, and Keith Blackwell.

Special thanks to Joanna Krueger, who gave me my first chance in science and taught me lessons I will never forget.

Thanks to Ethan Ford for keeping me company in lab for so many years, and lots of help in the early days.

Thanks to Greg Liszt, my classmate, labmate, roommate, fellow aging research nut, musician, St. Barth's traveler, gap-toothed yokel, and friend. You made the tough times bearable and the good times even better.

Thanks to my adventure buddies for some amazing experiences in the world outside MIT. Matthew, Paul, Alex, Sarah: some of the best times in my life. What more can I say.

Thanks to all my friends and classmates at MIT, who helped make it all so much fun. Especially my climbing partner Andy Tolonen, who has gotten me through my last year in style. Hana, Sarah, Rico, Bill, Megan, Anu, Kimberly, Melissa and everyone else: thanks for everything.

Very special thanks to my girlfriend Michelle for her love and support, especially during the preparation of this thesis. You couldn't have been more amazing – even if you had brought me a pie.

Finally, the greatest of thanks to my family: Dad, who first instilled the love of discovery in me, and Mom and Joanna, who taught me to love the rest of life, too.

TABLE OF CONTENTS

Title	1
Abstract	3
Dedication	5
Acknowledgements	6
Table of Contents	7
Chapter 1:	9
Dietary Restriction-Induced Longevity in Model Organisms and the Hypothesis of Neuroendocrine Control	
Dietary restriction: an intervention that extends healthy lifespan	11
<i>Studies in model organisms can identify single genes controlling aging</i>	11
<i>Studying DR in C. elegans</i>	13
<i>A conserved neural basis for DR longevity?</i>	14
Hypothalamic energy sensing in mammals	16
<i>Energy-sensing hypothalamic nuclei and neuropeptides</i>	16
<i>Cell-intrinsic sensing of energy availability</i>	17
<i>Afferent hormones modulate hypothalamic energy sensing</i>	20
Dietary Restriction in Yeast	21
<i>Genetics of increased longevity under mild DR</i>	22
<i>Genetics of increased longevity under severe DR</i>	23
<i>Genetic mimics of DR</i>	24
A role for the hypothalamus in DR?	25
<i>Neural regulation of DR longevity in invertebrates</i>	28
<i>Other nutrient-sensitive genes that regulate invertebrate lifespan</i>	30
Conclusions and future directions	32
References	35
Tables and Figures	43
Chapter 2:	
<i>skn-1</i> Acts in Two Neurons to Mediate Dietary Restriction- Induced Longevity in <i>C. elegans</i>	69
Summary Paragraph	71
Results and Discussion	71
Methods	78

Acknowledgements	86
References	87
Tables and Figures	91
Chapter 3:	143
A Conserved MAPK Pathway Mediates Dietary Restriction-Induced Longevity in <i>C. elegans</i>	
Summary Paragraph	145
Results	145
<i>DR Increases Lifespan by a Different Mechanism Than Known Longevity Mutants</i>	146
<i>Mutants Disrupting the sek-1 MAPKK Pathway Cause Defects in Multiple Physiological Responses to DR</i>	147
<i>sek-1 Regulates skn-1 Expression in the ASI Neurons</i>	149
<i>sek-1 Acts Separately in the ASI Neurons and the Intestine to Influence Lifespan by Two Different Mechanisms</i>	151
Discussion	152
Methods	155
Acknowledgements	160
References	161
Tables and Figures	165
Chapter 4:	197
Conclusions and Future Directions	
Summary of Results	199
Future Research Directions	199
<i>What are the signals of energy status integrated by the ASI neurons?</i>	200
<i>What genes act downstream of sek-1 and skn-1 to mediate DR longevity?</i>	201
<i>What hormone(s) mediate the DR longevity response?</i>	203
<i>What other genetic pathways are required for DR longevity?</i>	204
Conclusions	204
References	207
Figures	209
Appendix 1:	221
Additional Mutants Tested for a Role in DR Longevity	
Biographical Note	225

CHAPTER 1

Dietary Restriction-Induced Longevity in Model Organisms and the Hypothesis of Neuroendocrine Control

Portions of this chapter will be submitted for publication. The authors will be Nicholas A. Bishop and Leonard Guarente.

Dietary restriction: an intervention that extends healthy lifespan

Dietary restriction (DR), the limitation of food intake below the *ad libidum* (AL) level without malnutrition, extends mean and maximum lifespan in every organism in which it has been tested, including yeast¹, worms², flies³, and rodents⁴. Studies are presently underway to test the effect of DR on lifespan in primates, with promising preliminary results⁵. Perhaps even more significantly, DR has also been shown in animal models to slow progression of, or even prevent entirely, an array of age-dependent pathologies, including cardiovascular disease⁶, multiple types of cancer⁷, several neurodegenerative disorders^{8,9}, and diabetes¹⁰. Short-term DR also reduces the risk of coronary disease and stroke in humans⁶. Clearly, identification of the genetic mechanisms underlying these protective effects of DR would have profound implications for the development of novel medical interventions affecting diseases of aging. DR induces alterations in the physiology of many organ systems in rodents, which have been characterized extensively over the last several decades¹¹. However, which of these myriad changes are causally relevant in the increased longevity and improved health of DR animals has remained elusive.

Studies in model organisms can identify single genes controlling aging

In contrast to the limited progress on DR longevity specifically, the last fifteen years have seen a great deal learned about the general genetic regulation of aging in model organisms, principally the yeast *S. cerevisiae*, the worm *C. elegans*, and the

fruitfly *D. melanogaster*. Studies of these organisms have revealed that aging is not simply an inevitable “wearing out” of the body with time, but a regulated process controlled by a few critical genetic pathways. The rate of physiological aging can be modulated by a relatively small set of regulatory genes, defining several general pathways of lifespan control, many of which are conserved across taxa even unto mammals (Figure 1). A very well-characterized and conserved longevity intervention is reduced insulin-IGF axis signaling. Insulin signaling was first determined to be a lifespan control pathway when the worm gene *daf-2*, mutation of which was known to cause increased lifespan, was cloned and found to encode a homologue of the insulin receptor¹². Reduced insulin-IGF axis signaling has since been shown also to extend lifespan in flies and mice¹³. Most other interventions that extend lifespan have also first been identified in *C. elegans*, including germline ablation¹⁴, sensory neuron defects¹⁵, and reduced mitochondrial function during development¹⁶, among others. The worm model permits systematic whole-genome RNAi screens for genes affecting longevity^{17,18}, the results of which have led some investigators to suggest that “we may now be aware of most of the major biological pathways in *C. elegans* that, when inhibited, can produce large extensions in lifespan¹⁸.” It is therefore perhaps surprising that, unlike most other mechanisms of aging control, almost nothing is known of the genetic control of lifespan extension by dietary restriction in any metazoan, including *C. elegans*.

Studying DR in C. elegans

The first genetic determinants of DR longevity were identified seven years ago using yeast as a model system, and now quite robust genetic pathways controlling DR longevity in yeast have been elucidated (see below). The lagging progress on genetic control of DR longevity in *C. elegans* is likely due largely to the relative technical difficulty of inducing DR in the worm. One method of achieving DR has been the use of *eat-2* mutant strains, which have a reduced rate of pharyngeal pumping and reduced food ingestion¹⁹. *eat-2* mutants have been reported to live up to 50% longer than wild-type²⁰, but in the hands of the author and others²¹ the lifespan extension is much shorter or absent (data not shown). Thus, DR by *eat-2* mutation seems unreliable. The *eat-2* method of DR is also potentially subject to confounding effects during development under DR that might influence adult lifespan, as well as a dichotomy between low food in the worm and high food in the environment. The other reported method of inducing DR in worms is growth in liquid medium with controlled high or low bacterial density². This method is limited in that it does not lend itself to the traditional form of the worm lifespan assay, which is to follow a population of a few dozen individuals throughout its entire lifespan. This limitation, along with the use of medium and culture conditions that differ substantially from standard worm plates, complicates comparisons to existing studies on any given mutant. Furthermore, the magnitude of lifespan extension induced by this liquid culture approach has been underwhelming in most recent reports²². To address the shortcomings of existing DR induction approaches, I developed a novel method of inducing DR in *C. elegans* based on culture in a few milliliters of liquid with

controlled bacterial density (Chapter 2). This method permits monitoring of a population of individuals during the entire lifespan and produces a robust and extremely reproducible lifespan extension. Furthermore, the composition of the medium differs from plates only by the exclusion of agar, and wild type and mutant worms show a similar lifespan in high food concentration liquid culture as they do on plates, permitting reasonably direct comparison of studies in my DR conditions and those done on traditional plates.

Using this novel method, I screened strains carrying mutants in known or candidate longevity genes (Chapter 3 and data not shown). Initially, this work demonstrated that DR extends lifespan in representative mutant backgrounds covering essentially all known lifespan-control pathways. These results argue that DR extends lifespan by a mechanism different from known longevity pathways. Continuing the candidate gene approach, I identified a novel genetic pathway specifically required for DR-induced longevity (Chapters 2 and 3). Analysis of this genetic pathway revealed that it functions exclusively in a pair of neuroendocrine cells in the head, called the ASI neurons, to mediate DR longevity.

A conserved neural basis for DR longevity?

The discovery that cell-nonautonomous signaling from central neurons mediates DR longevity in a metazoan represents the central conceptual advance of this thesis. For the remainder of this chapter, I will review other recent findings that are beginning to point toward a conserved neural basis of DR longevity control across species. By this

comparative approach, I hope to provide the reader with the relevant background on what is known and suspected about the control of DR longevity in different model organisms. I also hope the reader will be inspired to share my excitement over the tantalizing evidence that the emerging mechanisms of DR longevity control in lower organisms will prove to be conserved in mammals.

Current evidence strongly suggests that DR is mediated by brain neurons that sense energy availability and translate energy limitation into longevity during DR. In mammals, homeostatic energy balance is principally monitored and maintained by a brain region called the hypothalamus. The hypothalamus senses changes in energy balance and reflexively modulates energy intake and expenditure, by altering feeding behavior and peripheral metabolism, respectively. Here I present evidence supporting the hypothesis that increased longevity induced by DR is also controlled by the hypothalamus. I begin by reviewing the current understanding of the genetic mechanisms of energy sensing in the mammalian hypothalamus. I then outline the known pathways mediating DR longevity in the organism in which they are best-understood, yeast, and highlight similarities between mechanisms of hypothalamic energy sensing and DR longevity in yeast. I describe recent direct evidence for central neuronal control of dietary restriction-induced longevity in worms, flies, and mammals. Finally, I identify potential novel DR genes based on their role in both invertebrate lifespan control and hypothalamic energy sensing.

Hypothalamic energy sensing in mammals

The hypothalamus is the principal vertebrate brain region responsible for maintaining homeostatic energy balance. The hypothalamus detects changes in energy availability and mediates appropriate modifications of energy intake and expenditure (Figure 2a). Specifically, the hypothalamus modulates energy balance by causing behavioral responses to hunger, such as increased feeding and foraging, and can alter energy expenditure in peripheral tissues via efferent hormonal and autonomic nervous signaling. In addition, the hypothalamus controls other nutrient-dependent processes such as growth, sexual maturation and reproduction. Very recently, the hypothalamus has been proven also to be capable of controlling mammalian lifespan (see below). Much has been learned about the genetic mechanisms of hypothalamic energy sensing in recent years, an overview of which will be presented here. The reader is directed to several recent reviews for further detail²³⁻²⁵.

Energy-sensing hypothalamic nuclei and neuropeptides

The behavior- and metabolism-modifying outputs of the hypothalamus result from the integrated activity of several populations of energy-sensitive neurons (Figure 2b). The best characterized of these are two neuronal populations within the arcuate nucleus: the anorexigenic proopiomelanocortin (POMC) neurons and the orexigenic agouti-related peptide (AgRP) neurons. When energy is in excess, AgRP neurons are repressed, while POMC neurons are active and release alpha-melanocyte stimulating

hormone (α -MSH), which is a product of POMC proteolytic cleavage. α -MSH is an agonist of the melanocortin 4 receptor (MC4R), which is expressed in neurons of the paraventricular and ventromedial hypothalamus. Activation of MC4R causes reduced energy intake and increased peripheral energy expenditure, restoring homeostatic energy balance. When energy availability is low, POMC neurons are repressed, while AgRP neurons are activated, causing increased release of AgRP, an antagonist of MC4R that reduces its activity and promotes increased feeding and decreased peripheral energy expenditure. Knockout of MC4R causes hyperphagia and obesity²⁶, while ablation of AgRP neurons in adults suppresses feeding²⁷, confirming the critical role of this pathway in regulating energy balance.

In addition to the neurons already described, two populations of neurons in the lateral hypothalamus, expressing either hypocretin (Hcrt) or melanin concentrating hormone (MCH), also play a role in promoting feeding, as ablation of either the MCH gene or the Hcrt neurons causes hypophagia and altered energy expenditure^{28,29}. The hypocretin neurons also appear to have complex roles in the regulation of arousal, as deletion of Hcrt causes narcolepsy³⁰.

Cell-intrinsic sensing of energy availability

Hypothalamic neurons integrate information from several sources in order to generate an overall picture of organismal energy status. One mechanism by which hypothalamic neurons sense energy availability is the sampling of levels of certain key

metabolites within the cell, including glucose, fatty acids, ATP, and possibly amino acids (Figure 3).

The hypothalamus contains many glucose-sensitive neurons, which are either glucose-excited or glucose-inhibited. For example, anorexigenic POMC neurons are glucose-excited³¹ and orexigenic AgRP neurons are glucose-inhibited³². Glucose-excited hypothalamic neurons sense glucose concomitantly with its metabolism, in a manner analogous to that of pancreatic β cells (Figure 3a). Most glucose-sensitive hypothalamic neurons, unlike most other brain neurons, express the pancreatic form of glucokinase, which is required for glucose sensing in both neurons and β -cells³³. Glycolysis produces pyruvate and elevates cytoplasmic NADH. Both metabolites must be produced and transported into the mitochondria for glucose to be sensed³⁴. NADH and pyruvate in the mitochondria cause increased ATP production, which closes ATP-sensitive potassium channels, leading ultimately, in neurons, to increased action potential frequency. The mechanism of glucose inhibition in glucose-inhibited neurons is not as well understood, though pancreatic glucokinase activity and production of cytoplasmic NADH by glycolysis are essential for glucose sensing in these cells also³⁵.

To an even greater degree than glucose, perception of energy status by hypothalamic neurons depends on the intracellular levels of certain intermediates of fatty acid metabolism²⁴ (Figure 3b). Experimental manipulation that results in a constitutively low intracellular level of long-chain fatty acyl-CoA (LCFA) molecules in hypothalamic neurons is sufficient to increase expression of AgRP, cause hyperphagia, and decrease peripheral energy expenditure, leading to obesity³⁶. Physiological control of LCFA level is heavily dependent on the steady-state level of malonyl-CoA, an intermediate in fatty

acid biosynthesis. In the absence of malonyl-CoA, LCFA-CoAs are transported by carnitine-palmitoyl transferase 1 (CPT1) into the mitochondria for β -oxidation. When malonyl-CoA is abundant, CPT1 is inhibited and LCFA-CoA levels remain high, promoting anorexigenic hypothalamic outputs²⁴.

Malonyl-CoA is produced from acetyl-CoA by acetyl-CoA carboxylase (ACC). ACC is primarily regulated via inhibitory phosphorylation by AMP-activated protein kinase (AMPK), which is activated by low ATP levels in most eukaryotic cells³⁷. AMPK controls hypothalamic energy sensing, acting both to promote expression of orexigenic peptides in the arcuate nucleus and to promote appropriate response in the paraventricular receiving cells³⁸. AMPK is thought to act in part by inhibiting ACC and thus reducing malonyl-CoA levels. mTOR has recently been shown to inhibit food intake by acting in the hypothalamus, particularly in response to injected leucine³⁹. AMPK is an important inhibitor of mTOR in many tissues, and therefore may exert its hypothalamic effects on energy homeostasis in part by inhibition of mTOR⁴⁰.

Recently, it was shown that fasting induces expression of uncoupling protein 2 (UCP2) in AgRP neurons⁴¹. Uncoupling proteins reduce metabolic efficiency by dissipating the proton gradient across the mitochondrial membrane, necessitating more rapid respiration to maintain ATP production rate. Fasting also caused an increase in mitochondrial number in the AgRP neurons, perhaps to compensate for this reduced metabolic efficiency. In UCP2 KO animals, fasting did not cause mitochondrial uncoupling or biogenesis, orexigenic peptide expression was not induced by fasting, and rebound feeding following fasting was diminished. Thus, fasting-induced uncoupling of mitochondrial respiration is a critical step in activation of orexigenic AgRP neurons. It is

not known how increased uncoupling in these neurons leads to perception of a low-energy state, but it is worth noting that increased uncoupling should lower NADH levels and/or ATP levels, possibly reducing glucose inhibition and/or increasing AMPK activity by the mechanisms discussed above.

Afferent hormones modulate hypothalamic energy sensing

In addition to the essentially cell-intrinsic energy sensing mechanisms described above, hypothalamic energy sensing pathways are modulated by an ever-expanding group of afferent hormones carrying information about the long- and short-term energy status of the body²³. I will limit my discussion to two of the most important, leptin and insulin.

Leptin is produced by adipocytes in proportion to fat mass, and promotes anorexic hypothalamic signaling²³. Mutation of the leptin gene *ob* causes hyperphagia and massive obesity⁴², due in large part to repression of AgRP neurons and activation of POMC neurons^{23, 43}. The binding of leptin to its receptors on arcuate neurons activates the transcription factor Stat3 and also activates PI3 kinase, which promotes Akt-dependent phosphorylation and nuclear exclusion of the transcription factor FoxO1⁴⁴ (Figure 4). Stat3 and FoxO1 oppositely regulate orexigenic and anorexigenic neuropeptide gene expression.

Insulin also promotes hypothalamic anorexigenic signaling, but plays a more minor role than leptin. Neuron-specific insulin receptor knockout causes mild obesity⁴⁵, and central administration of insulin causes suppression of feeding⁴⁶. Interestingly,

insulin signaling affects the PI3K-Akt-Foxo1 cascade in the same direction as leptin signaling in arcuate neurons, so it has been suggested that the insulin signaling pathway may act to modulate the dominant leptin signal⁴⁴. Consistently with this model, Stat3 and Foxo1 bind to partially overlapping sites on orexigenic and anorexigenic peptide gene promoters and oppositely regulate them, providing a mechanism by which insulin signaling could cooperate with leptin signaling by removing the repressive effect of FoxO1⁴⁷ (Figure 4). In addition, pharmacological inhibition of hypothalamic PI3 kinase suppresses the effects of both leptin and insulin, indicating that leptin and insulin signaling pathways converge on PI3K^{48, 49}.

Neuropeptide regulation is not the only mechanism by which leptin and insulin promote hypothalamic anorexigenic signals. For instance, leptin and insulin both inhibit hypothalamic AMPK signaling³⁸. Leptin also upregulates mTOR in the hypothalamus³⁹.

Dietary restriction in yeast

The first genes involved in dietary restriction-induced lifespan increase were identified in the yeast *S. cerevisiae*⁵⁰. In yeast, replicative lifespan is defined as the number of daughter cells a mother cell can produce before senescing, and this lifespan is controlled by many of the same genes that control metazoan lifespan. A report published in 2000 showed that reducing glucose concentration in the medium from 2% to 0.5% could extend replicative lifespan, establishing a model of DR in yeast⁵⁰. A number of genes mediating this DR-induced longevity were identified using this model. More recently, however, it has been found that more extreme glucose limitation, to 0.05%, can

apparently induce an entirely separate set of genes that mediate an even longer lifespan extension⁵¹⁻⁵³. The controversy surrounding the genetics of DR in yeast has been expertly reviewed elsewhere⁵⁴, so I will present only a brief overview here.

Genetics of increased longevity under mild DR

A mild reduction in glucose concentration in the medium, from 2% to 0.5%, caused an increase in replicative lifespan via genetic pathway dependent on a shift of carbon metabolic flux away from anaerobic fermentation and toward aerobic respiration¹ (Figure 5). Increased mitochondrial carbon metabolism was inferred from an increase in oxygen consumption during DR. This respiration increase was necessary for DR to increase lifespan, because deletion of the cytochrome c1 gene *cyt1* suppressed respiration and prevented the longevity increase. Furthermore, blocking oxidative metabolism of carbon by deleting a subunit of the pyruvate dehydrogenase complex, *lat1*, prevented DR longevity, and *lat1* overexpression increased the lifespan of 2% glucose cells but not DR cells⁵³. Reduced glycolysis and increased respiration during DR raises the cellular NAD⁺/NADH ratio, and this elevated ratio is necessary and sufficient to increase longevity⁵⁵. The change in NAD⁺/NADH ratio produced by altered glucose metabolism during mild DR activates the lifespan-regulating NAD-dependent deacetylase SIR2 and its homologues, which drive increased lifespan¹. Deletion of all the *sir2* homologues suppresses DR longevity under mild glucose restriction in the hands of most investigators^{53, 56}, though there has been one reported exception⁵⁷.

Genetics of increased longevity under severe DR

More recently, it has been reported that a severe limitation of glucose, to 0.05%, produces a robust extension in yeast replicative lifespan mediated by a genetic pathway that apparently requires neither the electron transport chain nor any sirtuin homologues^{51,52}. The genetic determinants of this pathway are not well understood at this time, but a role for the Akt homologue *sch9* or the Tor homologue *tor1* has been suggested, because deletion of either of these genes produces a striking lifespan increase that cannot be further extended by 0.05% glucose⁵¹.

The interpretation of the *sir2*- and respiration-independent lifespan increase under extreme glucose limitation has been a matter of some debate recently, with two possibilities being proposed^{52, 58}. First, subtle *sir2*-independent lifespan increases might have been originally masked by suboptimal DR conditions at 0.5% glucose; alternately, mild and severe DR conditions might induce separate longevity pathways. I favor the second interpretation for a number of reasons. First, numerous experiments from different laboratories have repeatedly confirmed that deletion of *sir2* and its homologues prevent lifespan extension by 0.5% glucose, though not 0.05% glucose^{53, 56}. Second, the physiological responses of yeast to 0.5% and 0.05% glucose differ, with growth and cell cycle being minimally affected by 0.5% glucose, but severely slowed by 0.05% glucose⁵⁹. It is therefore reasonable to suppose that responses that limit protein synthesis and increase autophagy, such as reduction of *tor1* activity, would be engaged in 0.05% glucose, but not 0.5%. Third, the NAD⁺/NADH ratio is strongly increased in cells under 0.5% glucose, but much less so in cells under 0.05% glucose, suggesting a different

metabolic response to the two conditions⁵³. Fourth, mutations that block DR longevity at 0.5%, such as *cyt1Δ* and *sir2Δ*, actually have the opposite effect at 0.05% glucose, instead enhancing the longevity response^{53,60}. This observation suggests that the 0.5%-response genes inhibit the 0.05%-response genes, allowing the cell to fine-tune its responses to various levels of nutrient availability (Figure 5). Notably, mutations that extend replicative lifespan at 0.05% glucose also generally increase the chronological lifespan of stationary phase cells that lack nutrients entirely, while genes extending replicative lifespan at 0.5% glucose generally do not^{61,62}. This observation supports the view that genes such as *sch9* and *tor1* become increasingly important in lifespan control as food restriction becomes more extreme, while genes such as *sir2* decrease in importance.

Interestingly, both 0.5% glucose and 0.05% glucose increase lifespan by a mechanism dependent on the pyruvate dehydrogenase subunit *lat1*⁵³. Undoubtedly, future work will uncover many more cross-regulations between longevity pathways responding to different degrees of food limitation.

Genetic mimics of DR

In addition to physical limitation of available glucose, several mutations affecting glucose transporting or sensing genes have been shown to extend lifespan in yeast. These include the *cdc25-10* mutation that disrupts a glucose-sensing GTP/GDP exchange factor, Hap4 overexpression that increases respiration, and deletion of the hexokinase *hxx2*, which prevents glucose entry into glycolysis⁵⁰. As mentioned above, mutation of the Akt

homolog *sch9* has also been suggested to be a mimic of DR⁵¹. Interestingly, these “DR mimic” mutations can be divided into two classes based on genetic epistasis, and this also supports the view that there is more than one genetic pathway controlling nutrient-dependent lifespan. The first class of mutations, including the *cdc25-10* mutant and Hap4 overexpressor, appear to share characteristics with the response to 0.5% glucose: like 0.5% glucose, *cdc25-10* and Hap4 overexpression required *sir2* and *lat1* to increase lifespan⁵³. *hxx2Δ* and *sch9Δ* fall into a separate class of nutrient-responsive longevity genes, their effects on lifespan being independent of *sir2* and *lat1*⁵³. Presumably at least one additional class of nutrient-responsive genes exists which, like 0.05% glucose, have longevity effects that are independent of *sir2* but dependent on *lat1*⁵³.

A role for the hypothalamus in DR?

It will be apparent from the preceding discussion that considerable parallels exist between the genetic pathways in yeast that translate low glucose perception into long lifespan and the genetic pathways in the hypothalamus that translate perception of low energy availability into appropriate efferent signals (Table 1). Glucose sensing in both yeast and hypothalamic neurons is coupled to glucose metabolism in similar ways. Both cell types depend on a hexokinase enzyme to detect glucose, and use elevated NADH as a signal of high glucose. Increased respiration is a critical step in sensing low nutrients in both yeast and AgRP neurons. In addition, *tor1*/TOR, *snf1*/AMPK, and *sch9*/Akt homologues play a role in both nutrient-sensitive longevity in yeast and nutrient sensing in the hypothalamus. It is not known whether malonyl-CoA/LCFA levels affect lifespan

in yeast, but yeast do contain homologues of all the essential mammalian components of this biochemical pathway. The apparent similarities between pathways that sense nutrients and affect DR longevity in yeast and pathways that sense nutrients in the hypothalamus beg the question: is DR longevity in mammals mediated by afferent hypothalamic signaling?

Answering this question would require perturbing the hypothalamus in some way and then demonstrating insensitivity to DR in the manipulated animal. To my knowledge, an experiment of this type has not yet been performed in a mammal. However, there is excellent evidence that the mammalian hypothalamus can control longevity, in addition to its well-established role in energy balance. For some years, a role of the hypothalamus in mammalian lifespan control has been indirectly inferred from the critical role of the pituitary in mammalian aging. The pituitary is a master endocrine gland that is chiefly controlled by hypothalamic input, both by direct innervation and by short-range hormonal signals relayed by a portal vein system. Removal of the pituitary (hypophysectomy) can extend lifespan^{63,64}, though it is not known whether hypophysectomy increases lifespan by the same mechanism as DR. Testing the DR response in hypophysectomized animals is somewhat confounded by the fact that these animals exhibit lower voluntary food intake, possibly imposing DR on themselves⁶⁴. Apart from surgical removal of the pituitary, any of several mutations that reduce growth hormone release, or its reception in peripheral tissues, also extend lifespan⁶⁵⁻⁶⁷. These mutations appear to have effects quite distinct from those of hypophysectomy, as they induce hyperphagia and age-dependent obesity⁶⁸. This reduced growth hormone longevity pathway is thought to act by a separate mechanism than DR⁶⁸. This conclusion is partly based on the finding that long-lived

mutants with reduced growth hormone secretion live even longer when subjected to DR⁶⁹.

Another indirect indication that the hypothalamus may control mammalian aging comes from a fat-specific knockout of the murine insulin receptor. This mutation caused a dramatic reduction in fat mass and plasma leptin level, promoting hyperphagia mediated by the hypothalamus, and also caused a significant lifespan extension⁷⁰. It remains untested whether the hypothalamus is involved in the lifespan increase. However, DR and fat-specific insulin receptor knockout produce similar alterations in fat mass, leptin level, appetite and metabolism, suggesting possible commonalities in mechanism.

Recently, an exciting direct connection between nutrient-sensitive cells of the hypothalamus and mammalian longevity was demonstrated by Conti and colleagues⁷¹. UCP2 was overexpressed specifically in the orexigenic hypocretin neurons in the lateral hypothalamus of mice. The intent of this manipulation was to cause thermogenesis in the hypocretin neurons and thus raise the temperature of nearby temperature-sensitive centers of the hypothalamus, causing lowered core body temperature, all of which did, in fact, occur. However, overexpression of UCP2 would also be predicted to increase hunger perception in the hypocretin neurons. (Although it is not known whether hypocretin neurons normally elevate UCP2 expression as a signal of hunger, as the AgRP neurons do, increased mitochondrial uncoupling would be expected to induce a low energy state in any cell due to reduced efficiency of ATP production.) Consistent with this prediction, these mice showed mild hyperphagia: despite their reduced daily calorie requirement due to reduced core body temperature, transgenic mice ate as much food as wild-type controls

and males gradually became obese as they aged. Remarkably, the UCP2-overexpressing mice also had longer mean and maximum lifespan than controls, by 12% in males and 20% in females. Thus, altered gene expression in a single population of hypothalamic neurons is sufficient to modify energy balance and increase lifespan. It remains to be tested whether the hypocretin neurons play a role in DR longevity, but Conti and colleagues do note that the change in lifetime mortality of the long-lived transgenic mice resembles that observed when *Drosophila* is diet-restricted, and differs from that observed when *Drosophila* is raised at lowered temperature. This is consistent with the idea that hypocretin neurons and dietary restriction affect aging by the same mechanism. If increased hypocretin neuron activity could be shown to extend lifespan by the same mechanism as DR, this would suggest that the DR longevity pathway is separable from the low adiposity of DR animals, since the UCP2 overexpressors are obese. This would raise the intriguing possibility that the influence of DR on lifespan is not a mere passive consequence of altered peripheral metabolism, but a separate, active response coupled to nutrient sensing, as is the case in yeast.

Neural regulation of DR longevity in invertebrates

Several reports in the last few years have established that the nervous system is a critical regulator of invertebrate lifespan. In *C. elegans*, loss of chemosensory ability in all neurons dramatically extends lifespan¹⁵, as does laser ablation of specific neurons⁷², and in *Drosophila*, ablation of specific insulin-producing neurons in the head is sufficient to extend lifespan⁷³. Strong evidence for a critical role of neurons in mediating the DR

longevity response of metazoans has recently been obtained from two invertebrate studies, one in flies and one in worms.

The fly study⁷⁴ reported two important findings. First, the authors showed that the odor of food alone was sufficient to reduce the longevity response of dietary-restricted flies, suggesting that odor-sensitive neuronal pathways modulate DR longevity. Second, this study showed that mutation of a pan-neuronally expressed chemoreceptor called Or83b disrupted the function of many sensory neurons and extended lifespan significantly. These long-lived mutant flies responded less robustly to DR than the wild type, suggesting that the lifespan extension mediated by these neurons might overlap mechanistically with DR longevity. Interestingly, it was shown in a separate study that neuron-specific overexpression of human UCP2 in flies extended lifespan⁷⁵. The interaction of this lifespan extension with DR was not examined, but given the importance of UCP2 in hypothalamic nutrient sensing and possibly lifespan control, it is tempting to speculate that this neuronal UCP2 overexpression may have driven the fly nervous system to perceive hunger and activated concomitant DR-like lifespan extension pathways. Consistent with this interpretation, an endogenous *Drosophila* uncoupling protein, dUCP5, is required specifically in neurons to mediate normal adaptation to low energy conditions⁷⁶, suggesting that the neuronal uncoupling-dependent mechanism of mammalian energy sensing is conserved in flies.

The second recent study to implicate neurons in the control of DR longevity is described in the remainder of this thesis. A brief summary follows. A pair of sensory neuroendocrine cells in the worm head, called the ASI neurons, are in many ways functionally analogous to the hypothalamus. The ASI neurons sense food in the

environment and integrate this information with intrinsic energy availability to modulate hormonal signaling that controls dauer entry in larvae and fat metabolism in adults⁷⁷⁻⁷⁹. In Chapter 2, I show that a transcription factor called *skn-1* is required to act specifically in the ASI neurons in order for worms to increase lifespan in response to DR. Furthermore, ablation of the ASI neurons prevents the DR longevity response. This and other studies show that, as in yeast, DR causes increased respiration in worms^{22,80}. This respiration increase is also mediated by *skn-1* activity in the ASI neurons, suggesting that metabolic changes in peripheral tissues induced by DR are dependent on cell-nonautonomous signaling from the ASIs.

Taken together, the recent evidence linking energy-sensitive neurons to lifespan control suggests a model in which DR produces longevity by a mechanism very similar to that of yeast, except that the effectors of metazoan DR longevity are cell-nonautonomous (Figure 6). Many of the mechanisms by which yeast senses nutrient deprivation are conserved in the mammalian hypothalamus. However, where the unicellular yeast induces longevity effectors in the same cell, the hypothalamus likely induces cell-nonautonomous signals that induce effectors of metabolic changes and longevity in peripheral tissues.

Other nutrient-sensitive genes that regulate invertebrate lifespan

Many of the homologues of genes known to regulate DR longevity in yeast and/or nutrient sensing in the hypothalamus have also been shown to regulate lifespan in worms

and/or flies (Table 1). Some of these have been suggested to function by the same mechanism as DR. Almost none have yet been tested for a neural basis of action.

The *daf-2* insulin receptor homolog in *C. elegans* was one of the first genes shown to control metazoan lifespan⁸¹. Mutation of *daf-2* extends lifespan by reducing activation of homologues of PI3K and Akt, causing dephosphorylation and nuclearization of *daf-16*, a worm Forkhead homolog⁸² (Figure 1a). *daf-2* functions at least partly in neurons to regulate lifespan^{83,84}. Because *daf-16* mutation completely suppresses the longevity of well-fed *daf-2* mutants⁸¹, whereas DR produces a normal lifespan extension in *daf-16* mutants^{20,85} (see Chapter 2), it has been argued that DR longevity is independent of insulin signaling in worms. However, several groups have observed significantly greater lifespan extension by DR in *daf-2* animals compared to the wild type (ref. 85 and Chapter 2), suggesting that insulin signaling may in fact antagonize DR longevity by a *daf-16*-independent mechanism. The control of lifespan by insulin signaling is conserved in flies and mammals⁸². It has been argued that reduced insulin signaling and DR increase lifespan by a common mechanism in flies⁸⁶, though the interpretation of this data has been disputed⁸⁷. Further work is clearly needed to clarify the influence of neural insulin signaling on the lifespan of well-fed and diet-restricted metazoans.

Reduced TOR signaling can extend lifespan in yeast⁵¹, worms⁸⁸, and flies⁸⁹. This conservation across taxa strongly suggests TOR will also prove to regulate mammalian lifespan. Dietary restriction is unable to further extend the lifespan of yeast, worms, or flies with reduced TOR signaling^{51,89,90}, suggesting a common mechanism of action of these two interventions. An assessment of the possible neural basis of TOR

effects on lifespan and the interaction of neural TOR activity with DR lifespan extension is required.

Another energy-sensitive kinase, AMPK, has been shown to extend lifespan when hyperactivated in worms⁹¹. The relevant tissue(s) of action are not known. Surprisingly, deletion of a worm AMPK α -subunit, *aak-2*, did not affect dietary restriction-induced longevity⁹² (and my unpublished observations), though this may be due to redundancy with another α -subunit in the worm genome.

Finally, homologues of the first DR effector gene ever identified, yeast *sir2*, have been shown to play roles in DR in other organisms. In flies, dSir2 is required for DR to extend lifespan⁹³; the tissue(s) in which dSir2 acts during DR is not known. Interestingly, though, a neural activity mediated by a sirtuin during mammalian DR has been suggested by a study showing that *Sirt1*, the nearest mammalian homologue of yeast *sir2*, is specifically required for the increase in spontaneous movement typically observed in DR animals⁹⁴. *Sir2* genes have not thus far been convincingly connected with DR in worms; however, only one of the four worm *sir2* homologues has been tested to date⁹⁰.

Conclusions and future directions

We stand on the edge of a mechanistic understanding of how dietary restriction extends lifespan. The latest results from invertebrates indicate that energy-sensing neurons play a critical role in the control of DR-induced longevity, but the critical experiments have not yet been done to determine whether similar mechanisms function in mammals. At present, we have a strong understanding of how energy-sensing pathways

function in the mammalian brain and an extensive catalogue of genes that regulate aging in invertebrates. As has been described in this chapter, considerable overlap between these two categories exists, but in most cases, it is not known whether the longevity mutants function in the same genetic pathway as DR, nor whether they function in neurons. DR interaction studies of the type that have been described⁸⁶ are needed in invertebrate longevity mutants to determine whether the mutant genes mediate DR. For genes that act in the DR longevity pathway, tissue specificity should be determined to identify possible neuronal roles. As a first step in evaluating the importance of the hypothalamus in DR longevity in mammals, the DR longevity response should be tested in hypophysectomized animals or in mutant animals with defective hypothalamic energy sensing.

If mammalian hypothalamic energy sensing is convincingly linked to DR longevity by future studies, one of the more exciting possibilities that should be explored is the question of whether the DR longevity response is separable from the other hypothalamic outputs caused by perception of low energy balance, such as reduced peripheral metabolic rate, feelings of hunger, and impaired reproduction. This is important for potential future medical activation of putative hypothalamic DR longevity pathways, as few patients are likely to tolerate concomitant obesity, hunger, and sterility. Excitingly, there is preliminary evidence that the longevity effects of DR can, in fact, be uncoupled from metabolic effects. Dietary restriction of genetically obese *ob/ob* mice results in an extended lifespan equal to that of diet-restricted wild-type, even though the *ob/ob* mice retain greater adiposity than AL wild-type⁹⁵. Thus, the effects of DR on lifespan can be uncoupled from low adiposity. Separability of different hypothalamic

outputs during DR is further suggested by the study showing that *Sirt1* KO mice have a specific defect in the increased spontaneous movement response to DR, whereas many other physiological parameters change normally⁹⁴. It will be interesting to see whether future experiments reveal general separability of distinct hypothalamic outputs during DR, particularly the putative longevity signals. Eventual development of specific activators of DR longevity pathways holds the promise of therapeutic panaceas against hosts of age-related diseases, and perhaps increased healthy lifespan for all of humankind.

References

1. Lin, S. J., Kaeberlein, M., Andalis, A. A., Sturtz, L. A., Defossez, P.A., Culotta, V. C., Fink, G. R. & Guarente, L. Calorie restriction extends *Saccharomyces cerevisiae* lifespan by increasing respiration. *Nature* **418**, 344-8 (2002).
2. Klass, M. R. Aging in the nematode *Caenorhabditis elegans*: major biological and environmental factors influencing life span. *Mech Ageing Dev* **6**, 413-29 (1977).
3. Loeb, J. & Northrop, J. H. On the influence of food and temperature upon the duration of life. *J Biol Chem* **32**, 103-121 (1917).
4. McCay, C. M., Crowell, M. F. & Maynard, L. A. The effect of retarded growth upon the length of life span and upon the ultimate body size. *J Nutr* **10**, 63-79 (1935).
5. Mattison, J. A., Roth, G. S., Lane, M. A. & Ingram, D. K. Dietary restriction in aging nonhuman primates. *Interdiscip Top Gerontol* **35**, 137-58 (2007).
6. Mattson, M. P. & Wan, R. Beneficial effects of intermittent fasting and caloric restriction on the cardiovascular and cerebrovascular systems. *J Nutr Biochem* **16**, 129-37 (2005).
7. Klebanov, S. Can short-term dietary restriction and fasting have a long-term anticarcinogenic effect? *Interdiscip Top Gerontol* **35**, 176-92 (2007).
8. Wang, J., Ho, L., Qin, W., Rocher, A. B., Seror, I., Humala, N., Maniar, K., Dolios, G., Wang, R., Hof, P. R. & Pasinetti, G. M. Caloric restriction attenuates beta-amyloid neuropathology in a mouse model of Alzheimer's disease. *Faseb J* **19**, 659-61 (2005).
9. Maswood, N., Young, J., Tilmont, E., Zhang, Z., Gash, D. M., Gerhardt, G. A., Grondin, R., Roth, G. S., Mattison, J., Lane, M. A., Carson, R. E., Cohen, R. M., Mouton, P. R., Quigley, C., Mattson, M. P. & Ingram, D. K. Caloric restriction increases neurotrophic factor levels and attenuates neurochemical and behavioral deficits in a primate model of Parkinson's disease. *Proc Natl Acad Sci USA* **101**, 18171-6 (2004).
10. Anson, R. M., Guo, Z., de Cabo, R., Iyun, T., Rios, M., Hagepanos, A., Ingram, D. K., Lane, M. A. & Mattson, M. P. Intermittent fasting dissociates beneficial effects of dietary restriction on glucose metabolism and neuronal resistance to injury from calorie intake. *Proc Natl Acad Sci USA* **100**, 6216-20 (2003).
11. Koubova, J. & Guarente, L. How does calorie restriction work? *Genes Dev* **17**, 313-21 (2003).
12. Kimura, K., Tissenbaum, H. A., Liu, Y. & Ruvkun, G. *daf-2*, an insulin receptor-like gene that regulates longevity and diapause in *Caenorhabditis elegans*. *Science* **277**, 942-46 (1997).

13. Holzenberger, M., Kappeler, L. & De Magalhaes Filho, C. IGF-1 signaling and aging. *Exp Gerontol* **39**, 1761-4 (2004).
14. Hsin, H. & Kenyon, C. Signals from the reproductive system regulate the lifespan of *C. elegans*. *Nature* **399**, 362-6 (1999).
15. Apfeld, J. & Kenyon, C. Regulation of lifespan by sensory perception in *Caenorhabditis elegans*. *Nature* **402**, 804-9 (1999).
16. Dillin, A. Hsu, A. L., Arantes-Oliveira, N., Lehrer-Graiwer, J., Hsin, H., Fraser, A. G., Kamath, R. S., Ahringer, J. & Kenyon, C. Rates of behavior and aging specified by mitochondrial function during development. *Science* **298**, 2398-401 (2002).
17. Lee, S. S. Lee, R. Y., Fraser, A. G., Kamath, R. S., Ahringer, J. & Ruvkun, G. A systematic RNAi screen identifies a critical role for mitochondria in *C. elegans* longevity. *Nat Genet* **33**, 40-8 (2003).
18. Hansen, M., Hsu, A. L., Dillin, A. & Kenyon, C. New genes tied to endocrine, metabolic, and dietary regulation of lifespan from a *Caenorhabditis elegans* genomic RNAi screen. *PLoS Genet* **1**, 119-28 (2005).
19. Avery, L. The genetics of feeding in *Caenorhabditis elegans*. *Genetics* **133**, 897-917 (1993).
20. Lakowski, B. & Hekimi, S. The genetics of caloric restriction in *Caenorhabditis elegans*. *Proc Natl Acad Sci USA* **95**, 13091-6 (1998).
21. Walker, G., Houthoofd, K., Vanfleteren, J. R. & Gems, D. Dietary restriction in *C. elegans*: from rate-of-living effects to nutrient sensing pathways. *Mech Ageing Dev* **126**, 929-37 (2005).
22. Houthoofd, K., Braeckman, B. P., Lenaerts, I., Brys, K., De Vreese, A., Van Eygen, S. & Vanfleteren, J. R. No reduction of metabolic rate in food restricted *Caenorhabditis elegans*. *Exp Gerontol* **37**, 1359-69 (2002).
23. Flier, J. S. Obesity wars: molecular progress confronts an expanding epidemic. *Cell* **116**, 337-50 (2004).
24. Lam, T. K., Schwartz, G. J. & Rossetti, L. Hypothalamic sensing of fatty acids. *Nat Neurosci* **8**, 579-84 (2005).
25. Levin, B. E., Routh, V. H., Kang, L., Sanders, N. M. & Dunn-Meynell, A. A. Neuronal glucosensing: what do we know after 50 years? *Diabetes* **53**, 2521-8 (2004).

26. Huszar, D., Lynch, C. A., Fairchild-Huntress, V., Dunmore, J. H., Fang, Q., Berkemeier, L. R., Gu, W., Kesterson, R. A., Boston, B. A., Cone, R. D., Smith, F. J., Campfield, L. A., Burn, P. & Lee, F. Targeted disruption of the melanocortin-4 receptor results in obesity in mice. *Cell* **88**, 131-41 (1997).
27. Luquet, S., Perez, F. A., Hnasko, T. S. & Palmiter, R. D. NPY/AgRP neurons are essential for feeding in adult mice but can be ablated in neonates. *Science* **310**, 683-5 (2005).
28. Shimada, M., Tritos, N. A., Lowell, B. B., Flier, J. S. & Maratos-Flier, E. Mice lacking melanin-concentrating hormone are hypophagic and lean. *Nature* **396**, 670-4 (1998).
29. Hara, J., Beuckmann, C. T., Nambu, T., Willie, J. T., Chemelli, R. M., Sinton, C. M., Sugiyama, F., Yagami, K., Goto, K., Yanagisawa, M. & Sakurai, T. Genetic ablation of orexin neurons in mice results in narcolepsy, hypophagia, and obesity. *Neuron* **30**, 345-54 (2001).
30. Chemelli, R. M., Willie, J. T., Sinton, C. M., Elmquist, J. K., Scammell, T., Lee, C., Richardson, J. A., Williams, S. C., Xiong, Y., Kisanuki, Y., Fitch, T. E., Nakazato, M., Hammer, R. E., Saper, C. B. & Yanagisawa, M. Narcolepsy in orexin knockout mice: molecular genetics of sleep regulation. *Cell* **98**, 437-51 (1999).
31. Ibrahim, N., Bosch, M. A., Smart, J. L., Qiu, J., Rubinstein, M., Ronnekleiv, O. K., Low, M. J. & Kelly, M. J. Hypothalamic proopiomelanocortin neurons are glucose responsive and express K(ATP) channels. *Endocrinology* **144**, 1331-40 (2003).
32. Muroya, S., Yada, T., Shioda, S. & Takigawa, M. Glucose-sensitive neurons in the rat arcuate nucleus contain neuropeptide Y. *Neurosci Lett* **264**, 113-6 (1999).
33. Mobbs, C. V., Mastaitis, J. W., Zhang, M., Isoda, F., Cheng, H. & Yen, K. Secrets of the lac operon. Glucose hysteresis as a mechanism in dietary restriction, aging and disease. *Interdiscip Top Gerontol* **35**, 39-68 (2007).
34. Eto, K., Tsubamoto, Y., Terauchi, Y., Sugiyama, T., Kishimoto, T., Takahashi, N., Yamauchi, N., Kubota, N., Murayama, S., Aizawa, T., Akanuma, Y., Aizawa, S., Kasai, H., Yazaki, Y. & Kadowaki, T. Role of NADH shuttle system in glucose-induced activation of mitochondrial metabolism and insulin secretion. *Science* **283**, 981-5 (1999).
35. Yang, X. J., Kow, L. M., Pfaff, D. W. & Mobbs, C. V. Metabolic pathways that mediate inhibition of hypothalamic neurons by glucose. *Diabetes* **53**, 67-73 (2004).
36. He, W., Lam, T. K., Obici, S. & Rossetti, L. Molecular disruption of hypothalamic nutrient sensing induces obesity. *Nat Neurosci* **9**, 227-33 (2006).

37. Hardie, D. G. & Carling, D. The AMP-activated protein kinase--fuel gauge of the mammalian cell? *Eur J Biochem* **246**, 259-73 (1997).
38. Minokoshi, Y., Alquier, T., Furukawa, N., Kim, Y. B., Lee, A., Xue, B., Mu, J., Fougère, F., Ferre, P., Birnbaum, M. J., Stuck, B. J. & Kahn, B. B. AMP-kinase regulates food intake by responding to hormonal and nutrient signals in the hypothalamus. *Nature* **428**, 569-74 (2004).
39. Cota, D., Proulx, K., Smith, K. A., Kozma, S. C., Thomas, G., Woods, S. C. & Seeley, R. J. Hypothalamic mTOR signaling regulates food intake. *Science* **312**, 927-30 (2006).
40. Xue, B. & Kahn, B. B. AMPK integrates nutrient and hormonal signals to regulate food intake and energy balance through effects in the hypothalamus and peripheral tissues. *J Physiol* **574**, 73-83 (2006).
41. Coppola, A., Liu, Z. W., Andrews, Z. B., Paradis, E., Roy, M. C., Friedman, J. M., Ricquier, D., Richard, D., Horvath, T. L., Gao, X. B. & Diano, S. A central thermogenic-like mechanism in feeding regulation: an interplay between arcuate nucleus T3 and UCP2. *Cell Metab* **5**, 21-33 (2007).
42. Zhang, Y., Proenca, R., Maffei, M., Barone, M., Leopold, L. & Friedman, J. M. Positional cloning of the mouse obese gene and its human homologue. *Nature* **372**, 425-32 (1994).
43. Ahima, R. S., Prabakaran, D., Mantzoros, C., Qu, D., Lowell, B., Maratos-Flier, E. & Flier, J. S. Role of leptin in the neuroendocrine response to fasting. *Nature* **382**, 250-2 (1996).
44. Plum, L., Belgardt, B. F. & Bruning, J. C. Central insulin action in energy and glucose homeostasis. *J Clin Invest* **116**, 1761-6 (2006).
45. Bruning, J. C., Gautam, D., Burks, D. J., Gillette, J., Schubert, M., Orban, P. C., Klein, R., Krone, W., Müller-Wieland, D. & Kahn, C. R. Role of brain insulin receptor in control of body weight and reproduction. *Science* **289**, 2122-5 (2000).
46. Schwartz, M. W., Woods, S. C., Porte, D., Jr., Seeley, R. J. & Baskin, D. G. Central nervous system control of food intake. *Nature* **404**, 661-71 (2000).
47. Kitamura, T., Feng, Y., Kitamura, Y. I., Chua, S. C., Jr., Xu, A. W., Barsh, G. S., Rossetti, L. & Accili, D. Forkhead protein FoxO1 mediates Agrp-dependent effects of leptin on food intake. *Nat Med* **12**, 534-40 (2006).
48. Niswender, K. D., Morrison, C. D., Clegg, D. J., Olson, R., Baskin, D. G., Myers, M. G., Jr., Seeley, R. J. & Schwartz, M. W. Insulin activation of phosphatidylinositol 3-

kinase in the hypothalamic arcuate nucleus: a key mediator of insulin-induced anorexia. *Diabetes* **52**, 227-31 (2003).

49. Niswender, K. D., Morton, G. J., Stearns, W. H., Rhodes, C. J., Myers, M. G., Jr. & Schwartz, M. W. Intracellular signalling. Key enzyme in leptin-induced anorexia. *Nature* **413**, 794-5 (2001).

50. Lin, S. J., Defossez, P. A. & Guarente, L. Requirement of NAD and SIR2 for life-span extension by calorie restriction in *Saccharomyces cerevisiae*. *Science* **289**, 2126-8 (2000).

51. Kaeberlein, M., Powers, R. W., 3rd, Steffen, K. K., Westman, E. A., Hu, D., Dang, N., Kerr, E. O., Kirkland, K. T., Fields, S. & Kennedy, B. K. Regulation of yeast replicative life span by TOR and Sch9 in response to nutrients. *Science* **310**, 1193-6 (2005).

52. Kaeberlein, M., Hu, D., Kerr, E. O., Tsuchiya, M., Westman, E. A., Dang, N., Fields, S. & Kennedy, B. K. Increased life span due to calorie restriction in respiratory-deficient yeast. *PLoS Genet* **1**, e69 (2005).

53. Easlon, E., Tsang, F., Dilova, I., Wang, C., Lu, S. P., Skinner, C. & Lin, S. J. The dihydrolipoamide acetyltransferase is a novel metabolic longevity factor and is required for calorie restriction-mediated life span extension. *J Biol Chem* **282**, 6161-71 (2007).

54. Longo, V. D. & Kennedy, B. K. Sirtuins in aging and age-related disease. *Cell* **126**, 257-68 (2006).

55. Lin, S. J., Ford, E., Haigis, M., Liszt, G. & Guarente, L. Calorie restriction extends yeast life span by lowering the level of NADH. *Genes Dev* **18**, 12-6 (2004).

56. Lamming, D. W., Latorre-Esteves, M., Medvedik, O., Wong, S. N., Tsang, F. A., Wang, C., Lin, S. J. & Sinclair, D. A. HST2 mediates SIR2-independent life-span extension by calorie restriction. *Science* **309**, 1861-4 (2005).

57. Kaeberlein, M., Steffen, K. K., Hu, D., Dang, N., Kerr, E. O., Tsuchiya, M., Fields, S. & Kennedy, B. K. Comment on "HST2 mediates SIR2-independent life-span extension by calorie restriction". *Science* **312**, 1312; author reply 1312 (2006).

58. Lin, S. J. & Guarente, L. Increased life span due to calorie restriction in respiratory-deficient yeast. *PLoS Genet* **2**, e33; author reply e34 (2006).

59. Sinclair, D. A., Lin, S. J. & Guarente, L. Life-span extension in yeast. *Science* **312**, 195-7; author reply 195-7 (2006).

60. Kaeberlein, M., Kirkland, K. T., Fields, S. & Kennedy, B. K. Sir2-independent life span extension by calorie restriction in yeast. *PLoS Biol* **2**, E296 (2004).

61. Powers, R. W., 3rd, Kaeberlein, M., Caldwell, S. D., Kennedy, B. K. & Fields, S. Extension of chronological life span in yeast by decreased TOR pathway signaling. *Genes Dev* **20**, 174-84 (2006).
62. Fabrizio, P., Gattazzo, C., Battistella, L., Wei, M., Cheng, C., McGrew, K. & Longo, V. D. Sir2 blocks extreme life-span extension. *Cell* **123**, 655-67 (2005).
63. Powers, R. W., 3rd, Harrison, D. E. & Flurkey, K. Pituitary removal in adult mice increases life span. *Mech Ageing Dev* **127**, 658-9 (2006).
64. Everitt, A. V., Seedsman, N. J. & Jones, F. The effects of hypophysectomy and continuous food restriction, begun at ages 70 and 400 days, on collagen aging, proteinuria, incidence of pathology and longevity in the male rat. *Mech Ageing Dev* **12**, 161-72 (1980).
65. Brown-Borg, H. M., Borg, K. E., Meliska, C. J. & Bartke, A. Dwarf mice and the ageing process. *Nature* **384**, 33 (1996).
66. Flurkey, K., Papaconstantinou, J., Miller, R. A. & Harrison, D. E. Lifespan extension and delayed immune and collagen aging in mutant mice with defects in growth hormone production. *Proc Natl Acad Sci USA* **98**, 6736-41 (2001).
67. Coschigano, K. T., Clemmons, D., Bellush, L. L. & Kopchick, J. J. Assessment of growth parameters and life span of GHR/BP gene-disrupted mice. *Endocrinology* **141**, 2608-13 (2000).
68. Bartke, A., Masternak, M. M., Al-Regaiey, K. A. & Bonkowski, M. S. Effects of dietary restriction on the expression of insulin-signaling-related genes in long-lived mutant mice. *Interdiscip Top Gerontol* **35**, 69-82 (2007).
69. Bartke, A., Wright, J. C., Mattison, J. A., Ingram, D. K., Miller, R. A. & Roth, G. S. Extending the lifespan of long-lived mice. *Nature* **414**, 412 (2001).
70. Blüher, M., Kahn, B. B. & Kahn, C. R. Extended longevity in mice lacking the insulin receptor in adipose tissue. *Science* **299**, 572-4 (2003).
71. Conti, B., Sanchez-Alavez, M., Winsky-Sommerer, R., Morale, M. C., Lucero, J., Brownell, S., Fabre, V., Huitron-Resendiz, S., Henriksen, S., Zorrilla, E. P., de Lecea, L. & Bartfai, T. Transgenic mice with a reduced core body temperature have an increased life span. *Science* **314**, 825-8 (2006).
72. Alcedo, J. & Kenyon, C. Regulation of *C. elegans* longevity by specific gustatory and olfactory neurons. *Neuron* **41**, 45-55 (2004).
73. Broughton, S. J., Piper, M. D., Ikeya, T., Bass, T. M., Jacobson, J., Drieger, Y., Martinez, P., Hafen, E., Withers, D. J., Leivers, S. J. & Partridge, L. Longer lifespan,

altered metabolism, and stress resistance in *Drosophila* from ablation of cells making insulin-like ligands. *Proc Natl Acad Sci USA* **102**, 3105-10 (2005).

74. Libert, S., Zwiener, J., Chu, X., Vanvoorhies, W., Roman, G. & Pletcher, S. D. Regulation of *Drosophila* life span by olfaction and food-derived odors. *Science* **315**, 1133-7 (2007).

75. Fridell, Y. W., Sanchez-Blanco, A., Silvia, B. A. & Helfand, S. L. Targeted expression of the human uncoupling protein 2 (hUCP2) to adult neurons extends life span in the fly. *Cell Metab* **1**, 145-52 (2005).

76. Sanchez-Blanco, A., Fridell, Y. W. & Helfand, S. L. Involvement of *Drosophila* uncoupling protein 5 in metabolism and aging. *Genetics* **172**, 1699-710 (2006).

77. Bargmann, C. I. & Horvitz, H. R. Chemosensory neurons with overlapping functions direct chemotaxis to multiple chemicals in *C. elegans*. *Neuron* **7**, 729-42 (1991).

78. Bargmann, C. I. & Horvitz, H. R. Control of larval development by chemosensory neurons in *Caenorhabditis elegans*. *Science* **251**, 1243-6 (1991).

79. Riddle, D. L. & Albert, P. S. in *C. elegans II* (eds. Riddle, D. L., Blumenthal, T., Meyer, B. J. & Preiss, J. R.) 739-68 (Cold Spring Harbor Laboratory Press, Plainview, NY, 1997).

80. Houthoofd, K., Braeckman, B. P., Lenaerts, I., Brys, K., De Vreese, A., Van Eygen, S. & Vanfleteren, J. R. Axenic growth up-regulates mass-specific metabolic rate, stress resistance, and extends life span in *Caenorhabditis elegans*. *Exp Gerontol* **37**, 1371-8 (2002).

81. Kenyon, C., Chang, J., Gensch, E., Rudner, A. & Tabtiang, R. A *C. elegans* mutant that lives twice as long as wild type. *Nature* **366**, 461-4 (1993).

82. Kenyon, C. The plasticity of aging: insights from long-lived mutants. *Cell* **120**, 449-60 (2005).

83. Wolkow, C. A., Kimura, K. D., Lee, M. S. & Ruvkun, G. Regulation of *C. elegans* life-span by insulinlike signaling in the nervous system. *Science* **290**, 147-50 (2000).

84. Libina, N., Berman, J. R. & Kenyon, C. Tissue-specific activities of *C. elegans* DAF-16 in the regulation of lifespan. *Cell* **115**, 489-502 (2003).

85. Houthoofd, K., Braeckman, B. P., Johnson, T. E. & Vanfleteren, J. R. Life extension via dietary restriction is independent of the Ins/IGF-1 signalling pathway in *Caenorhabditis elegans*. *Exp Gerontol* **38**, 947-54 (2003).

86. Clancy, D. J., Gems, D., Hafen, E., Leevers, S. J. & Partridge, L. Dietary restriction in long-lived dwarf flies. *Science* **296**, 319 (2002).
87. Tatar, M. Diet restriction in *Drosophila melanogaster*. Design and analysis. *Interdiscip Top Gerontol* **35**, 115-36 (2007).
88. Vellai, T., Takacs-Vellai, K., Zhang, Y., Kovacs, A. L., Orosz, L. & Muller, F. Genetics: influence of TOR kinase on lifespan in *C. elegans*. *Nature* **426**, 620 (2003).
89. Kapahi, P., Zid, B. M., Harper, T., Koslover, D., Sapin, V. & Benzer, S. Regulation of lifespan in *Drosophila* by modulation of genes in the TOR signaling pathway. *Curr Biol* **14**, 885-90 (2004).
90. Hansen, M., Taubert, S., Crawford, D., Libina, N., Lee, S. J. & Kenyon, C. Lifespan extension by conditions that inhibit translation in *Caenorhabditis elegans*. *Aging Cell* **6**, 95-110 (2007).
91. Apfeld, J., O'Connor, G., McDonagh, T., DiStefano, P. S. & Curtis, R. The AMP-activated protein kinase AAK-2 links energy levels and insulin-like signals to lifespan in *C. elegans*. *Genes Dev* **18**, 3004-9 (2004).
92. Curtis, R., O'Connor, G. & DiStefano, P. S. Aging networks in *Caenorhabditis elegans*: AMP-activated protein kinase (aak-2) links multiple aging and metabolism pathways. *Aging Cell* **5**, 119-26 (2006).
93. Rogina, B. & Helfand, S. L. Sir2 mediates longevity in the fly through a pathway related to calorie restriction. *Proc Natl Acad Sci USA* **101**, 15998-6003 (2004).
94. Chen, D., Steele, A. D., Lindquist, S. & Guarente, L. Increase in activity during calorie restriction requires Sirt1. *Science* **310**, 1641 (2005).
95. Harrison, D. E., Archer, J. R. & Astle, C. M. Effects of food restriction on aging: separation of food intake and adiposity. *Proc Natl Acad Sci USA* **81**, 1835-8 (1984).

Table 1. Conserved control of energy sensing, lifespan, and DR longevity response.

Gene or metabolic process	Energy sensing				Lifespan control				DR longevity			
	Y	W	F	M	Y	W	F	M	Y	W	F	M
gluco/fructokinases	✓			✓	✓	✓			✓			
NADH level	✓			✓	✓				✓			
respiration rate				✓	✓	✓	✓	✓	✓	✓		
neuronal signaling	na	✓	✓	✓	na	✓	✓	✓	na	✓	✓	
InsR	na	✓	✓	✓	na	✓	✓	✓	na	x?	✓?	x?
PI3K		✓	✓	✓		✓						
Akt	✓	✓	✓	✓	✓	✓			✓			
FoxO1	na	✓	✓	✓	na	✓	✓		na	x		
Sirtuins	✓	✓		✓	✓	✓	✓		✓	x?	✓	
AMPK	✓	✓	✓	✓	✓	✓			✓	x?		
TOR	✓	✓	✓	✓	✓	✓	✓		✓	✓	✓	

Y= yeast, W = worm, F = fly, M = mammal. “✓” symbol indicates that a given gene or process is connected with the energy sensing, lifespan control, or DR longevity in the corresponding model organism. “x” symbol indicates that there is evidence that the given gene or process is not involved in DR longevity in the corresponding model organism. na = not applicable. Blank table cells indicate that a potential interaction has not been tested.

Figure 1. Some lifespan control pathways that are conserved in multiple species.

(a) Insulin-like signaling accelerates aging. Yeast lack the insulin receptor, but retain downstream kinases such as the Akt homologue *sch9*. Abbreviations: GH, growth hormone; ILPs, insulin-like peptides; IGF-1 insulin-like growth factor 1.

(b) TOR signaling accelerates aging. AMPK activation slows aging, and may do so in part by inhibiting TOR signaling. *aak-2* is a homologue of the mammalian AMPK catalytic α subunit.

(c) Dietary restriction extends lifespan in all species shown. The lifespan extension depends on SIR2 in flies. Yeast DR longevity depends on *sir2* and/or related sirtuins under some circumstances (see text). Some physiological responses to DR depend on sirtuins in mammals, though a role in DR longevity for sirtuins remains to be tested. Sirtuins have not been linked to DR in worms, but do regulate lifespan.

(d) Small subsets of neurons can control lifespan in worms, flies, and mammals.

FIGURE 1

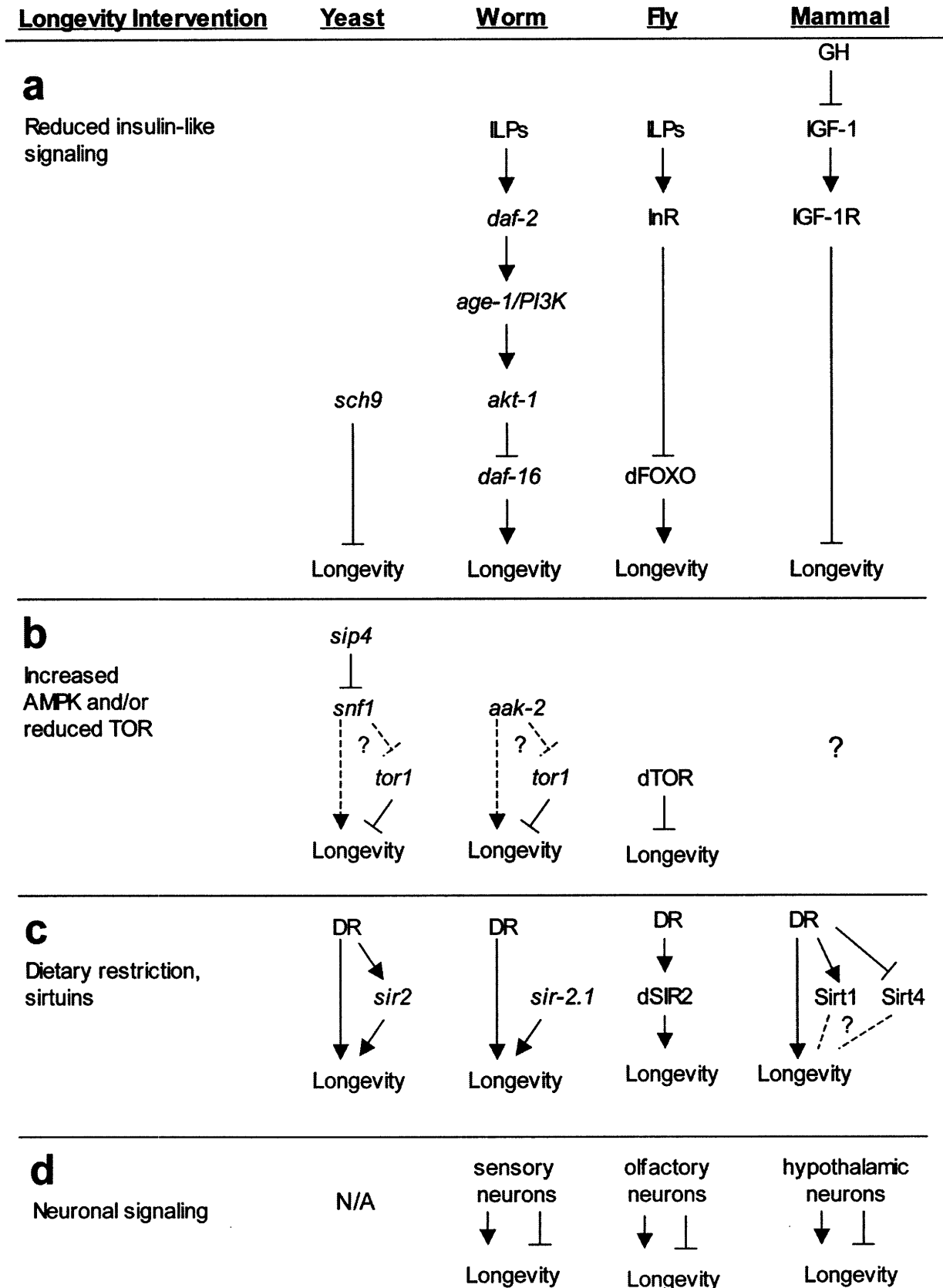


Figure 2. Homeostatic energy balance is maintained by the hypothalamus.

(a) Afferent signals, such as nutrient availability, energy status-dependent hormones from the periphery, and signals from sensory and reward centers of the brain are integrated by the hypothalamus and translated into nervous and hormonal outputs that modulate multiple physiological and behavioral processes.

(b) Principal hypothalamic nuclei modulating feeding and peripheral energy expenditure. Nuclei and pathways are color-coded according to whether they are orexigenic (green) or anorexigenic (blue). Nutrients, and the nutrient-dependent hormones leptin and insulin, activate anorexigenic POMC neurons and inhibit orexigenic AgRP neurons in the arcuate nucleus. When activated, POMC neurons secrete α -MSH, a proteolytic cleavage product of POMC, which is an agonist of the MC4R on anorexic neurons in the paraventricular and ventromedial hypothalamus. Activated AgRP neurons secrete AgRP, which antagonizes the MC4R. Orexigenic MCH and hypocretin (Hcrt) neurons in the lateral hypothalamus regulate energy balance in parallel to the MC4R neurons. Abbreviations: POMC: proopiomelanocortin; AgRP: agouti-related peptide; α -MSH: alpha-melanocyte stimulating hormone; MC4R: melanocortin-4 receptor; MCH: melanin-concentrating hormone.

FIGURE 2

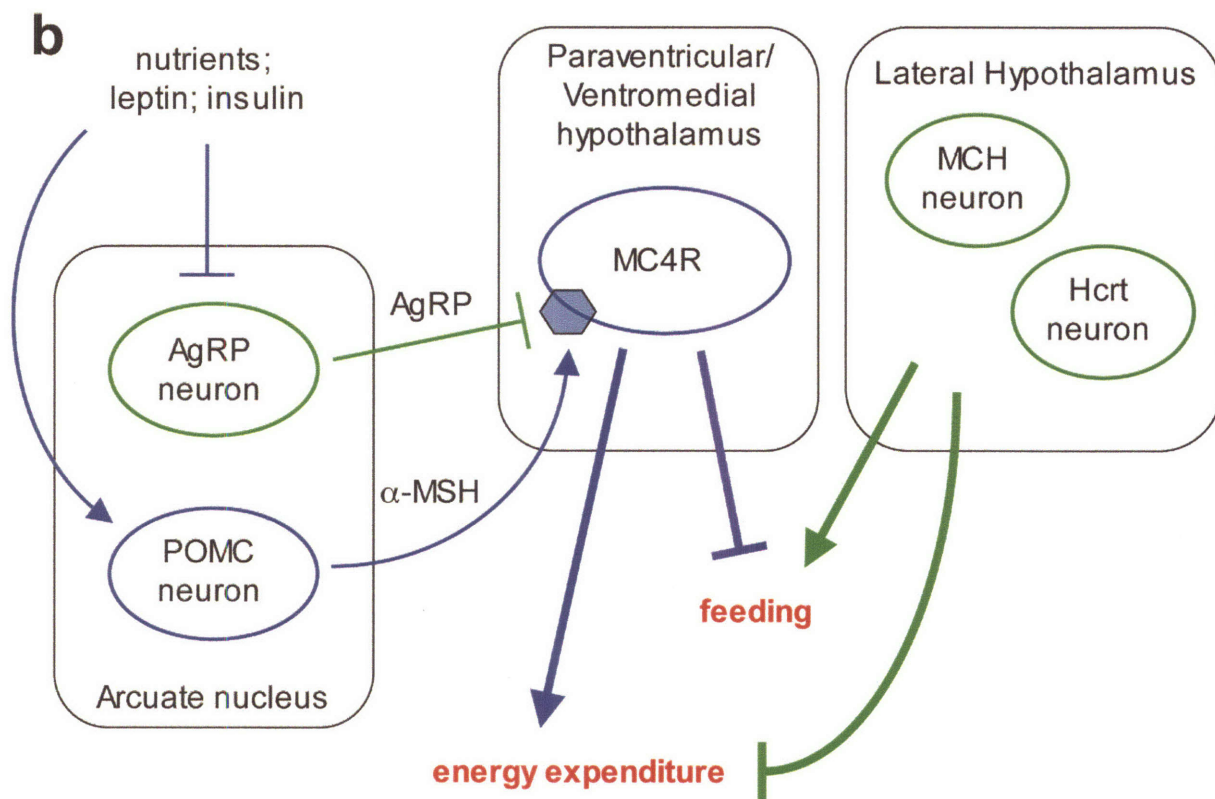
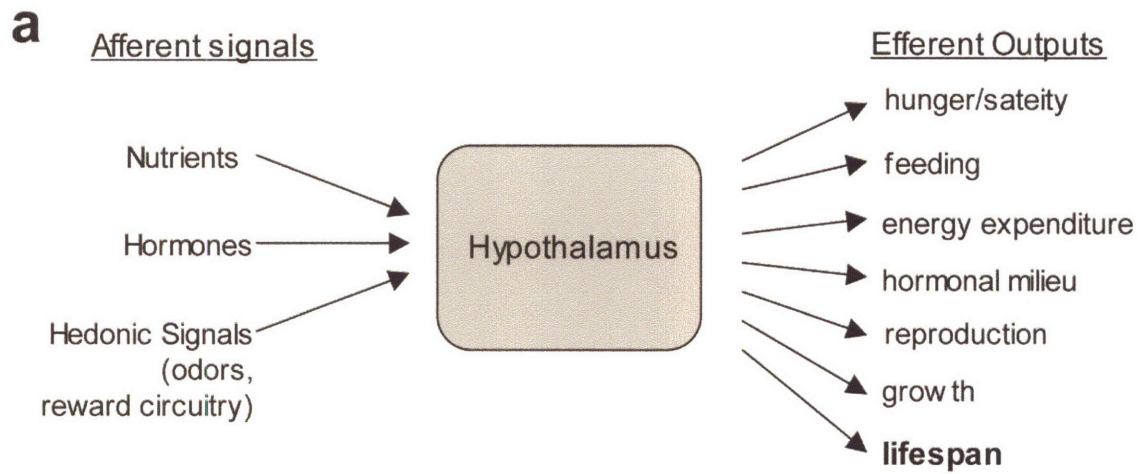


Figure 3. Intracellular energy sensing mechanisms in hypothalamic neurons.

(a) Glucose-excited hypothalamic neurons sense glucose by a mechanism similar to that used by pancreatic β -cells. The pancreatic form of glucokinase (GK) drives glucose entry into the glycolytic pathway. Glycolysis elevates cytosolic NADH and pyruvate. Shuttling of cytoplasmic NADH into the mitochondria is essential for subsequent electron transport chain (ETC)-dependent production of ATP. Increased ATP closes ATP-sensitive potassium channels, leading to neuronal activation.

(b) Additional intracellular energy sensing mechanisms responding to fat, ATP, glucose, and amino acids. In high energy conditions, intracellular long-chain fatty acid acyl-CoA (LCFA-CoA) levels in hypothalamic neurons are high, which causes anorexigenic responses. The LCFA-CoA level is increased by synthesis from LCFAs (by acyl CoA synthase, ACS). Also, malonyl-CoA is synthesized from glucose-derived acetyl-CoA by acetyl-CoA carboxylase (ACC). Malonyl-CoA increases LCFA-CoA levels by inhibiting their transport into the mitochondria (via inhibition of carnitine-palmitoyl transferase, CPT1), thus preventing LCFA β -oxidation. Malonyl-CoA also increases LCFA-CoA levels by direct contribution to synthesis, via fatty acid synthase (FAS). AMPK inhibits ACC, and is itself inhibited by high ATP. mTOR inhibits feeding, possibly in response to high amino acids.

FIGURE 3

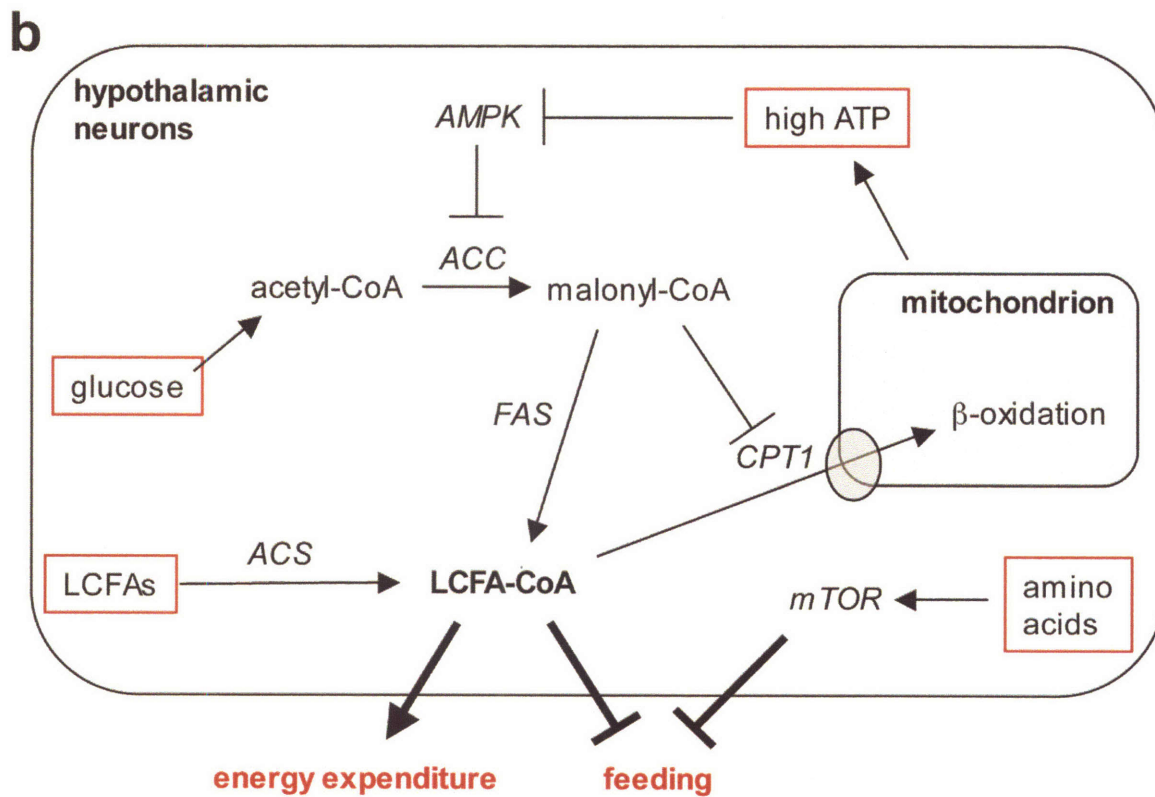
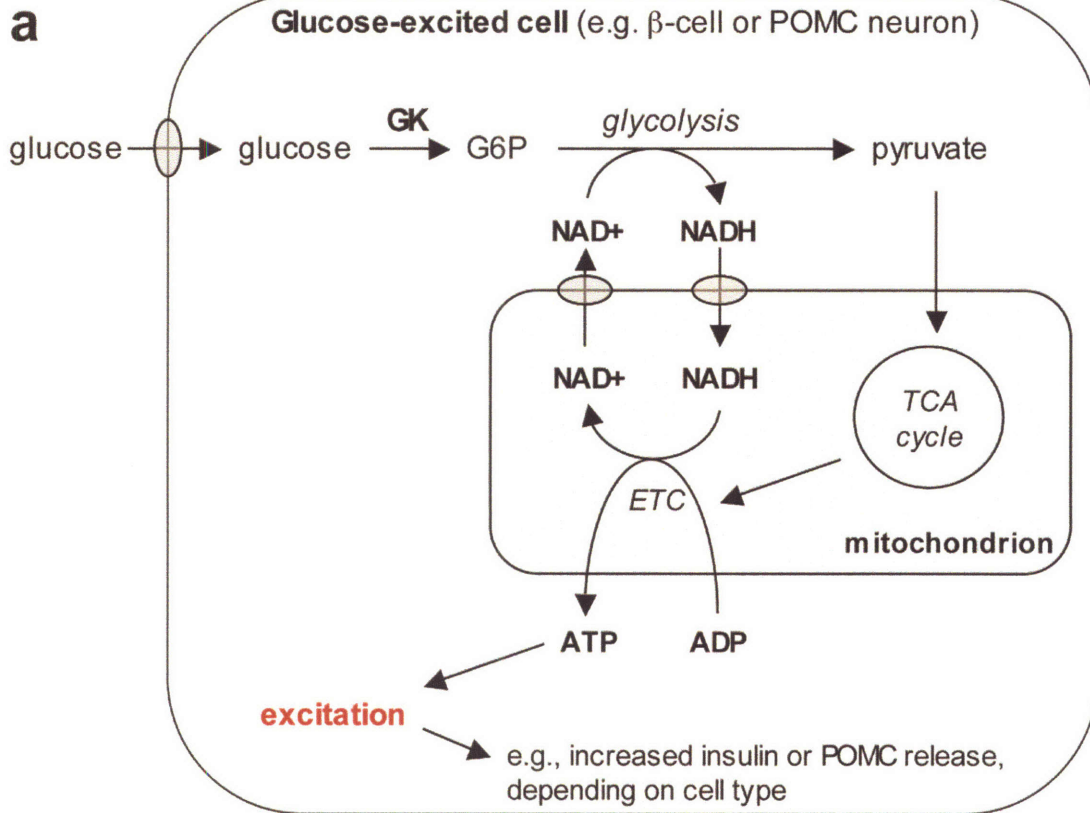


Figure 4. Interaction between leptin- and insulin-dependent neuropeptide regulatory pathways in POMC and AgRP neurons.

In both types of neurons, leptin binding to its receptor (LepR) causes phosphorylation of Stat3, which binds to the neuropeptide promoter. Insulin binding to its receptor activates PI3 kinase, which activates Akt/PKB, which phosphorylates FoxO1 and causes its exclusion from the nucleus. Leptin binding may also activate PI3K. Stat3 and FoxO1 bind to partially overlapping sites on the neuropeptide promoters, such that prior binding of one precludes the binding of the other. Stat3 activates POMC and inhibits AgRP, whereas FoxO1 inhibits POMC and activates AgRP. Thus, high leptin upregulates POMC and represses AgRP; high insulin derepresses POMC and downregulates AgRP.

FIGURE 4

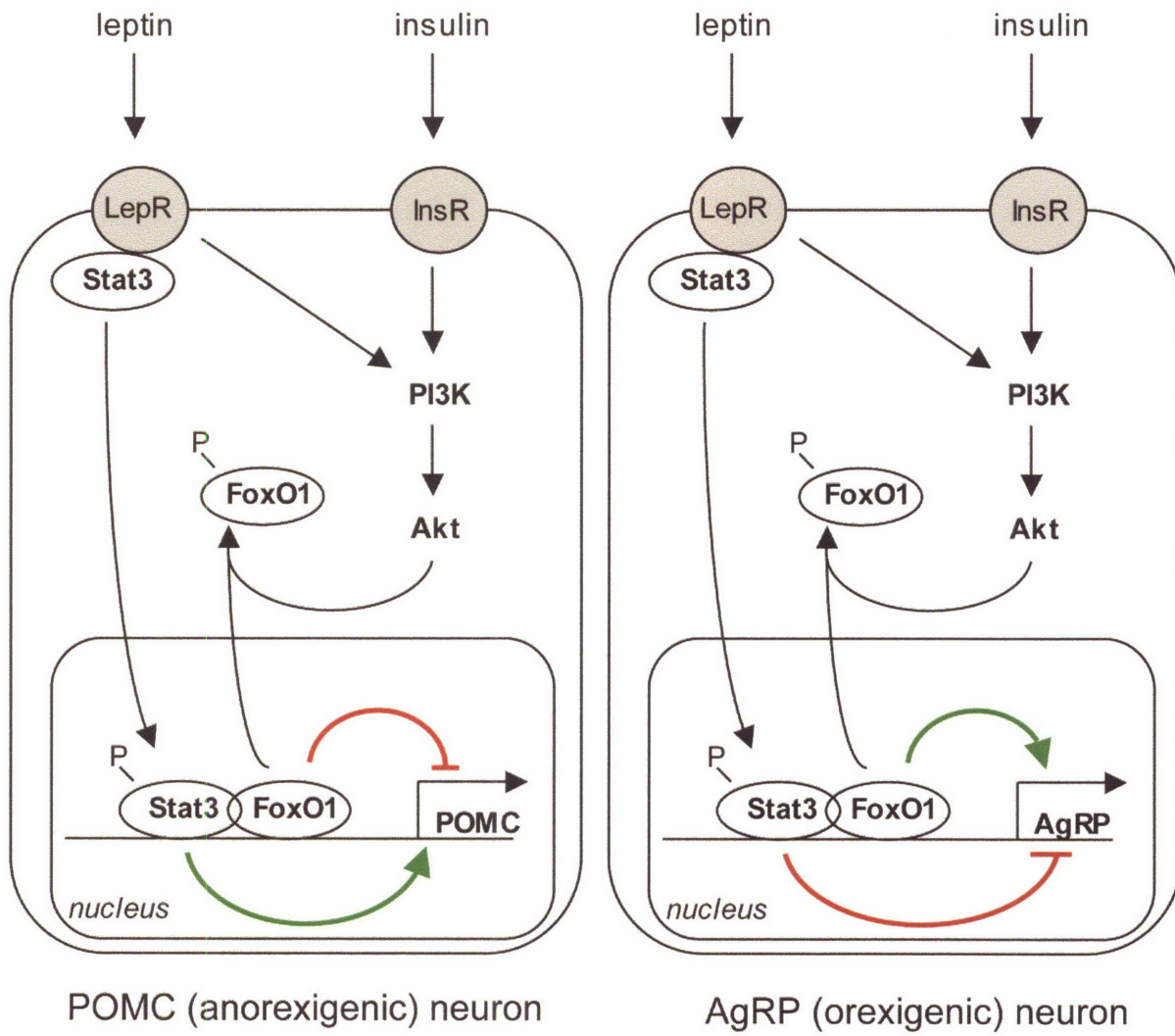
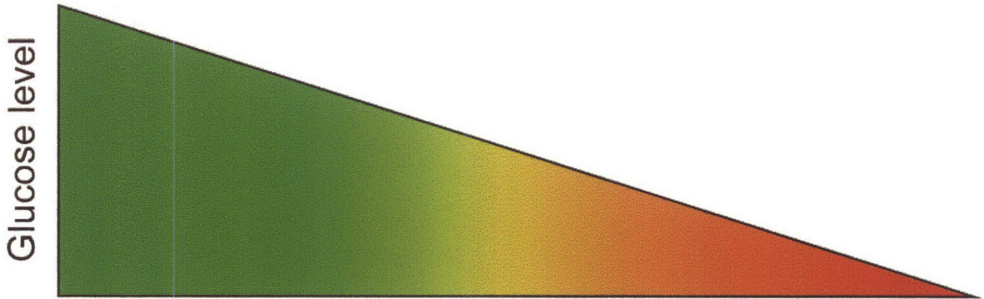


Figure 5. Different longevity pathways predominate at mild vs. extreme DR in yeast.

Yeast is normally cultured with 2% glucose in the medium. At mild (0.5%) glucose restriction, the longevity pathway on the left side of the figure is most important.

Reduced glycolysis leads to lower cytoplasmic NADH. Carbon flux through the pyruvate dehydrogenase complex (PDC), especially its subunit *lat1*, is increased under 0.5% glucose, which elevates mitochondrial respiration and further lowers NADH. The elevated NAD⁺/NADH ratio increases activity of *sir2* and/or the related genes *hst1* and *hst2*, which increases lifespan. At severe glucose restriction (0.05% glucose), an apparently separate longevity pathway predominates, which extends lifespan without requiring any of the genes in the 0.5% glucose longevity pathway except *lat1*. *sch9* and *tor1* inhibit lifespan, acting by the same mechanism as 0.05% glucose and downstream of or in parallel to *lat1*. The 0.5% glucose longevity pathway appears to antagonize the 0.05% longevity pathway, as 0.05% glucose extends lifespan much more effectively in strains bearing deletions in the three sirtuin genes or genes required for function of the electron transport chain.

FIGURE 5



Dominantly active longevity pathway

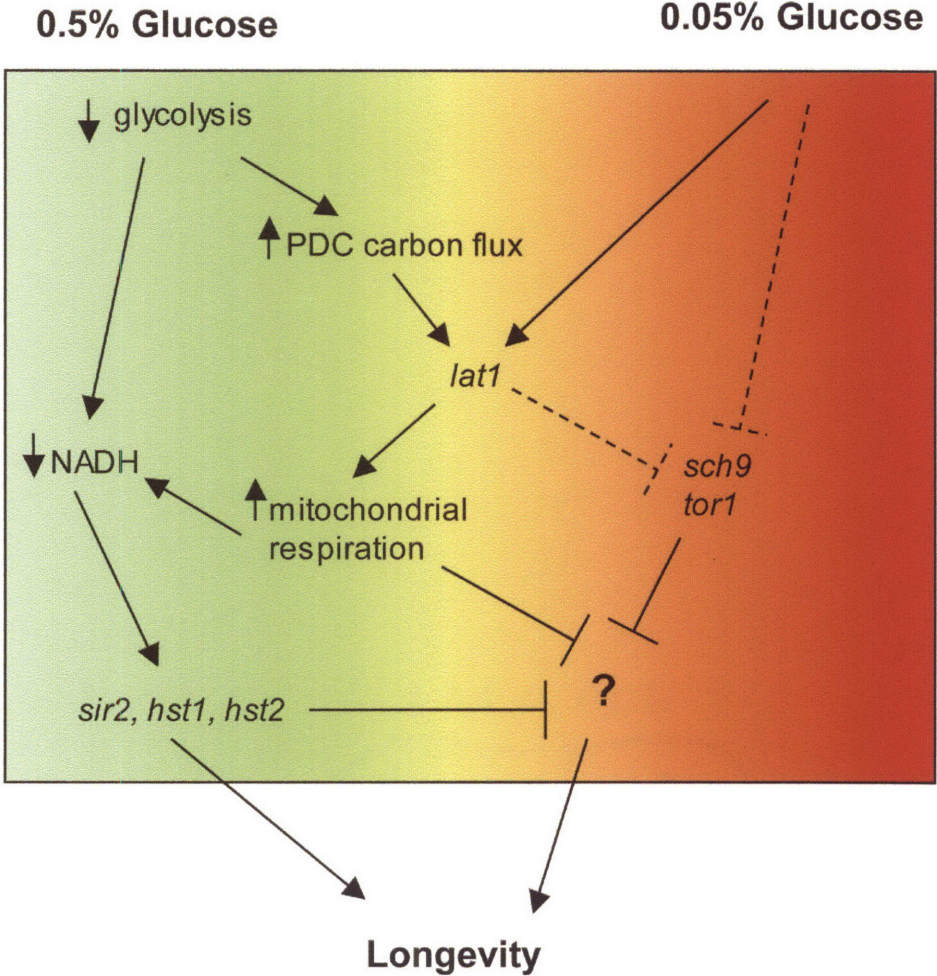
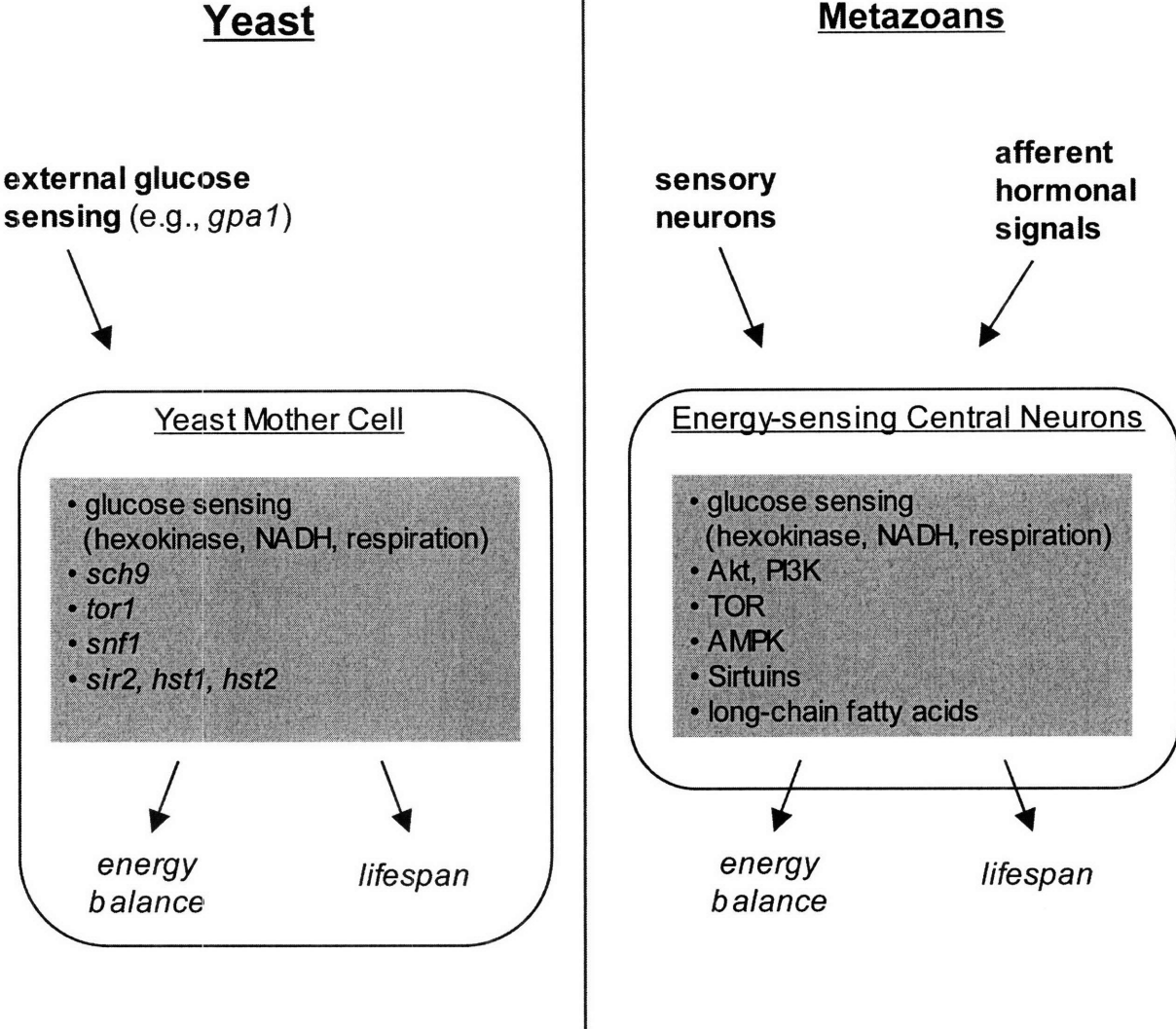


Figure 6. Model of potentially parallel mechanisms of DR longevity control in yeast and metazoans.

Both model systems sense external nutritional cues, in yeast via the glucose-sensitive GPCR *gpa1*, and in metazoans via sensory neurons. Both model systems integrate this environmental information with cellular energy status, sensed by similar pathways in both yeast and metazoan. Glucose is sensed in both models by a mechanism depending on hexokinases to drive glucose metabolism and on elevated NADH and mitochondrial activity. Nutrients are sensed and lifespan controlled by homologues of Akt, TOR, and AMPK in both systems. Sirtuins are involved in some responses to DR in both model systems. Long chain fatty acids are important in mammalian hypothalamic energy sensing, but their importance is not known in yeast. The primary difference between yeast and metazoan DR longevity control is that, in yeast, cellular energy-sensing pathways are coupled directly to cellular energy homeostasis and lifespan effectors, while in metazoans, cellular energy-sensing pathways are coupled to cell-nonautonomous signaling that achieves organismal energy homeostasis and lifespan control. A necessary consequence of this difference is that metazoan energy-sensing neurons receive additional afferent inputs from the periphery that are indicative of organismal energy status.

FIGURE 6



CHAPTER 2

skn-1* Acts in Two Neurons to Mediate Dietary Restriction-Induced Longevity in *C. elegans

This chapter is in press at *Nature*. The authors are Nicholas A. Bishop and Leonard Guarente.

Summary Paragraph

Dietary restriction (DR) extends lifespan and retards age-related disease in many species¹ and profoundly alters endocrine function in mammals². However, no causal role of any hormonal signal in diet-restricted longevity has been demonstrated. Here we show that increased longevity of diet-restricted *C. elegans* requires the transcription factor *skn-1* acting in the ASIs, a pair of neurons in the head. DR activates *skn-1* in the ASIs, thereby signalling peripheral tissues to increase metabolic activity. These findings demonstrate that increased lifespan in a diet-restricted metazoan depends on cell-nonautonomous signaling from central neuronal cells to non-neuronal body tissues, and suggest that the ASIs mediate dietary restriction-induced longevity by an endocrine mechanism.

Results and Discussion

Dietary restriction extends lifespan in many organisms and reduces incidence and progression of age-related disease¹. In mammals, DR dramatically alters central and secondary hormone production and target tissue responsiveness, suggesting a mechanism by which this regimen coordinately slows aging across a variety of tissues². A possible hormonal link of DR to longevity is suggested by the recent demonstration that serum from DR mice contains factors sufficient to induce many of the cellular phenotypes of DR *in vitro*³. However, no hormone has been shown to mediate DR longevity *in vivo*, and indeed mice that almost completely lack several pituitary hormones respond normally to

DR⁴, so the question of whether DR induces longevity by an endocrine mechanism remains unresolved.

DR has been shown to extend lifespan in the roundworm *C. elegans*⁵. We developed a DR protocol that reliably increases longevity in worms (see Methods; Fig. 1a). Worms cultured on standard plates seeded with the bacterial food source throughout larval development were then transferred to a small volume of liquid medium in which bacterial density was controlled at a range of different levels (see Methods). Worms maintained at high bacterial density (our *ad libitum*, or AL, condition) had a slightly longer lifespan than worms cultured on agar plates seeded with a bacterial lawn (Fig. 1a). Mean lifespan increased as bacterial density was reduced until a maximum lifespan was reached at an optimal dilution of 1:10 (our DR condition), while further dilutions caused reduced mean lifespan, presumably due to starvation (Fig. 1b). DR animals also exhibited reduced fat in the intestine and small body size (Supplementary Fig. S1a-b). Animals in the AL condition exhibited an optimal brood size, while DR animals had a reduced brood size and extended reproductive period (Supplementary Fig. S1c). As reported for other methods of DR^{6,7}, this DR protocol extended the lifespan of both *daf-16* and *daf-2* mutants (Figure 1c), which function in the well-characterized insulin-like signaling pathway⁸. Here, we describe the use of this protocol to identify a gene mediating DR longevity: *skn-1*.

skn-1 has previously been shown to be critical in endodermal development⁹ and control of the oxidative stress response¹⁰, functions that are shared by the most similar mammalian proteins, the NF-E2-related transcription factors. Since oxidative damage is thought to be a key cause of aging¹¹, it has been proposed that *skn-1* may be a

determinant of aging rate¹⁰. Notably, some isoforms of *skn-1* are expressed in an operon downstream of *bec-1*, the *C. elegans* homolog of mammalian beclin 1. Beclin 1 mediates autophagy induced by nutrient deprivation¹², suggesting that *skn-1* might be regulated in response to nutritional stress (Fig. 2a). We therefore tested whether *skn-1* functions in the DR-induced longevity response. Four loss-of-function alleles of *skn-1* all significantly impaired response to DR (Fig. 2b; Supplementary Fig. S2a and S3). *Skn-1* mutant lifespan was unresponsive to diet over a wide range of food concentrations (Fig 1b). *skn-1* mutations appeared to specifically interfere with the DR longevity response, as they did not impair the longevity increase caused by mutation of *daf-2* (Supplementary Fig. S4) or by treatment with a plant polyphenol extract¹³. We focused our subsequent analysis on two alleles, *skn-1(zu135)* and *skn-1(zu169)*, because they prevented the longevity increase on DR completely, yet had little or no effect on AL lifespan (Fig. 2b). These two alleles introduce premature stop codons before the sequence encoding the DNA-binding domain of all *skn-1* isoforms (Supplementary Fig S2a; also see below). The failure of both *skn-1* mutants to respond to DR was rescued by *Is007*, an integrated transgene expressing a *skn-1::gfp* fusion from its native promoter¹⁰ (Fig. 2a and 2c; Supplementary Fig. S2a), confirming that these *skn-1* mutations caused the DR longevity defect.

The rescuing *Is007* transgene is expressed in only two tissues: in the two ASI neurons, and in the intestine¹⁰. This is an intriguing expression pattern in the context of DR, since the intestine is the food absorption and storage organ, and the ASIs are sensory neurons in the head that are critical in translating information about food availability into endocrine signals that influence the dauer decision during development¹⁴. We asked in which tissue *skn-1* acts to mediate DR longevity. The *skn-1* gene encodes three protein

isoforms, SKN-1A, SKN-1B, and SKN-1C, which have different N-termini but a common C-terminus (Fig. 2a). Using 5' RACE, we obtained evidence that each of these isoforms is expressed from an independent promoter (Supplementary Fig. S2b-d). Because most of the unique 5' coding region of *skn-1a* is not included in the rescuing *Is007* transgene (Fig. 2a), we reasoned that *skn-1b* and/or *skn-1c* must be sufficient to rescue DR in the *skn-1* mutants. We used RNAi feeding clones corresponding to the unique 5' end of either *skn-1b* or *skn-1c* to knock down each isoform separately in GFP reporter strains, and determined that *skn-1b* is expressed in the ASI neurons but not detectably in the gut, and *skn-1c* is expressed in the gut but not detectably in the ASI neurons (Fig. 2d-f). An extrachromosomal transgene that drives *skn-1b::gfp* expression from the ASI-specific *gpa-4* promoter¹⁵ showed expression in the ASI neurons, but not the gut, and rescued the DR longevity defects of *skn-1(zu135)* animals completely (Fig. 2g). Similar results were obtained with the same transgene in a *skn-1(zu169)* background, and also with a chromosomally integrated version of the transgene (Supplementary Table S1). In contrast, extrachromosomal and integrated transgenes driving *skn-1c::gfp* from the *ges-1* promoter¹⁶ showed expression only in the gut, and had no effect on the DR defect of *skn-1(zu135)* (Fig. 2h). Furthermore, ectopic expression of *skn-1c::gfp* in the ASI neurons using the *gpa-4* promoter failed to rescue the DR longevity defect of *skn-1(zu135)* (Supplementary Table S1). Taken together, these data indicate that *skn-1b* functions in the ASI neurons to mediate DR longevity.

To confirm that the ASI neurons are required for DR-induced longevity, we used a laser microbeam to specifically kill these two cells and tested the effect in subsequent DR. Ablation of the ASI neurons completely suppressed the response to DR (Fig. 3a), but

also caused a small increase in basal longevity, consistently with a previous report¹⁷. The ASIs can apparently affect lifespan by two independent pathways, since the increase in basal longevity was previously reported to be dependent on *daf-16*¹⁷, and DR longevity is not (Fig. 1c). We reasoned that the use of a *daf-16* mutant would separate the two effects of ablating the ASI neurons and allow us to determine their role in DR longevity specifically. As expected, when we repeated the ASI ablation in *daf-16* animals, we found that basal longevity was unaffected by the ablation (Fig. 3b). Importantly, DR longevity was still suppressed (Fig. 3b). These results support the model that *skn-1* functions in the ASI neurons to extend lifespan in response to DR.

We next investigated how *skn-1* acts in the ASI to mediate DR longevity. To rule out the possibility that *skn-1* mutation disrupts development of the ASI neurons, we used a panel of ASI-specific GFP reporters to confirm that the ASI neurons exhibit normal morphology and cell fate in a *skn-1* background (Supplementary Fig. S5). We then tested whether SKN-1::GFP is induced by DR in *Is007* animals. Although we saw no specific induction in the intestine (data not shown), DR significantly increased SKN-1::GFP fluorescence in the ASI neurons (Fig. 4a). The fluorescence increase was specific to SKN-1::GFP expressed from its native promoter, because if the protein was expressed from the ASI-specific *gpa-4* promoter, we observed instead a slight decrease in expression during DR (Fig. 4a). This dependence of *skn-1* induction on the native promoter suggests that *skn-1* may be transcriptionally regulated during DR.

In yeast, DR induces an increase in respiratory rate¹⁸, and there is evidence that this is also the case in worms^{19,20}. We measured the whole-body oxygen consumption rate of large populations of wild-type worms on day 3 of AL and DR (see Methods), and

found that DR worms exhibited elevated respiration (Fig. 4b). The respiration rate increase on DR was absent in a *skn-1(zu135)* mutant, but could be rescued, and somewhat enhanced, by the *Is007* transgene (Fig. 4b), demonstrating that *skn-1* is necessary for the increased respiration. The increase in respiration is likely to be necessary for the DR longevity effect, because two different specific inhibitors of the mitochondrial electron transport chain (ETC) complex III, myxothiazol and antimycin, suppressed DR longevity without shortening AL lifespan (Fig. 4c-d). Further, myxothiazol completely suppressed the increase in respiration under DR (data not shown). The effect of inhibiting electron transport was specific to DR longevity, as the long life of a *daf-2* mutant was not affected by antimycin (Fig. 4e). Finally, to determine whether *skn-1* in the ASI neurons alone is sufficient to rescue the absence of increased respiration in the *skn-1(zu135)* mutant during DR, we constructed two stably integrated transgenes: *geIs9*, which drives *skn-1b::gfp* expression in the ASI neurons, and *geIs10*, which drives *skn-1c::gfp* expression in the intestine. *geIs9* expressed strongly in the ASIs, and also rescued and enhanced the respiration response to DR in the *skn-1(zu135)* mutant (Fig 4b). The *geIs9* line sometimes showed weak expression in a few cells apart from the ASIs, though these are unlikely to contribute to the observed rescue (see Methods and Supplementary Fig. S6). *geIs10*, in contrast, failed to rescue the DR respiration defect of *skn-1(zu135)*, despite expressing efficiently in the intestine (Supplementary Fig. S6). These findings suggest that DR-induced activation of *skn-1* in the ASIs causes release of a signal that promotes metabolism in peripheral tissues and leads to long life. Interestingly, it appears that *skn-1* has two functions in the adult that are separable by isoform and tissue of expression:

mediation of DR longevity by *skn-1b* in the ASI neurons, and resistance to oxidative stress by *skn-1c* in the intestine (Supplementary Fig. S6).

How might DR activate *skn-1* in the ASIs? Although the ASI is a sensory neuron²⁰, sensation of the environment by the ASI is unlikely to be necessary for DR to increase longevity, because mutants lacking functional sensory cilia still expressed SKN-1::GFP in the ASI neurons (not shown) and responded normally to DR (Fig. 4f). It has recently been shown that, within particular cells of the mammalian hypothalamus, levels of key intracellular metabolites indicative of energy availability control organismal food intake and energy metabolism²². We propose that the ASI neurons similarly detect their own cellular energy state and adjust the animal's overall metabolism in response to nutrient availability. Because increased expression of *skn-1::gfp* in the ASI is not sufficient by itself to extend AL lifespan or to enhance the response to DR (Supplementary Table 1), other pathways or neurons must act in parallel to *skn-1* to orchestrate DR longevity.

Here we demonstrate that cell-nonautonomous signals from central neuroendocrine cells to the periphery can mediate DR longevity in a metazoan. The ASIs have well-established endocrine functions, and express at least 15 known or potential hormones, including members of the insulin, TGF- β , and neuropeptide classes^{23,24}. We suggest that the ASIs release a hormonal signal upon sensing DR that promotes metabolic activity in the periphery and leads to increased respiration and long life. We anticipate that future work will dissect the critical central hormones mediating DR longevity of worms and mammals.

Methods

Strains

We used the following strains: the wild-type N2, EU1 *skn-1(zu67)/nT1[unc-?(n754);let-?]*, EU31 *skn-1(zu135)/nT1[unc-?(n754);let-?]*, EU35 *skn-1(zu169)/nT1[unc-?(n754);let-?]*, EU40 *skn-1(zu129)/nT1[unc-?(n754);let-?]*, LG335 *skn-1(zu135)/nT1[qIs51]*, LG336 *skn-1(zu169)/nT1[qIs51]*, LG333 *skn-1(zu135);Is007[skn-1::gfp]*, LG326 *skn-1(zu169);Is007*, LG340 *skn-1(zu135)/nT1[qIs51];Ex(gpa-4p::skn-1b::gfp)* #1, LG341 *skn-1(zu169)/nT1[qIs51];Ex(gpa-4p::skn-1b::gfp)* #2, LG343 *skn-1(zu135)/nT1[qIs51];Ex(ges-1p::skn-1c::gfp)*, LG344 *gels8[gpa-4p::skn-1b::gfp]*, LG345 *gels9[gpa-4p::skn-1b::gfp]*, LG348 *skn-1(zu135)/nT1[qIs51];gels9*, LG349 *gels10[ges-1p::skn-1c::gfp]*, LG357 *skn-1(zu135)/nT1[qIs51];gels10*, CB1370 *daf-2(e1370)*, GR1307 *daf-16(mgDf50)*, CX3596 *kyIs128[str-3p::gfp]*, LG347 *daf-16(mgDf50);kyIs128*, CB1124 *che-3(e1124)*, PR813 *osm-5(p813)*, LG331 *lin-35(n745);Is007*, LG360 *skn-1(zu135)/nT1[qIs51];kyIs128*, FK181 *ksIs2[daf-7p::gfp]*, LG359 *skn-1(zu135)/nT1[qIs51];ksIs2*, CX3594 *kyIs87[srd-1p::gfp]*, LG363 *skn-1(zu135)/nT1[qIs51];kyIs87*, CX3465 *kyIs39[sra-6p::gfp]*, LG367 *skn-1(zu135)/nT1[qIs51];kyIs39*, LG313 *kyIs140[str-2p::gfp]*, LG361 *skn-1(zu135)/nT1[qIs51];kyIs140*, AU10 *agIs1[dod-24p::gfp]* (a gift of D. Kim and F. Ausubel), and the *Is007[skn-1::gfp]* and *Ex(gcs-1Δ2)* strains¹⁰.

Transgenic strain construction

Extrachromosomal array-carrying transgenic strains were generated using standard microinjection methods³⁵, injecting 50 ng/μL each of the transgene plasmid and the co-injection marker plasmid pRF4. To make the *gpa-4p::skn-1b::gfp* construct, the last exon of *skn-1* and fused GFP coding sequence was amplified from *Is007* genomic DNA, and the resulting product cut with AhdI and NcoI. *skn-1b* cDNA was generated by RT-PCR using a 5' primer with a BamHI-site-containing linker and cut with BamHI and AhdI. These two restriction fragments were trimolecularly ligated into BamHI/NcoI-cut pPD95.75 to yield pNB117, a promoterless *skn-1b::gfp* fusion vector. Approximately 2.9 kb upstream of the *gpa-4* coding region was amplified from cosmid C04A12 using primers that added a 5' SphI site and a 3' BamHI site. This amplicon was digested with SphI and BamHI and ligated into SphI/BamHI cut pNB117 to yield the *gpa-4p::skn-1b::gfp* transgene plasmid (pNB121). Adult animals carrying this transgene exhibited GFP fluorescence in the nuclei of the ASI neurons, and nowhere else. In larvae, weak expression was observed in one other pair of head neuron nuclei, which may be the AWAs³⁶. Integrants of the *Ex(gpa-4p::skn-1b::gfp)* transgenes, called *gels8* and *gels9*, were isolated independently from a standard γ-ray integration screen³⁷, and were backcrossed three times to N2 prior to analysis. Following integration, nonspecific low-level GFP expression accumulated in the extreme posterior few gut nuclei of aged adult animals. It is improbable that this weak intestinal expression accounts for the observed effects on DR respiration in *gels9* for several reasons: 1) the intestinal expression is very low-level, detectable only in aged adult animals on normal plates and not in our AL or DR conditions, and limited to only a few posterior cells; 2) *skn-1b* is not normally present

in the intestine (Fig. 2e-f) and lacks the transactivation domain of the *skn-1* isoforms that are normally present (Fig. 2a), and therefore is not necessarily capable of performing any normal intestinal function of *skn-1*; 3) the low level of intestinal *skn-1b* that is present in *geIs9* animals is definitely not capable of rescuing the only intestine-specific function of *skn-1* that we are aware of, arsenate resistance (Supplementary Fig. S6).

To make the *ges-1p::skn-1c::gfp* construct, a promoterless *skn-1c::gfp* plasmid, pNB120, was first constructed analogously to pNB117 described above. Next, approximately 2.5 kb upstream of the *ges-1* coding region was amplified from cosmid C29B10 using primers with 5' SphI and 3' KpnI linkers. The amplicon was subcloned into SphI/KpnI-digested pNB117 to yield a *ges-1p::gfp* transcriptional reporter plasmid, pNB123. Worms transformed with this plasmid showed robust GFP expression throughout the gut, and nowhere else. Next, the entirety of *skn-1c::gfp* was amplified from pNB120 using a 5' primer with a KpnI linker. The amplicon was digested with KpnI and NcoI and ligated into KpnI/NcoI-cut pNB123 to yield the *ges-1p::skn-1c::gfp* transgene plasmid. 21 of 30 transgenic animals from the line used in this report exhibited nuclear GFP fluorescence in the intestine following heat shock for 20 hr at 29°C (this degree of nuclear localization is comparable to that observed with the *Is007* integrant, see Fig. 2e). No GFP fluorescence was ever observed outside the gut with or without heat shock. An integrant of the *Ex(ges-1p::skn-1c::gfp)* transgene, called *geIs10*, was isolated from a standard γ -ray integration screen³⁷, and was backcrossed three times to N2 prior to analysis.

To make the *gpa-4p::skn-1c::gfp* construct, pNB121[*gpa-4p::skn-1b::gfp*] and a cDNA clone of *skn-1c* that had been amplified with a 5' BamHI linker were cut with BamHI/SacI and ligated to yield pNB125.

Dietary restriction protocol

Lifespan assays were performed in the outer four wells of 6-well tissue culture plates, with each well containing 2.5 ml DR Bottom Medium and 2.5 ml DR Top Medium. DR Bottom Medium is composed of standard NGM medium²⁵, supplemented with 1 mg/ml erythromycin to prevent bacterial division, 12.5 µg/ml 5-fluoro-2'-deoxyuridine to inhibit progeny hatching, 50 µg/ml ampicillin, and 1 mM IPTG; DR Top Medium is identical to DR Bottom Medium, excluding the agar. Erythromycin inhibits prokaryotic protein synthesis, but is unable to penetrate the outer membrane of mammalian mitochondria³⁸. We confirmed that *C. elegans* mitochondria are also apparently insensitive to erythromycin, because the drug does not affect oxygen consumption rate or the time required for larval development (data not shown). The bacterial food source used was HT115(DE3) carrying the empty RNAi feeding vector pPD129.36²⁹, a strain routinely used as a vector control in RNAi feeding experiments in *C. elegans*. This strain remained viable for weeks without dividing in our DR medium. Bacteria were added from a concentrated stock to the desired concentration, and bacterial concentration in a 1 ml sample of each well was monitored spectrophotometrically on a rotating basis so that each well was sampled every fourth day. Additional bacteria were added as necessary to maintain starting concentration. AL bacterial concentration was approximately 2.5×10^8 .

cfu/ml, and the optimal DR level was ten-fold lower, at 2.5×10^7 cfu/ml. Worms were grown to the L4/young adult stage on NGM plates seeded with OP50 bacteria, then transferred individually into the wells and maintained at 20°C with gentle gyrotory shaking at 80 rpm.

For the progeny production assays, worms cultured as described except that FuDR was excluded to allow progeny production, and worms were transferred daily to fresh wells.

For oxygen consumption assays, the method was scaled up to allow mass culture of animals. The protocol was essentially identical, except that animals were grown in larger volumes of DR Top Medium in Erlenmeyer flasks, at a density of approximately 20 animals per ml, and DR Bottom Medium was not used.

Lifespan assay

Most lifespans in this report were measured in the liquid medium described above, except where noted; in these cases lifespans either were done on plates with the same composition as DR Bottom Medium seeded with 50 μ L concentrated bacteria (appx. 5×10^9 cfu/ml), or on standard NGM plates seeded with OP50 bacteria. Regardless of medium, the lifespan assay was performed by prodding individual animals with a worm pick every two days to determine when they died. Animals that were lost, or exploded, or died from internal hatching of progeny were censored at the time of the event, which allowed their incorporation into the dataset until the time of censorship as described³⁹.

Worms on plates containing erythromycin lived 30 - 40% longer than worms on plates

without the drug; we attribute this to the previously reported lifespan-extending effect of suppressing bacterial division⁴⁰. Some assays were done in the presence of respiration-inhibiting agents (Fig. 4c-e). In these cases the DR medium contained 1% DMSO plus 0 μ M, 30 μ M, or 60 μ M myxothiazol, or 0.1% ethanol plus 0 μ M or 1 μ M antimycin.

Survival curve p-values were calculated by the Mantel-Cox logrank test using Prism statistical software (Graphpad).

Laser ablation

The strain CX3596 *kyIs128[*str-3p:gfp*]*, which expresses GFP specifically in the ASI neuron²⁶, was used to facilitate identification of the ASI. Synchronized L1 animals were fed on OP50 for 4 – 8 hours to induce robust GFP expression, then mounted on microscope slides in 50 mM sodium azide anesthetic and ablated using a laser microbeam as described²⁷. Mock-ablated animals were treated identically in parallel, except that they were not exposed to the laser. Worms were recovered to OP50 plates and grown to the L4/young adult stage, at which time absence of GFP was taken to indicate successful ablation. (We confirmed in a separate control experiment that a cohort of ablated animals lacking GFP also all lacked the ASI itself, and we never observed a GFP-negative animal in any of the hundreds of mock-ablated controls). Lifespan of successfully ablated animals and mock-ablated controls was assayed as described above. The *kyIs128* strain proved to have a somewhat shorter lifespan than N2, but this was attributable to intrinsic strain differences and not to the mounting procedure (Supplementary Fig. S7). The

kyIs128 strains increased lifespan on DR by a similar percentage as does N2 (Supplementary Fig. S7).

Respiration assay

Mass plate cultures of synchronized worms were obtained by standard techniques and grown on OP50 plates to the L4 stage, then transferred to Erlenmeyer flasks containing AL or DR levels of bacteria, as described above. After three days of culture, animals were collected by centrifugation and washed free of bacteria in S buffer. Respiration rate was measured at 25°C as described²⁸, using a Clark-type oxygen electrode (Microelectrodes Inc.). At least three 1 ml samples containing approximately 500 worms each were measured for each strain and condition in each experiment. The entire sample was frozen at -80°C following the respiration assay. Protein concentration in each sample was measured as described²⁸, and oxygen consumption rates were normalized to protein content.

skn-1 mutants are maternal-effect lethal and must be maintained as balanced heterozygotes. To obtain nearly pure *skn-1(zu135)* and *skn-1(zu135);gels9* populations for the oxygen assays, we first balanced *skn-1(zu135)* with the reciprocal translocation *nT1[qIs51]*, which carries a transgene expressing GFP in the pharynx. We then isolated non-GFP-pharynx, *skn-1* homozygous animals from a synchronous L4 population using the COPAS Biosorter (Union Biometrica) prior to transfer to the AL or DR culture conditions. This procedure yielded greater than 95% non-GFP-pharynx populations,

which we confirmed to be *skn-1* homozygotes by verifying the embryonic lethality of progeny of samples of sorted worms.

Fluorescence intensity quantification

Fluorescent images were collected at 1000X magnification (Zeiss) from worms subjected to 5 days of AL or DR as described above. Fluorescence brightness in the ASI was quantified using NIH ImageJ software.

RNAi feeding

RNAi feeding assays were done as described²⁹. Worms were fed RNAi from L1 to L4. The *skn-1b(RNAi)* construct included the entire first exon of *skn-1b*. The *skn-1c(RNAi)* construct included the spliced first three exons from a *skn-1c* cDNA. In Fig. 2d, a *lin-35(n745)* mutation in the strain background was used because this mutation sensitizes the normally refractory ASI neurons to RNAi⁴¹.

Rapid amplification of cDNA ends

5' RACE (Invitrogen) was performed on total N2 RNA in accordance with the manufacturer's instructions, using a primer specific to the unique first exon of *skn-1b*.

Sudan Black fat staining

Day 3 adults cultured on plates, in AL conditions, and in DR conditions were stained as described³¹.

Acknowledgements

We thank H. R. Horvitz for generously allowing use of essential equipment, and members of the Guarente and Horvitz labs for advice and useful discussions. We thank D. Kim and F. Ausubel for the gift of an unpublished strain. Many of the strains used in this work were provided by the Caenorhabditis Genetics Center. This work was supported by a grant from the National Institutes of Health.

References

1. Koubova, J. & Guarente, L. How does calorie restriction work? *Genes Dev* **17**, 313-21 (2003).
2. Mobbs, C. V., Bray, G. A., Atkinson, R. L., Bartke, A., Finch, C. E., Maratos-Flier, E., Crawley, J. N. & Nelson, J. F. Neuroendocrine and pharmacological manipulations to assess how caloric restriction increases life span. *J Gerontol A Biol Sci Med Sci* **56** Spec No 1, 34-44 (2001).
3. de Cabo, R., Furer-Galban, S., Anson, R. M., Gilman, C., Gorospe, M. & Lane, M. A. An in vitro model of caloric restriction. *Exp Gerontol* **38**, 631-9 (2003).
4. Bartke, A., Wright, J. C., Mattison, J. A., Ingram, D. K., Miller, R. A. & Roth, G. S. Extending the lifespan of long-lived mice. *Nature* **414**, 412 (2001).
5. Walker, G., Houthoofd, K., Vanfleteren, J. R. & Gems, D. Dietary restriction in *C. elegans*: from rate-of-living effects to nutrient sensing pathways. *Mech Ageing Dev* **126**, 929-37 (2005).
6. Lakowski, B. & Hekimi, S. The genetics of caloric restriction in *Caenorhabditis elegans*. *Proc Natl Acad Sci USA* **95**, 13091-6 (1998).
7. Houthoofd, K., Braeckman, B. P., Johnson, T. E. & Vanfleteren, J. R. Life extension via dietary restriction is independent of the Ins/IGF-1 signalling pathway in *Caenorhabditis elegans*. *Exp Gerontol* **38**, 947-54 (2003).
8. Kenyon, C. The plasticity of aging: insights from long-lived mutants. *Cell* **120**, 449-60 (2005).
9. Bowerman, B., Eaton, B. A. & Priess, J. R. *skn-1*, a maternally expressed gene required to specify the fate of ventral blastomeres in the early *C. elegans* embryo. *Cell* **68**, 1061-75 (1992).
10. An, J. H. & Blackwell, T. K. SKN-1 links *C. elegans* mesendodermal specification to a conserved oxidative stress response. *Genes Dev* **17**, 1882-93 (2003).
11. Golden, T. R., Hinerfeld, D. A. & Melov, S. Oxidative stress and aging: beyond correlation. *Aging Cell* **1**, 117-23 (2002).
12. Zhenyu, Y., Jin, S., Yang, C., Levine, A.J., & Heintz, N. Beclin 1, an autophagy gene essential for early embryonic development, is a haploinsufficient tumor suppressor. *PNAS* **100**, 15077-82 (2003).
13. Wilson, M. A., Shukitt-Hale, B., Kalt, W., Ingram, D. K., Joseph, J. A. & Wolkow, C. A. Blueberry polyphenols increase lifespan and thermotolerance in *Caenorhabditis elegans*. *Aging Cell* **5**, 59-68 (2006).

14. Bargmann, C. I. & Horvitz, H. R. Control of larval development by chemosensory neurons in *Caenorhabditis elegans*. *Science* **251**, 1243-6 (1991).
15. Jansen, G., Thijssen, K. L., Werner, P., van der Horst, M., Hazendonk, E. & Plasterk, R. H. The complete family of genes encoding G proteins of *Caenorhabditis elegans*. *Nat Genet* **21**, 414-9 (1999).
16. Libina, N., Berman, J. R. & Kenyon, C. Tissue-specific activities of *C. elegans* DAF-16 in the regulation of lifespan. *Cell* **115**, 489-502 (2003).
17. Alcedo, J. & Kenyon, C. Regulation of *C. elegans* longevity by specific gustatory and olfactory neurons. *Neuron* **41**, 45-55 (2004).
18. Lin, S. J., Ford, E., Haigis, M., Liszt, G. & Guarente, L. Calorie restriction extends *Saccharomyces cerevisiae* lifespan by increasing respiration. *Nature* **418**, 344-8 (2002).
19. Houthoofd, K., Braeckman, B. P., Lenaerts, I., Brys, K., De Vreese, A., Van Eygen, S. & Vanfleteren, J. R. Axenic growth up-regulates mass-specific metabolic rate, stress resistance, and extends life span in *Caenorhabditis elegans*. *Exp Gerontol* **37**, 1371-8 (2002).
20. Houthoofd, K., Braeckman, B. P., Lenaerts, I., Brys, K., De Vreese, A., Van Eygen, S. & Vanfleteren, J. R. No reduction of metabolic rate in food restricted *Caenorhabditis elegans*. *Exp Gerontol* **37**, 1359-69 (2002).
21. Bargmann, C. I. & Horvitz, H. R. Chemosensory neurons with overlapping functions direct chemotaxis to multiple chemicals in *C. elegans*. *Neuron* **7**, 729-42 (1991).
22. Dowell, P., Hu, Z. & Lane, M. D. Monitoring energy balance: metabolites of fatty acid synthesis as hypothalamic sensors. *Annu Rev Biochem* **74**, 515-34 (2005).
23. Li, C. The ever-expanding neuropeptide gene families in the nematode *Caenorhabditis elegans*. *Parasitology* **131** Suppl, S109-27 (2005).
24. Ren, P., Lim, C. S., Johnsen, R., Albert, P. S., Pilgrim, D. & Riddle, D. L. Control of *C. elegans* larval development by neuronal expression of a TGF- β homolog. *Science* **274**, 1389-91 (1996).
25. Brenner, S. The genetics of *Caenorhabditis elegans*. *Genetics* **77**, 71-94 (1974).
26. Peckol, E. L., Zallen, J. A., Yarrow, J. C. & Bargmann, C. I. Sensory activity affects sensory axon development in *C. elegans*. *Development* **126**, 1891-902 (1999).
27. Avery, L. & Horvitz, H. R. Pharyngeal pumping continues after laser killing of the pharyngeal nervous system of *C. elegans*. *Neuron* **3**, 473-85 (1989).

28. Braeckman, B. P., Houthoofd, K. & Vanfleteren, J. R. Assessing metabolic activity in aging *Caenorhabditis elegans*: concepts and controversies. *Aging Cell* **1**, 82-8 (2002).
29. Timmons, L., Court, D. L. & Fire, A. Ingestion of bacterially expressed dsRNAs can produce specific and potent genetic interference in *Caenorhabditis elegans*. *Gene* **263**, 103-12 (2001).
30. Apfeld, J. & Kenyon, C. Regulation of lifespan by sensory perception in *Caenorhabditis elegans*. *Nature* **402**, 804-9 (1999).
31. McKay, R. M., McKay, J. P., Avery, L. & Graff, J. M. *C. elegans*: a model for exploring the genetics of fat storage. *Dev Cell* **4**, 131-42 (2003).
32. Blumenthal, T. & Steward, K. in *C. elegans II* (eds Riddle, D. L., Blumenthal, T., Meyer, B. J., & Preiss, J. R.) 117-146 (Cold Spring Harbor Laboratory Press, Cold Spring Harbor, New York, 1997).
33. Culetto, E., Combes, D., Fedon, Y., Roig, A., Toutant, J. P. & Arpagaus, M. Structure and promoter activity of the 5' flanking region of *ace-1*, the gene encoding acetylcholinesterase of class A in *Caenorhabditis elegans*. *J Mol Biol* **290**, 951-66 (1999).
34. Inoue, H., Hisamoto, N., An, J. H., Oliveira, R. P., Nishida, E., Blackwell, T. K. & Matsumoto, K. The *C. elegans* p38 MAPK pathway regulates nuclear localization of the transcription factor SKN-1 in oxidative stress response. *Genes Dev* **19**, 2278-83 (2005).
35. Mello, C. C., Kramer, J. M., Stinchcomb, D. & Ambros, V. Efficient gene transfer in *C. elegans*: extrachromosomal maintenance and integration of transforming sequences. *EMBO J* **10**, 3959-70 (1991).
36. Kim, K., Colosimo, M. E., Yeung, H. & Sengupta, P. The UNC-3 Olf/EBF protein represses alternate neuronal programs to specify chemosensory neuron identity. *Dev Biol* **286**, 136-48 (2005).
37. Jin, Y. in *C. elegans: A Practical Approach* (ed. Hope, I. A.) 69-96 (Oxford University Press, New York, 1999).
38. Ibrahim, N. G., Burke, J. P. & Beattie, D. S. The sensitivity of rat liver and yeast mitochondrial ribosomes to inhibitors of protein synthesis. *J Biol Chem* **249**, 6806-11 (1974).
39. Lawless, J. F. *Statistical Models and Methods for Lifetime Data* (Wiley, New York, 1982).

40. Garigan, D., Hsu, A. L., Fraser, A. G., Kamath, R. S., Ahringer, J. & Kenyon, C. Genetic analysis of tissue aging in *Caenorhabditis elegans*: a role for heat-shock factor and bacterial proliferation. *Genetics* **161**, 1101-12 (2002).

41. Wang, D., Kennedy, S., Conte, D., Jr., Kim, J. K., Gabel, H. W., Kamath, R. S., Mello, C. C. & Ruvkun, G. Somatic misexpression of germline P granules and enhanced RNA interference in retinoblastoma pathway mutants. *Nature* **436**, 593-597 (2005).

Supplementary Table S1. Lifespan data for main figures.

Strain and condition	# deaths/# censored(# trials)	mean \pm s.e.m	p-value vs. AL control
N2 on agar plates with bacterial lawn	218/25(5)	23.7 \pm 0.31	
N2 in 2.5x10 ⁸ cfu/ml ("AL")	832/50(17)	25.7 \pm 0.14	
N2 in 1.7x10 ⁸ cfu/ml	22/31(1)	25.6 \pm 1.00	
N2 in 8.5x10 ⁷ cfu/ml	25/27(1)	33.0 \pm 0.99	
N2 in 5.7x10 ⁷ cfu/ml	51/1(1)	34.9 \pm 0.72	
N2 in 2.5x10 ⁷ cfu/ml ("DR")	792/60(16)	32.8 \pm 0.18	P < 0.0001
N2 in 2.5x10 ⁶ cfu/ml	20/32(1)	26.3 \pm 1.56	
N2 in 2.5x10 ⁵ cfu/ml	34/17(1)	23.2 \pm 0.85	
N2 with no bacteria	37/12(1)	18.1 \pm 0.66	
<i>skn-1(zu135)</i> in 2.5x10 ⁸ cfu/ml ("AL")	202/2(4)	25.6 \pm 0.31	
<i>skn-1(zu135)</i> in 2.5x10 ⁷ cfu/ml ("DR")	207/1(4)	25.7 \pm 0.31	P = 0.6200
<i>skn-1(zu135)</i> in 2.5x10 ⁶ cfu/ml	51/2(1)	24.2 \pm 0.65	
<i>skn-1(zu135)</i> in 2.5x10 ⁵ cfu/ml	51/1(1)	23.0 \pm 0.63	
<i>daf-2(e1370)</i> AL	23/22(1)	39.0 \pm 2.11	
<i>daf-2(e1370)</i> DR	32/21(1)	60.0 \pm 2.7	P < 0.0001
<i>daf-16(mg50)</i> AL	51/2(1)	20.7 \pm 0.80	
<i>daf-16(mg50)</i> DR	53/1(1)	28.4 \pm 0.37	P < 0.0001
<i>skn-1(zu135);Is007</i> AL	55/1(1)	26.3 \pm 0.47	
<i>skn-1(zu135);Is007</i> DR	48/8(1)	33.4 \pm 0.69	P < 0.0001
<i>skn-1(zu135);Ex(gpa-4p::skn-1b::GFP)</i> line #1 AL	16/0(1)	25.4 \pm 0.87	
<i>skn-1(zu135);Ex(gpa-4p::skn-1b::GFP)</i> line #1 DR	15/2(1)	31.2 \pm 1.22	P = 0.0005
<i>skn-1(zu135);Ex(gpa-4p::skn-1b::GFP)</i> line #2 AL	42/1(1)	26.0 \pm 0.56	
<i>skn-1(zu135);Ex(gpa-4p::skn-1b::GFP)</i> line #2 DR	44/1(1)	33.5 \pm 0.79	P < 0.0001
<i>skn-1(zu135);gels9[gpa-4p::skn-1b::GFP]</i> AL	39/0(1)	24.7 \pm 0.65	
<i>skn-1(zu135);gels9[gpa-4p::skn-1b::GFP]</i> DR	55/1(1)	34.6 \pm 0.69	P < 0.0001
<i>skn-1(zu169)</i> AL	127/3(3)	24.3 \pm 0.39	
<i>skn-1(zu169)</i> DR	150/0(3)	25.6 \pm 0.46	P = 0.0062
<i>skn-1(zu169);Is007</i> AL	54/0(1)	25.9 \pm 0.52	
<i>skn-1(zu169);Is007</i> DR	61/1(0)	33.4 \pm 0.60	P < 0.0001
<i>skn-1(zu169);Ex(gpa-4p::skn-1b::GFP)</i> AL ^a	10/1(1)	23.5 \pm 1.22	
<i>skn-1(zu169);Ex(gpa-4p::skn-1b::GFP)</i> DR ^a	10/0(1)	33.2 \pm 1.98	P = 0.0006
<i>skn-1(zu135);Ex(ges-1p::skn-1c::GFP)</i> AL	28/1(1)	24.9 \pm 0.52	
<i>skn-1(zu135);Ex(ges-1p::skn-1c::GFP)</i> DR	29/0(1)	25.4 \pm 0.81	P = 0.5829
<i>skn-1(zu135);gels10[gpa-4p::skn-1c::GFP]</i> AL	44/1(1)	27.6 \pm 0.61	
<i>skn-1(zu135);gels10[gpa-4p::skn-1c::GFP]</i> DR	51/0(1)	27.8 \pm 0.60	P = 0.7373
<i>skn-1(zu135);Ex(gpa-4p::skn-1c::GFP)</i> AL ^a	41/2(1)	22.7 \pm 0.47	
<i>skn-1(zu135);Ex(gpa-4p::skn-1c::GFP)</i> DR ^a	90/1(2)	22.3 \pm 0.64	P = 0.9584
<i>kyIs128</i> mock AL	96/1(2)	21.1 \pm 0.37	
<i>kyIs128</i> mock DR	99/2(2)	26.2 \pm 0.50	P < 0.0001
<i>kyIs128</i> ASI-ablated AL	54/0(2)	23.4 \pm 0.73	
<i>kyIs128</i> ASI-ablated DR	56/1(2)	24.4 \pm 0.65	P = 0.3485
<i>daf-16(mg50);kyIs128</i> mock AL	50/0(1)	18.0 \pm 0.52	
<i>daf-16(mg50);kyIs128</i> mock DR	53/0(1)	23.6 \pm 0.51	P < 0.0001
<i>daf-16(mg50);kyIs128</i> ASI-ablated AL	32/0(1)	18.9 \pm 0.60	
<i>daf-16(mg50);kyIs128</i> ASI-ablated DR	33/0(1)	19.6 \pm 0.74	P = 0.4342

N2 + DMSO AL	156/7(3)	26.6 ± 0.35	
N2 + DMSO DR	143/19(3)	32.2 ± 0.43	P < 0.0001
N2 + DMSO/30 μM myxothiazol AL	41/0(1)	26.6 ± 0.57	
N2 + DMSO/30 μM myxothiazol DR	44/2(1)	28.6 ± 0.40	P = 0.0063
N2 + DMSO/60 μM myxothiazol AL	44/2(1)	26.2 ± 0.58	
N2 + DMSO/60 μM myxothiazol DR	51/0(1)	25.7 ± 0.60	P = 0.6307
N2 + EtOH AL	101/5(2)	25.6 ± 0.37	
N2 + EtOH DR	63/27(2)	32.1 ± 0.66	P < 0.0001
N2 + EtOH/1 μM antimycin AL	98/5(2)	25.1 ± 0.35	
N2 + EtOH/1 μM antimycin DR	101/2(2)	23.1 ± 0.52	P = 0.0499
N2 plate + EtOH	44/3(1)	24.0 ± 0.49	
N2 plate + EtOH/1 μM antimycin	42/6(1)	25.6 ± 0.59	P = 0.0177 ^b
<i>daf-2(e1370)</i> plate + EtOH	48/2(1)	42.7 ± 0.87	
<i>daf-2(e1370)</i> plate + EtOH/1 μM antimycin	48/2(1)	42.8 ± 0.92	P = 0.8973 ^b
<i>che-3(e1124)</i> AL	57/48(2)	31.6 ± 0.71	
<i>che-3(e1124)</i> DR	48/4(1)	38.5 ± 0.74	P < 0.0001
<i>osm-5(p813)</i> AL	68/38(2)	34.3 ± 0.81	
<i>osm-5(p813)</i> DR	47/6(1)	41.1 ± 0.98	P < 0.0001
<i>Is007</i> AL ^a	47/0(1)	25.5 ± 0.72	
<i>Is007</i> DR ^a	54/5(1)	32.8 ± 0.37	P < 0.0001

Shaded bars indicate the conditions used for all subsequent *ad lib* and calorie-restricted lifespans.

^aLifespan curve is not shown in figures.

^bThis P-value is vs. the non-antimycin control that immediately precedes it.

Supplementary Table S2. Lifespan data for supplementary figures.

Strain and condition	# deaths/# censored(# trials)	mean ± s.e.m	p-value vs. AL control
N2 AL	832/50(17)	25.7 ± 0.14	
N2 DR	792/60(16)	32.8 ± 0.18	P < 0.0001
<i>skn-1(zu67)</i> AL	92/11(2)	22.0 ± 0.38	
<i>skn-1(zu67)</i> DR	102/0(2)	24.1 ± 0.53	P = 0.0005
<i>skn-1(zu129)</i> AL	51/1(1)	22.2 ± 0.43	
<i>skn-1(zu129)</i> DR	38/14(1)	23.1 ± 0.74	P = 0.0243
N2 ^a	46/4(1)	22.5 ± 0.65	
<i>skn-1(zu135)</i> ^a	45/5(1)	21.8 ± 0.76	
<i>daf-2(e1370)</i> ^a	48/2(1)	39.8 ± 1.33	
<i>skn-1(zu135);daf-2(e1370)</i> ^a	45/2(1)	45.2 ± 1.17	
<i>kyIs128</i> unmounted AL	51/2(1)	21.6 ± 0.50	
<i>kyIs128</i> unmounted DR	53/0(1)	26.7 ± 0.63	P < 0.0001
<i>kyIs128</i> mounted AL	96/1(2)	21.1 ± 0.37	
<i>kyIs128</i> mounted DR	99/2(2)	26.2 ± 0.50	P < 0.0001

^aThis lifespan was performed on standard NGM + OP50 plates containing FuDR.

Figure 1. Lifespan extension by DR.

Lifespan curves represent combined data from independent experiments as indicated in Supplementary Table S1. Complete lifespan data are presented in Supplementary Table S1.

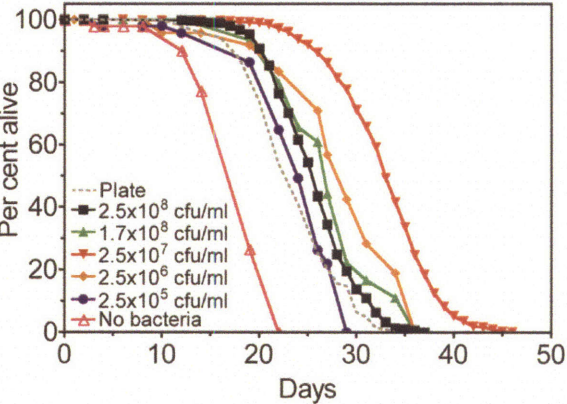
(a) Survival curves of wild-type N2 animals fed various concentrations of bacteria in liquid medium, or on agar plates of otherwise identical composition seeded with a bacterial lawn.

(b) Local maximum in N2 mean lifespan at optimal level of bacteria dilution. In contrast, the lifespan of *skn-1(zu135)* is not altered by food level.

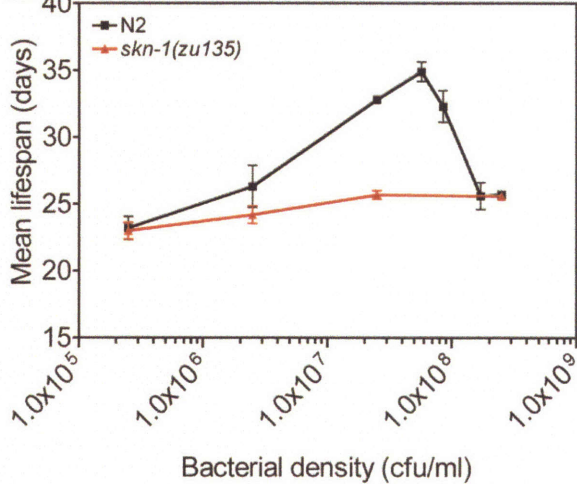
(c) The DR protocol extends lifespan of the insulin pathway mutants *daf-16(mgDf50)* and *daf-2(e1370)*. AL bacterial concentration = 2.5×10^8 cfu/ml; DR = 2.5×10^7 cfu/ml.

FIGURE 1

a



b



c

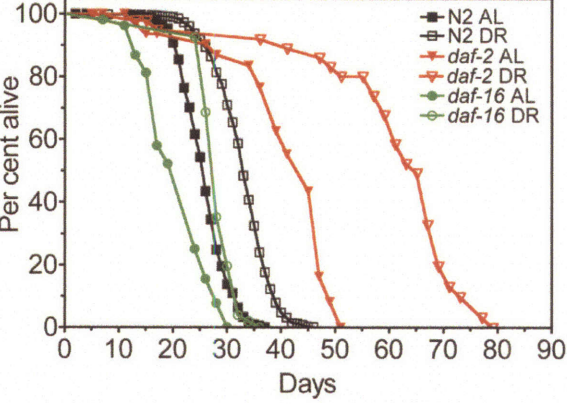


Figure 2. *skn-1* functions in the ASI neurons to mediate DR longevity.

- (a) The *skn-1* gene encodes three protein isoforms, with different N-termini but a common C-terminus. Predicted transcripts (Wormbase) and their genomic organization are depicted, with exons shown in blue and UTRs in gray. Striped boxes indicate an operonic transcript including the upstream gene, the beclin-1 homolog *bec-1*, and downstream *skn-1a*. The extent of the *Is007[skn-1::gfp]* integrated transgene¹⁰ and the insertion site of GFP in the transgene are also indicated. The purple and red dotted lines indicate the DNA segments used in the *skn-1(RNAi)* and *skn-1b(RNAi)* constructs, respectively (see text); the *skn-1c(RNAi)* construct was made using a fusion of the exons indicated by the green dotted line. The sites of the *zu169* and *zu135* nonsense mutations are shown. DBD = DNA binding domain. See Supplementary Fig. S2a for more detail.
- (b) Two strains carrying *skn-1* mutations, *zu135* and *zu169*, have normal basal lifespans, but fail to respond to DR.
- (c) Both *skn-1* mutants are rescued by the integrated transgene *Is007*, which drives *skn-1::gfp* from its native promoter and expresses *skn-1::gfp* in the ASI neurons and the gut.
- (d-f) The *skn-1b* isoform is expressed primarily in the ASI neuron, and *skn-1c* is expressed primarily in the intestine. RNAi constructs specific to the unique 5' end of either *skn-1b* or *skn-1c* (see panel a) were used to examine *skn-1* isoform expression. Note that the *skn-1c* RNAi construct will also knock down endogenous *skn-1a* due to sequence identity in this region. The *skn-1(RNAi)* clone targets the 3' region common to all *skn-1* isoforms (see panel a).

(d) *Is007* expresses SKN-1B::GFP, but not SKN-1C::GFP, in the ASI. The indicated RNAi constructs were fed to *lin-35(n745);Is007[skn-1::gfp]* animals. *skn-1b(RNAi)*, but not *skn-1c(RNAi)*, reduced GFP expression in the ASI. Data shown is from two independent experiments; errors are s.e.m. Total *n* of animals observed in trial 1, trial 2: vector: 24, 29; *skn-1(RNAi)*: 20, 24; *GFP(RNAi)*: 22, 26; *skn-1b(RNAi)*: 36, 24; *skn-1c(RNAi)*: 23,20.

(e) *Is007* expresses SKN-1C::GFP, but not SKN-1B::GFP, in the intestine. Following RNAi exposure, *Is007* worms were heat-shocked to induce nuclear accumulation of SKN-1::GFP in the intestine. *skn-1c(RNAi)* reduced SKN-1::GFP, while *skn-1b(RNAi)* had no effect. Data shown is from two independent experiments; errors are s.e.m. Total *n* of animals examined in trial 1, trial 2: vector: 24, 25; *skn-1(RNAi)*: 25, 23; *skn-1b(RNAi)*: 28, 24; *skn-1c(RNAi)*: 28, 21.

(f) *skn-1a* and/or *skn-1c* account for the majority of basal *skn-1* transcriptional activity in the intestine. The gene *dod-24* has several *skn-1* consensus binding sites in its promoter region and is expressed in a *skn-1*-dependent manner (data not shown). An integrated *dod-24p::gfp* transgenic strain (a gift of D. Kim and F. Ausubel) was therefore used as a reporter for intestinal *skn-1* activity. *skn-1c(RNAi)* reduced reporter expression, while *skn-1b(RNAi)* did not. Scale bars, 100 μ m.

(g) An extrachromosomal array that drives *skn-1b::gfp* expression from the *gpa-4* promoter exclusively in the ASI neurons of adult animals rescues the *skn-1(zu135)* DR longevity defect. Two independently transformed lines, labeled “#1” and “#2”, are shown. (h) An extrachromosomal array driving *skn-1c::gfp* expression from the *ges-1*

promoter exclusively in the gut does not rescue *skn-1(zu135)* DR longevity. *gels10*, an integrated version of the same array, also fails to rescue.

FIGURE 2

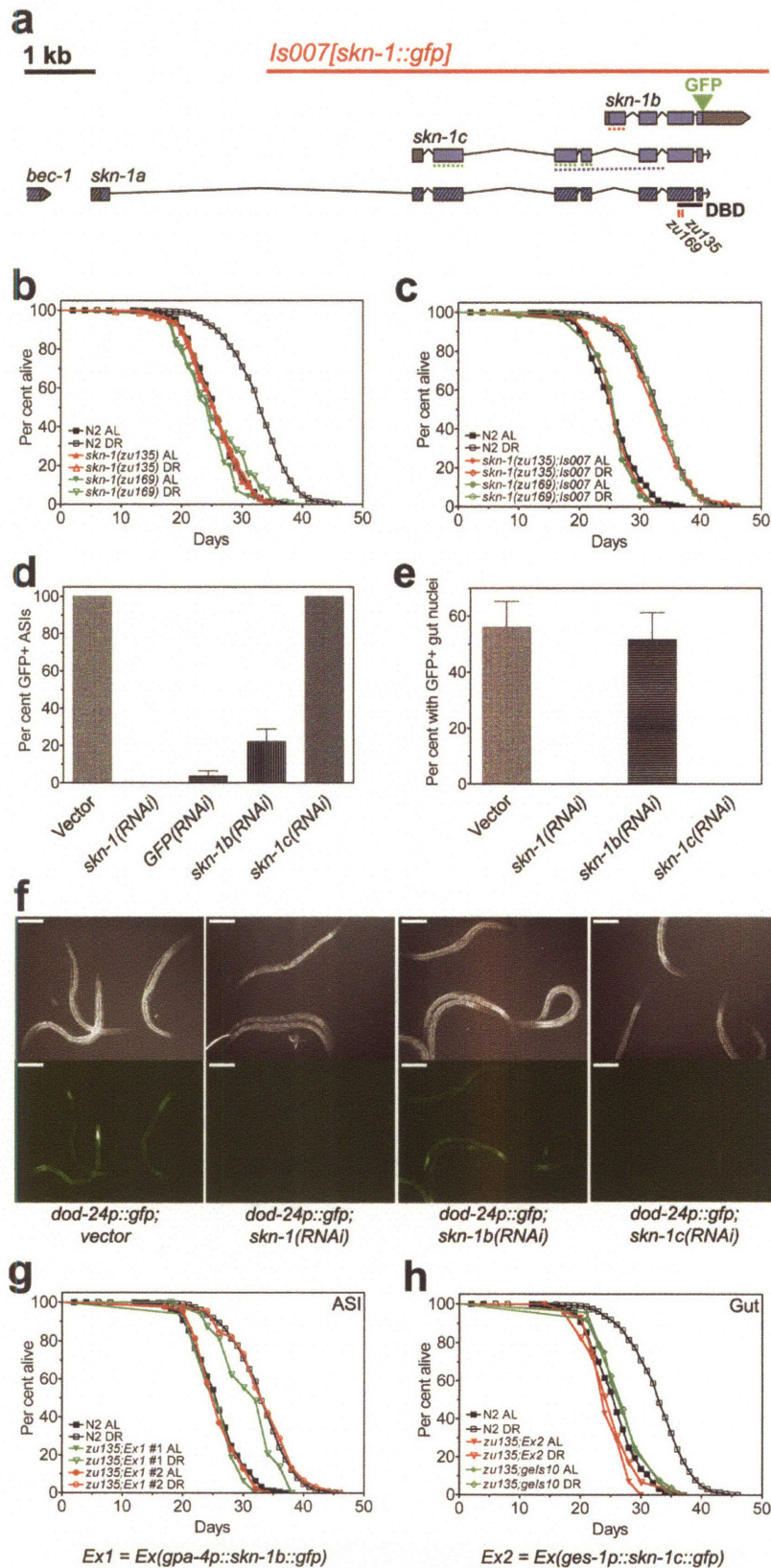


Figure 3. The ASI neurons are necessary for DR longevity.

ASIs were laser-ablated in strains carrying the integrated array *kyIs128*, which expresses GFP from the ASI-specific *str-3* promoter²⁶. “Mock” strains represent non-operated controls (see Methods).

(a) Animals with killed ASIs do not respond to DR. These animals have a longer basal lifespan, as previously reported¹⁷ (for *kyIs128* ASI⁻ AL vs. *kyIs128* mock AL, Mantel-Cox logrank $P < 0.0001$).

(b) *daf-16* mutation suppresses the longer basal lifespan caused by ASI ablation (for *daf-16(mgDf50);kyIs128* ASI⁻ AL vs. *daf-16(mgDf50);kyIs128* mock AL, $P = 0.3902$), but ASI-ablated animals remain refractory to DR.

FIGURE 3

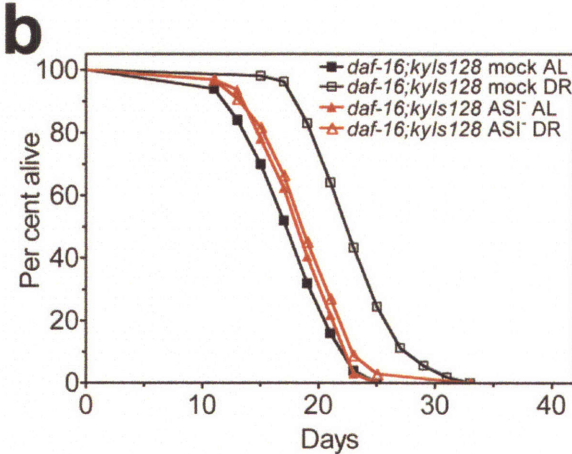
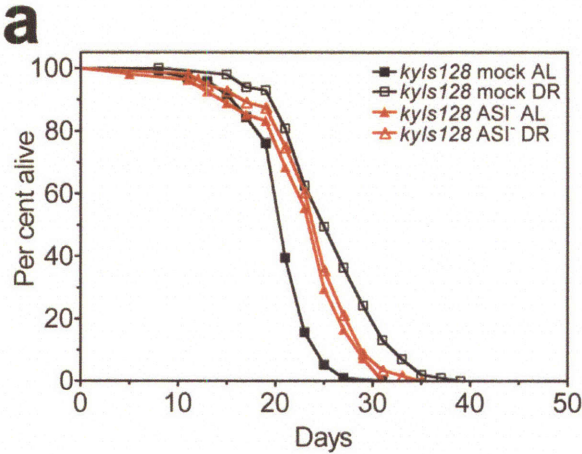


Figure 4. DR activates *skn-1* in the ASI neurons and increases whole-body respiration.

(a) 5 days of DR increases *skn-1::gfp* expression in the ASI neurons of *Is007*. Left, bright field and fluorescence Nomarski images. Scale bars, 10 μ m. Right, quantification of fluorescence in *Is007* and in *geIs8*, a specificity control strain that drives *skn-1::gfp* expression from the ASI-specific *gpa-4* promoter. Each value represents pooled data from two independent trials; errors are s.e.m. *n* for trial 1, trial 2: *Is007* AL: *n* = 42, 42. *Is007* DR: *n* = 58, 21 (unpaired two-tailed t-test $P < 0.0001$). *geIs8* AL: *n* = 19, 31; *geIs8* DR: *n* = 19, 39 ($P < 0.0001$).

(b) Respiration rate is increased in N2 animals assayed on day 3 of DR. The *skn-1(zu135)* mutation prevents the respiration increase on DR. Integrated transgenes driving *skn-1::gfp* expression, either from the native promoter (*Is007*), or from the ASI-specific *gpa-4* promoter (*geIs9*), rescue the DR respiration defect of *skn-1(zu135)*, elevating respiration rates above the wildtype level. The integrated transgene *geIs10*, which drives *skn-1::gfp* expression in the gut using the *ges-1* promoter, fails to rescue the respiration defect of *skn-1(zu135)* on DR. Unpaired two tailed t-test p-values, AL vs. DR for each strain: N2: $P = 0.0221$; *skn-1(zu135);Is007*: $P = 0.0011$; *skn-1(zu135);geIs9*: $P = 0.0005$. No other values differ significantly from N2 AL. N2 data represents pooled triplicate measurements from each of four independent experiments. Other strains were measured in triplicate in two experiments each; errors are s.e.m.

(c – d) Electron transport chain inhibiting drugs prevent the DR longevity response without shortening AL lifespan. The ETC complex III inhibitor myxothiazol partially

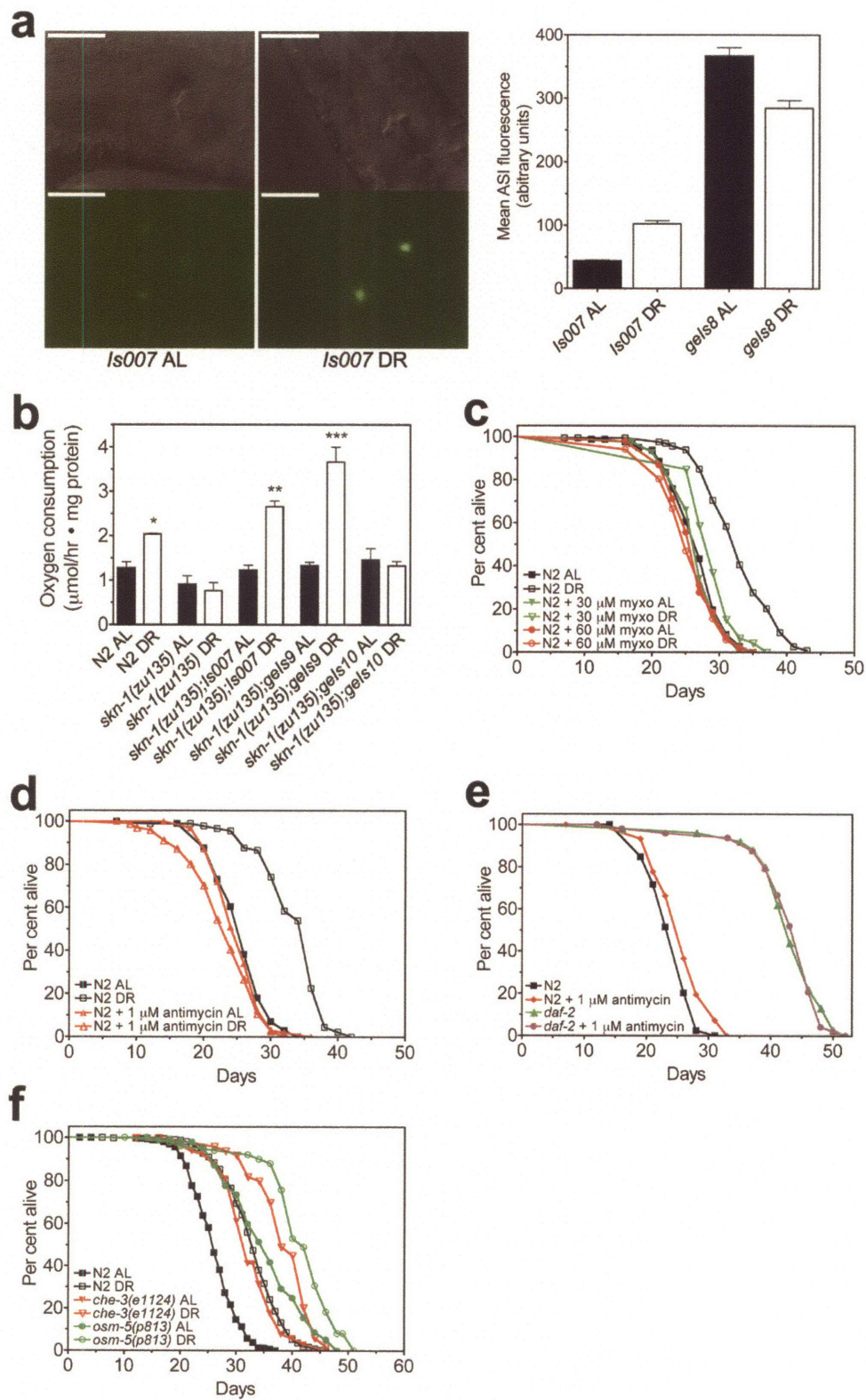
blocks DR longevity at 30 μ M, and completely blocks DR longevity at 60 μ M (c).

Another complex III inhibitor, antimycin, also blocks DR longevity (d).

(e) Antimycin does not affect the longevity induced by *daf-2(e1370)* mutation. This assay was performed on agar plates with otherwise identical composition to the liquid medium used for DR experiments.

(f) The DR longevity response does not require environmental chemosensation. *che-3(e1124)* and *osm-5(p813)* mutants lack functional sensory neuron cilia and are long-lived under AL conditions³⁰, but DR still increases lifespan in these mutants by a similar percentage as it does in N2.

FIGURE 4



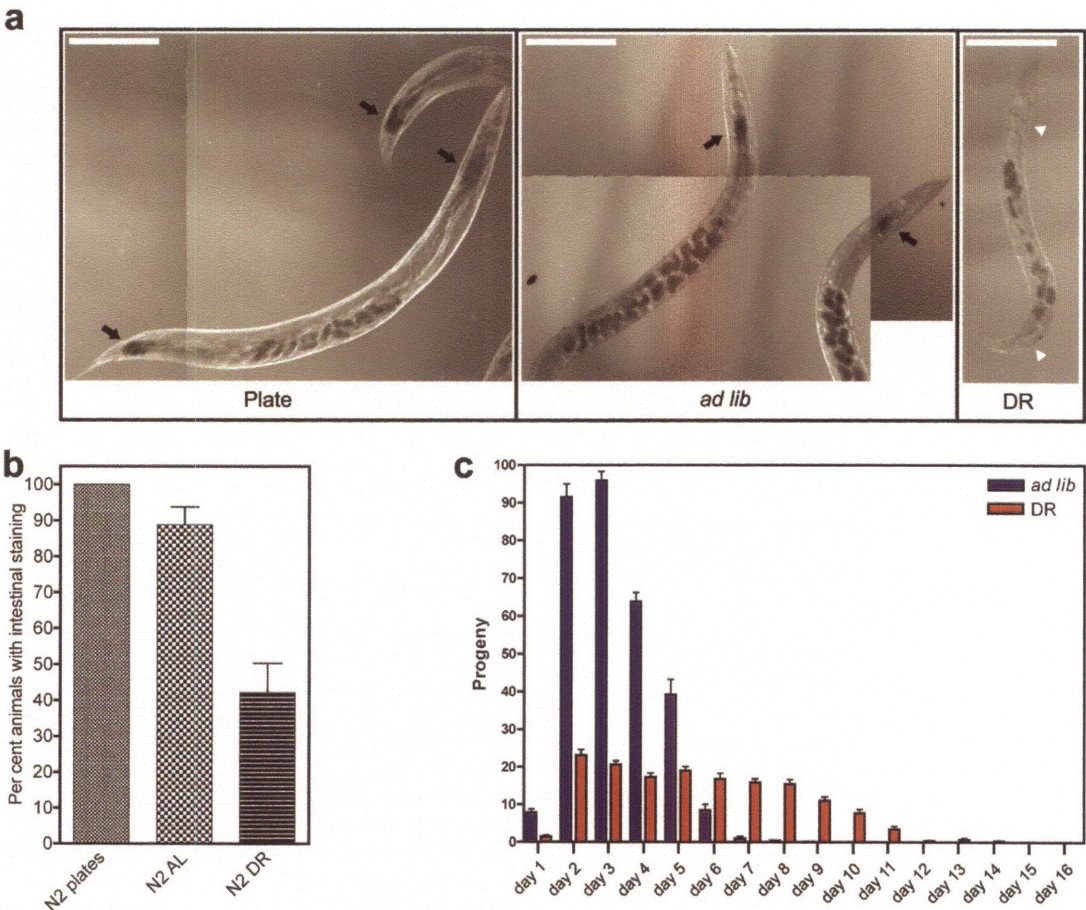
Supplementary Figure S1. Fat storage and progeny production are reduced in DR animals.

(a) Representative day 3 adult animals cultured on plates, in AL liquid medium, or DR liquid medium, with fat stained by Sudan Black³¹. Staining is observed in the anterior and posterior gut of plate-cultured and AL-cultured animals (black arrows), but is reduced or invisible in DR animals (white arrowheads). Staining is also visible in intrauterine eggs in all conditions. Also note the small size of the DR animals. Scale bars, 100 μm .

(b) Quantification of individuals with any visible intestinal fat staining on day 3 of plate feeding, AL feeding, or DR feeding. Fat staining is significantly reduced in DR vs. AL animals (unpaired two-tailed t-test, $p < 0.0001$). Similar results were obtained at later timepoints (data not shown). Each value on the graph represents two independent experiments; errors are s.e.m. Total n of animals examined in trial 1, trial 2: N2 plate: $n = 24, 35$; N2 AL: $n = 23, 31$; N2 DR: $n = 27, 32$.

(c) Progeny production is optimal in AL animals, while DR animals have reduced overall progeny production and extended reproductive period. Errors on graph are s.e.m. Total progeny \pm SD, total n animals examined: AL: $308 \pm 26, 21$; DR: $152 \pm 34, 20$.

SUPPLEMENTARY FIGURE S1



Supplementary Figure S2. 5' RACE indicates that the *skn-1b* mRNA is derived from a different promoter than those of *skn-1a* and *skn-1c*.

(a) The *skn-1* genomic locus encodes three protein isoforms, SKN-1A, SKN-1B, and SKN-1C, which have different N-termini but identical C-termini. Predicted transcripts (Wormbase) are depicted, with exons shown in blue and UTRs in gray. (Pink exons indicate predicted gene T19E7.1, which is transcribed from the opposite strand.) Striped boxes indicate an operonic transcript including the upstream gene, the beclin-1 homolog *bec-1*, and downstream *skn-1a*. The identities of the mutants described in this report are indicated; amino acid positions are relative to the first amino acid in SKN-1C. The extent of the *Is007* transgene and the insertion site of GFP in the transgene are also indicated. DBD = DNA binding domain. P1 – P4 indicate the positions of primers used for 5' RACE and RT-PCR (see panels b – c). *C. elegans* mRNAs are often trans-spliced at their 5' ends to short RNA leaders encoded elsewhere in the genome, termed SL1 and SL2³². PSL1 and PSL2 are primers identical to the SL1 and SL2 leader sequences, which will anneal to the 5' ends of SL1 and SL2 trans-spliced cDNAs. PSL1 and PSL2 are positioned on the diagram at the sites of predicted SL1 and SL2 trans-splice acceptor sequences in the *skn-1a* and *skn-1c* transcripts (Wormbase).

(b – c) RT-PCR confirms that *skn-1a* and *skn-1c* mRNAs are trans-spliced, but provides no evidence that *skn-1b* mRNA is trans-spliced. This difference in the 5' ends of the three *skn-1* isoforms' transcripts suggests that the *skn-1b* transcript is derived from a separate promoter than those of *skn-1a* and *skn-1c*, rather than resulting from alternative splicing

of *skn-1a* and/or *skn-1c* transcripts. Ladder sizes in bp are indicated to the left of each gel. Low molecular weight smears in each lane are unincorporated nucleotides.

(b) RT-PCR confirms predicted SL1 and SL2 trans-splicing in *skn-1a* and *skn-1c* mRNA.

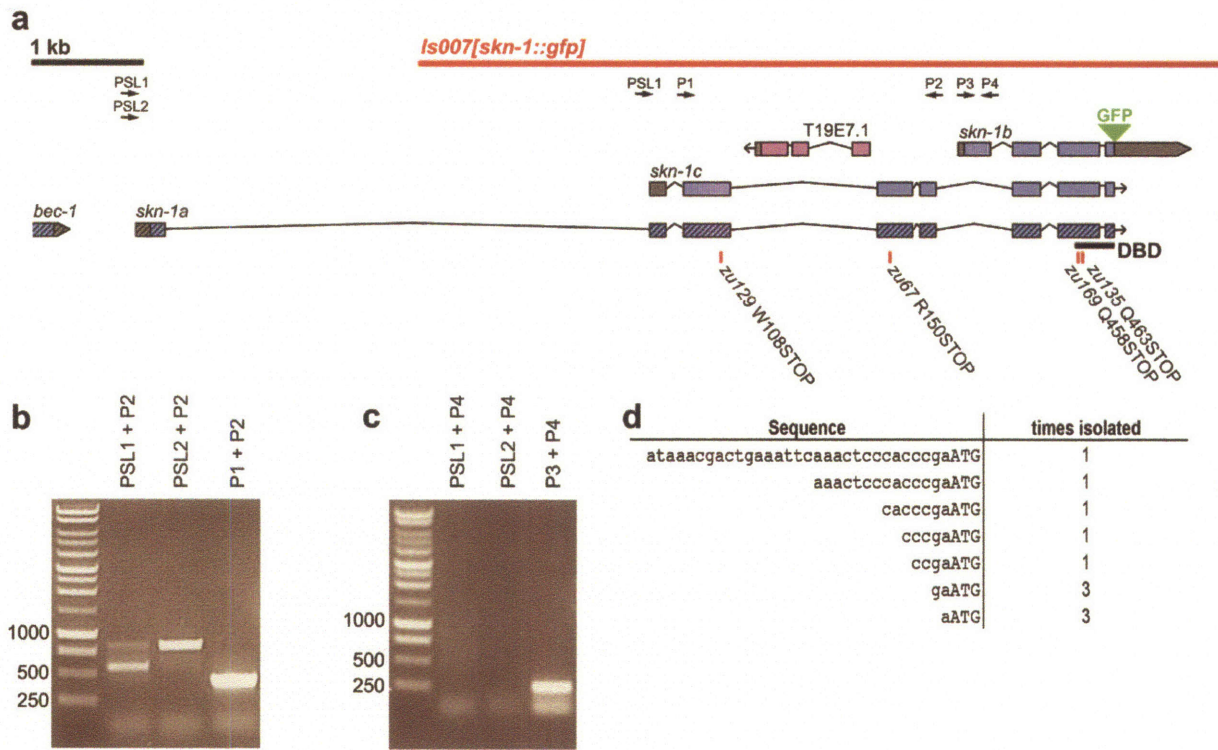
Primer PSL1, which anneals to the trans-spliced *skn-1a* and *skn-1c* cDNAs, and primer P2, which spans the *skn-1c* exon 3-exon 4 junction, produce two products of the expected 0.6 kb and 0.9 kb sizes. Primer PSL2, which anneals to the trans-spliced *skn-1a* cDNA, and primer P2 produce a product of the expected 0.9 kb size. A positive control amplification with primer P1, which is at the 5' end of *skn-1c* exon 1, and primer P2 produces a band of the expected 0.3 kb size, confirming that *skn-1c* and/or *skn-1a* cDNA was present in the template.

(c) RT-PCR does not indicate any trans-splicing of the *skn-1b* transcript. Primer PSL1, which is not predicted to anneal to *skn-1b* cDNA since *skn-1b* cDNA is not predicted to be trans-spliced, and primer P4, which spans the *skn-1b* exon 1-exon 2 junction, produce no product. Primer PSL2, which is not predicted to anneal to *skn-1b* cDNA, and primer P4 produce no product. A positive control amplification with primer P3, which is at the 5' end of *skn-1b* exon 1, and primer P4 produces a band of the expected 0.2 kb size, confirming that *skn-1b* cDNA was present in the template.

(d) 5' RACE using a primer specific for *skn-1b* also indicates no trans-splicing. The 5' cDNA ends cloned in the RACE reaction are listed, with the translational start codon in capital letters. Each clone carried between 1 and 31 bp of genomic sequence immediately upstream of the translational start. Heterogeneous transcriptional initiation within a 30 – 50 bp range is typically observed in *C. elegans* genes (cf. ref 33), suggesting that some or all of these products represent bona fide full-length transcripts. The results of the 5'

RACE suggest that *skn-1b* is transcribed from a promoter that lies almost immediately upstream of the translational start site, rather than being derived from one of the other *skn-1* transcripts by alternate splicing.

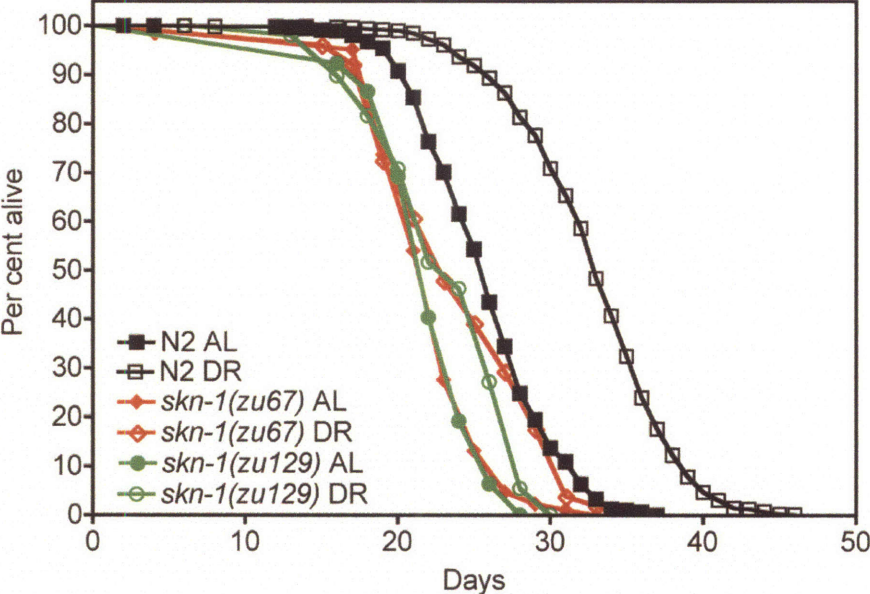
SUPPLEMENTARY FIGURE S2



Supplementary Figure S3. Two additional alleles of *skn-1* impair the DR longevity response.

N2 mean lifespan is extended by 27.6%, while *skn-1(zu67)* and *skn-1(zu129)* are extended only 9.5% and 4.1%, respectively. Complete lifespan data are presented in Supplementary Table S2.

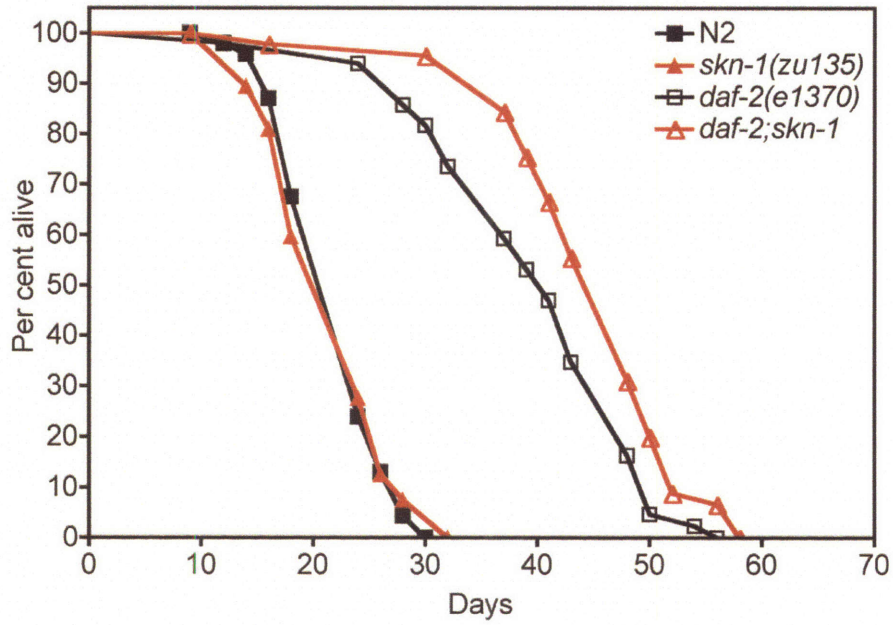
SUPPLEMENTARY FIGURE S3



Supplementary Figure S4. *skn-1(zu135)* does not suppress the long lifespan of *daf-2(e1370)*.

This assay was performed on standard NGM + OP50 plates containing FuDR. Complete lifespan data are presented in Supplementary Table S2.

SUPPLEMENTARY FIGURE S4



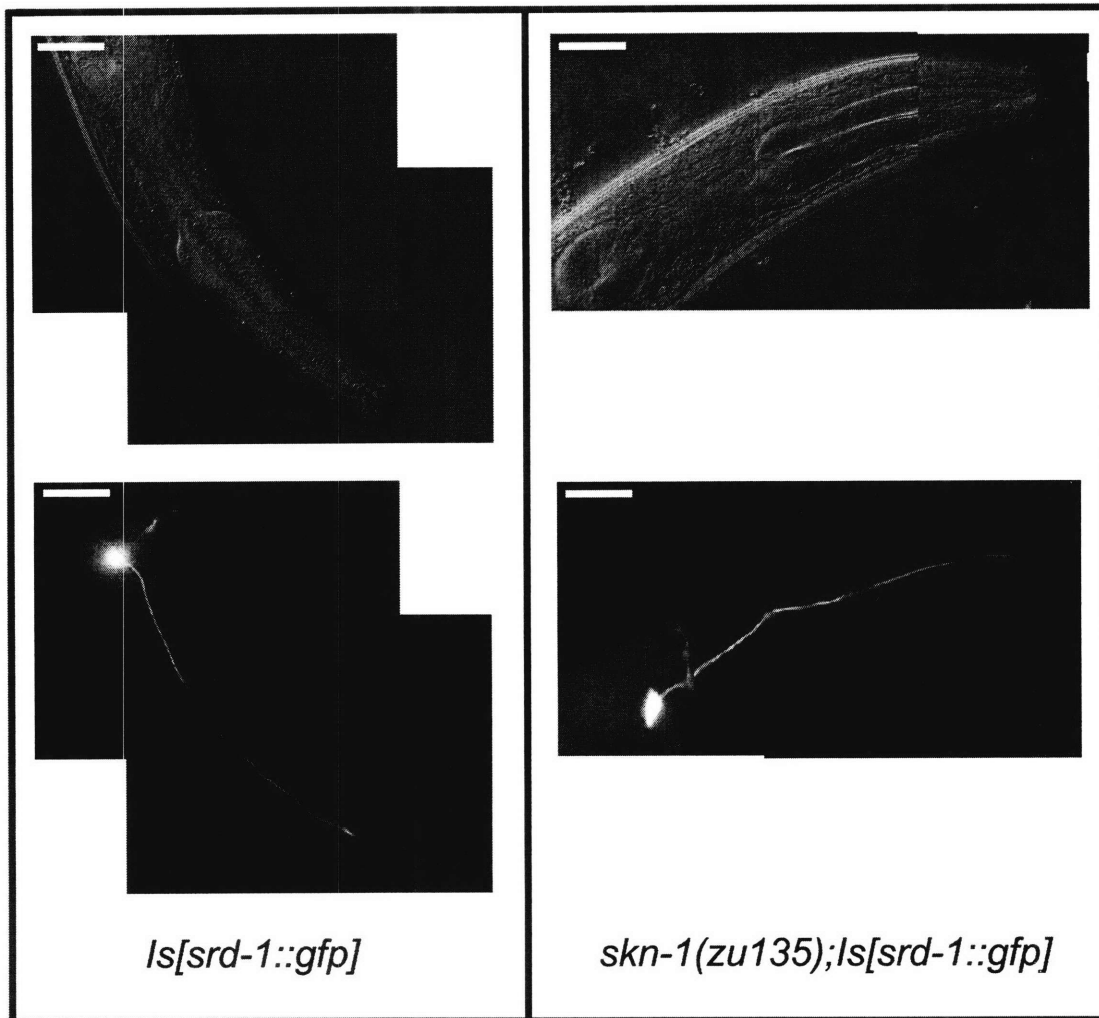
Supplementary Figure S5. The gross morphology and cell fate of the ASI neurons are not disrupted by *skn-1(zu135)*.

(a) Gross morphology of the ASI neurons is normal in *skn-1(zu135)* mutants. Nomarski bright field (top) and fluorescence images; the ASI is highlighted by expression of an integrated *srd-1p::gfp* transgene. Axon (black arrowheads), cell body, and dendrite all appear normal. Scale bars, 10 μ m.

(b) ASI cell fate is not altered by *skn-1(zu135)*. Expression of integrated GFP reporter constructs that serve as markers of ASI cell fate was examined in AL and DR conditions. Four of the five reporters were expressed normally in a *skn-1(zu135)* background, indicating that ASI cell identity is broadly preserved. The expression level of these four reporters was not altered by DR (data not shown). One ASI reporter construct, *sra-6p::gfp*, was dependent on *skn-1* for expression, and showed a modest increase in expression level on DR (N.B. and L.G., unpublished results). *Ex(gcs-1::gfp)* has previously been reported to be dependent on *skn-1* for expression in the ASI neurons¹⁰. We confirmed that *skn-1(zu135);Ex(gcs-1::gfp)* does not express GFP in the ASI neurons under AL conditions, but we did observe *skn-1*-independent expression under DR conditions. The expression level of *Ex(gcs-1::gfp)* was not significantly altered by DR (data not shown).

SUPPLEMENTARY FIGURE S5

a



b

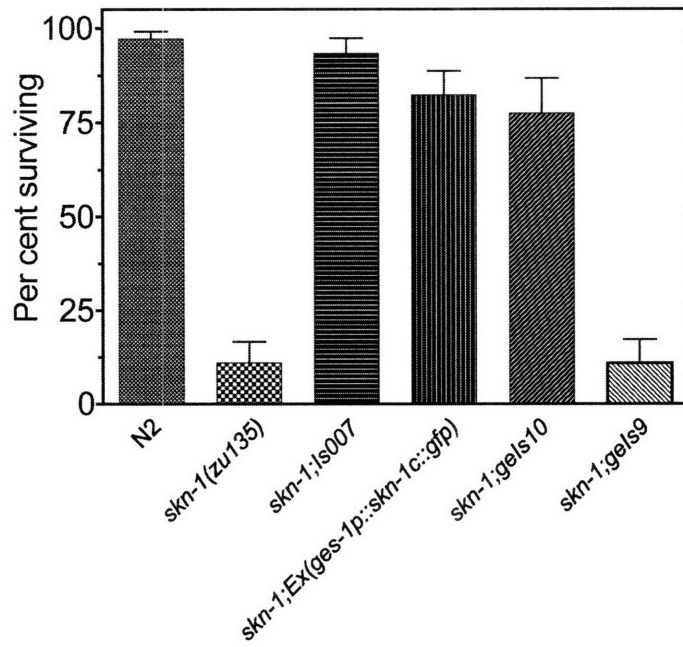
GFP reporter	Expression pattern	ASI expression	
		WT	<i>skn-1(zu135)</i>
<i>str-2::gfp</i>	ASI(faint), AWC	+	+
<i>str-3::gfp</i>	ASI	+	+
<i>srd-1::gfp</i>	ASI	+	+
<i>daf-7::gfp</i>	ASI	+	+
<i>sra-6::gfp</i>	ASI(faint), ASH, PVQ	+	-
<i>Ex(gcs-1::gfp)</i>	ASI, gut	+	- ^a

^a *Ex(gcs-1::gfp)* was not expressed in the ASI of *skn-1* animals under *ad lib* conditions, but was expressed independently of *skn-1* during DR.

Supplementary Figure S6. Arsenate resistance is mediated by intestinal activity of *skn-1*.

Adult animals were placed on 5 mM sodium arsenate NGM plates seeded with OP50, and survival was assayed after 48 hr. *skn-1(zu135)* exhibited marked arsenate sensitivity that could be rescued by *Is007[skn-1::gfp]*, consistently with a previous report³⁴. The intestine-specific *Ex(ges-1p::skn-1c::gfp)* transgene efficiently rescues arsenate sensitivity, as does *geIs10*, an integration of the same transgene. In contrast, a transgene expressing primarily in the ASI neuron, *geIs9[gpa-4p::skn-1b::gfp]*, does not rescue arsenate sensitivity. Each value represents pooled data from multiple independent experiments; errors are s.e.m. Number of trials, *n* for each experiment: N2: 3 trials, *n* = 18, 24, 22; *skn-1(zu135)*: 4 trials, *n* = 25, 22, 19, 16; *skn-1(zu135);Is007*: 3 trials, *n* = 23, 35, 27; *skn-1(zu135);Ex(ges-1p::skn-1c::gfp)*: 2 trials, *n* = 15, 34; *skn-1(zu135);geIs10*: 2 trials, *n* = 16, 20. *skn-1(zu135);geIs9*: 2 trials, *n* = 20, 23.

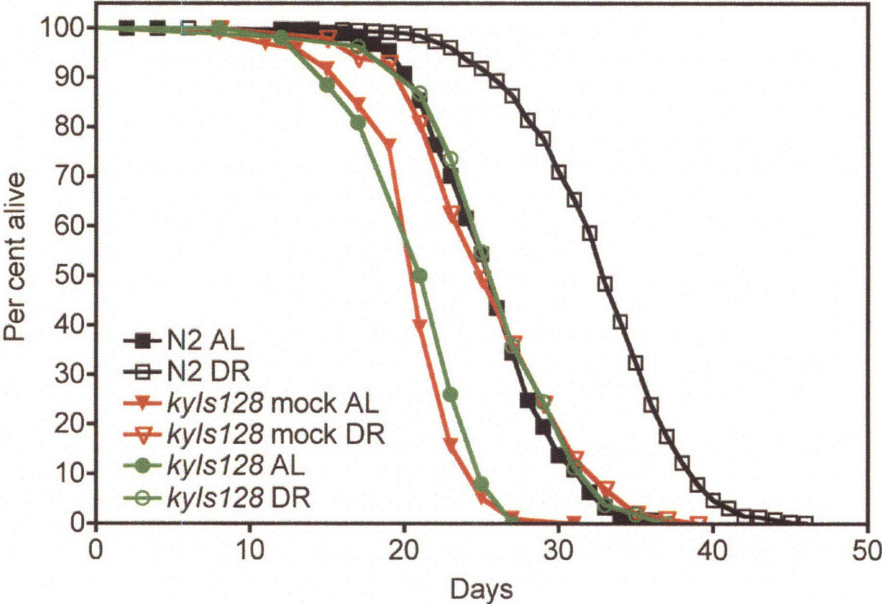
SUPPLEMENTARY FIGURE S6



Supplementary Figure S7. The short lifespan of *kyIs128/str-3p::gfp* is intrinsic to the strain, and not due to the laser-ablation mounting procedure.

“Mock” worms were mounted in sodium azide; other strains were not. Even without mounting, the *kyIs128* strain lives shorter than N2. Mounting had no effect on the lifespan. Complete lifespan data are presented in Supplementary Table S2.

SUPPLEMENTARY FIGURE S7



CHAPTER 3

A Conserved MAPK Pathway Mediates Dietary Restriction-Induced Longevity in *C. elegans*

This chapter will be submitted for publication. The authors will be Nicholas A. Bishop and Leonard Guarente.

Summary Paragraph

Dietary restriction (DR) extends the lifespan of many organisms and reduces incidence and progression of age-related disease in mammals¹. Until recently, almost nothing was known of the genetic pathways underlying DR-induced longevity in metazoans. We previously reported that the transcription factor *skn-1* acts specifically in two *C. elegans* head neurons, called the ASIs, to mediate DR-induced longevity by signaling to peripheral body tissues (Chapter 2). Here, we identify *sek-1*, a conserved stress-responsive MAPKK homologous to mammalian MEK3/6²⁻⁸, as essential for DR-induced longevity and several other physiological responses to DR. We show that *sek-1* acts in the ASI neurons to maintain *skn-1* expression and mediate the DR longevity response. During DR, *sek-1* functions downstream of the MAPKKK *nsy-1*, a homolog of the mammalian MAPKKK ASK1^{9,10}. Thus, we have established a three-member genetic pathway that mediates DR longevity by acting in the ASI neurons. These results provide new genetic insight into the DR response in metazoans, and suggest that activation of a stress-sensitive MAPK pathway in the brain is a crucial initial event in DR-induced longevity.

Results

We developed a method of imposing DR in *C. elegans* in which worms are cultured in a small volume of liquid medium with controlled bacterial density (see Methods). In wild-type worms, lifespan increases as bacterial concentration is reduced

until a maximum is reached at an optimal food level, but further food reduction causes reduced longevity due to starvation (Figure 1A, Table S1). The genetic mechanisms underlying the DR-induced increase in lifespan are poorly understood.

DR Increases Lifespan by a Different Mechanism Than Known Longevity Mutants

Many mutations have been identified in *C. elegans* that alter longevity by modulating several parallel genetic pathways¹¹, but very little is known about the genetic mechanism by which DR increases lifespan. We therefore tested a panel of mutants affecting known lifespan control pathways for a role in DR longevity by exposing each mutant to the optimal level of DR and evaluating epistasis (Table 1; also see reference 12). As we previously reported (Chapter 2), DR extends the lifespan of mutations affecting the insulin signaling pathway¹¹ or sensory perception¹³ at least as effectively as the wild type. Sterile *mes-1(bn7)* animals, which are long-lived due to absence of the germline^{14,15}, showed a lifespan increase under DR, as did two mutants that disrupt the germlineless longevity pathway, *daf-9(rh50)* and *daf-12(m20)*^{15,16}. Importantly, observation of DR-induced longevity in animals lacking the germline argues that the longevity effect of DR is separable from the concomitant reduction in fecundity observed in any species undergoing DR¹⁷. Sir2 regulates lifespan in several species and is required for dietary restriction to increase longevity in yeast and flies^{18,19}. A deletion mutant, *sir-2.1(ok434)*²⁰, did not prevent a normal DR-induced lifespan extension. In summary, all the longevity mutants tested, including representatives of the insulin signaling, sensory perception, germline, and sirtuin longevity pathways, responded robustly to DR,

suggesting that DR increases lifespan by a genetic pathway largely distinct from these. A caveat of this conclusion is that the *daf-2*, *daf-9*, and *daf-12* alleles tested were partial loss of function mutations, rather than null alleles, so it remains formally possible that any of these could play some role in DR longevity.

Mutants Disrupting the sek-1 MAPKK Pathway Cause Defects in Multiple Physiological Responses to DR

We previously reported that, in contrast to the wild type, the lifespan of worms carrying mutations in the transcription factor *skn-1* was not altered by food concentration, indicating that *skn-1* is required for the DR longevity response (Chapter 2). Because the MAPKK *sek-1* has been shown to regulate *skn-1*, at least in the intestine⁶, we tested whether *sek-1* might also function in DR longevity. The lifespan of *sek-1(km4)* animals was not altered by diet (Figure 1A, Table S1), consistent with a requirement for *sek-1* in the DR longevity response. An additional allele, *sek-1(ag1)*, also exhibited a dramatic reduction in lifespan increase under DR (Figure 1B, Table S1). *sek-1(km4)* is a large deletion and a presumed null allele, while *sek-1(ag1)* is a missense mutation in a single amino acid (Figure 2A), likely accounting for the more modest mutant phenotype of *sek-1(ag1)*. Although worms carrying either allele of *sek-1* exhibited a slightly shorter basal lifespan than the wild type at the AL food level (Figure 1B), this defect of *sek-1* mutants is separable from the failure to increase lifespan on DR (see below). Because *sek-1(km4)* is a probable null allele and has the stronger effect on DR, we focused our subsequent analyses on this allele. The possibility that *sek-1* mutation might simply impose an

absolute limit on lifespan was ruled out by the observation that the *daf-2(e1370)* mutation could extend the lifespan of a *sek-1* mutant (Figure S1), consistent with a previous report²¹. The longevity defects of *sek-1* animals, in both response to DR and basal lifespan, were rescued by an extrachromosomal array carrying a 10 kb genomic fragment including the wild-type *sek-1* gene (Figures 1C and 2A, Table S1), confirming that the mutation in *sek-1* was responsible for the observed phenotype.

The MAPKKK NSY-1 phosphorylates SEK-1 as part of a signaling module, and *nsy-1* mutants phenocopy *sek-1* mutants in most respects^{3, 5}. We therefore tested the longevity of *nsy-1(ky397)* mutants under DR, and found that, like *sek-1* mutants, *nsy-1* animals failed to increase lifespan in response to DR and had a slightly short basal lifespan (Figure 1D, Table S1), suggesting that *nsy-1* acts upstream of *sek-1* in the DR response. The CamKII *unc-43* acts immediately upstream of *nsy-1* during the development of the AWC neurons¹⁰, but the *unc-43(n1186)* mutant exhibited a normal lifespan increase during DR (Table S1), so the genes acting upstream of *nsy-1* during DR remain to be identified.

We next tested whether other physiological responses to DR, in addition to lifespan modulation, were affected by *sek-1* mutation. Multiple organisms, including yeast, worms, and mammals, increase respiratory rate during DR²²⁻²⁵, and there is evidence that this respiration increase is necessary for DR to increase longevity in yeast²² and worms (Chapter 2). Wild-type worms increased respiration during DR, but *sek-1* mutants, in contrast, had decreased respiratory rate under AL conditions that was not increased by DR (Figure 1E). Both the low basal respiration and the defect in DR-induced respiration were rescued by the extrachromosomal wild-type *sek-1* transgene,

confirming that the mutation in *sek-1* was responsible for the observed respiratory defects (Figure 1E).

DR leads to reduced body fat²⁶. In *C. elegans*, the intestine serves as the primary fat storage organ. We measured steady-state intestinal fat levels in AL and DR worms using the triglyceride stain Sudan Black, and found that wild-type worms exhibited fat levels during DR that were reduced by about half relative to AL worms (Figure 1F and S2). Interestingly, *sek-1* mutant worms had a fat level comparable to that observed in DR wild-type animals regardless of food concentration (Figure 1F and S2), indicating that *sek-1* is necessary for appropriate coupling of fat storage to diet.

Taken together, these findings show that mutants that disrupt *sek-1* activity cause defects in the translation of food availability into appropriate modulation of multiple physiological responses.

sek-1 Regulates skn-1 Expression in the ASI Neurons

To gain further insight into how *sek-1* acts to mediate DR longevity, we characterized the expression pattern of *gels7*, an integrated translational *sek-1::gfp* reporter (Figure 2A). The reporter expressed strongly in many, though not all, neurons, including a number of head and tail neurons and the dorsal and ventral nerve cords (Figure 2B). The reporter also expressed in the intestine, spermathecae, and distal tip cells. Importantly, *sek-1::gfp* expression was observed in the two ASI neurons in the head (Figure 2C), which play a crucial role in DR longevity (Chapter 2).

skn-1 acts specifically in the ASI neurons to mediate DR-induced lifespan extension. Given the known regulation of *skn-1* by *sek-1* in the intestine⁶, we investigated whether *skn-1* is also regulated by *sek-1* in the ASI neurons. Using *Is007*, an integrated *skn-1::gfp* reporter²⁷, we found that *sek-1* is required for maintenance of *skn-1* expression in the ASI neurons of adult animals. By the fifth day of adulthood, ASI neuronal SKN-1::GFP expression is maintained in the wild-type but almost completely lost in the *sek-1* background (Figure 2D). We confirmed that *sek-1* acts cell-autonomously to maintain SKN-1 expression in the ASI neurons by rescuing the SKN-1::GFP expression defect of *sek-1(km4);Is007* worms with an extrachromosomal transgene that drives a *sek-1::mStrawberry* red-fluorescent fusion²⁸ from the ASI-specific *gpa-4* promoter²⁹ (Figure 2D and S3).

Regulation of *skn-1* by *sek-1* in the ASIs was dependent on the native *skn-1* promoter, because *gels8*, an integrated transgene driving *skn-1::gfp* expression from the *gpa-4* promoter (Chapter 2), was not affected by *sek-1* mutation (Figure 2E). This observation suggests that *sek-1* regulates *skn-1* at the transcriptional level. Transcriptional regulation of *skn-1* by *sek-1* in the ASI neurons differs from the situation in the intestine. In the intestine, SEK-1 activates SKN-1 by first phosphorylating the p38 MAPK homologue PMK-1, which then phosphorylates cytoplasmic SKN-1 protein, driving relocation of SKN-1 to the nucleus⁶. The dominant SKN-1 protein isoform expressed in the ASI neurons, by contrast, is constitutively nuclear and lacks one of the two p38 phosphorylation sites present in the dominant intestinal SKN-1 isoform⁶. This suggests that the genes connecting *sek-1* to *skn-1* in the ASIs are likely to differ from those connecting the two in the intestine. In confirmation of this prediction, *pmk-1* was not

required for normal SKN-1::GFP expression in the ASI neurons or for normal lifespan increase in response to DR (Figure 2D, Table S1). There are two other p38 MAPK homologues in *C. elegans*, *pmk-2* and *pmk-3*, which could act downstream of *sek-1* in the ASI³⁰. However, the deletion *pmk-3(ok169)* responded normally to DR (Table S1), and a strain carrying the *pmk-2(gk21)* deletion exhibited completely penetrant larval arrest, so its lifespan could not be tested. Therefore, the genes acting downstream of *sek-1* to regulate *skn-1* in the ASI remain to be identified.

sek-1 Acts Separately in the ASI Neurons and the Intestine to Influence Lifespan by Two Different Mechanisms

DR induces an increase in SKN-1::GFP expression in the ASI neurons of *Is007* worms (Chapter 2). The very low expression level of SKN-1::GFP in *sek-1;Is007* animals was not increased by DR (Figure 2F), indicating that *sek-1* acts downstream of or in parallel to DR to regulate *skn-1*. Given the known requirement of *skn-1* in the ASI neurons for DR-induced longevity, this result suggested that *sek-1* mutant worms might fail to respond to DR due to lack of *sek-1* activity specifically in the ASI neurons. We tested this hypothesis by introducing an ASI-specific *gpa-4p::sek-1::gfp* transgene into *sek-1(km4)* animals and assessing rescue of DR longevity defects. In each of two independent transgenic lines, we observed full rescue of the DR longevity response (Figure 3A). Interestingly, the short basal lifespan was not substantially rescued by this transgene. This result indicates that *sek-1* is required specifically in the ASI neurons to

mediate the DR longevity response, but also has a separate function in another tissue(s) to assure normal basal lifespan.

sek-1 has known stress-resistance functions in the intestine⁶, so we examined whether *sek-1* activity is needed in the intestine to promote normal basal longevity. Two transgenic lines in which the intestine-specific *ges-1* promoter³¹ drove *sek-1::gfp* expression revealed that intestinal *sek-1::gfp* expression is sufficient to rescue the short basal lifespan of the *sek-1(km4)* mutant (Figure 3B). Unlike the ASI-specific *sek-1::gfp* transgene, this intestinal transgene did not appreciably rescue the DR-induced longevity defect, confirming that *sek-1* influences two separate lifespan control pathways in the two tissues.

Discussion

Taken together, these results suggest a model in which *sek-1* and *nsy-1* act in two separate tissues to affect lifespan in two different ways (Figure 4). First, *sek-1* and *nsy-1* act in the intestine to assure a normal basal lifespan under all dietary conditions. Because *pmk-1* is known to mediate most effects of *sek-1* in the intestine²¹, and *pmk-1(km25)* itself has a short basal lifespan (Table S1), *pmk-1* is likely also to act in this intestinal basal lifespan pathway. Second, *sek-1* and *nsy-1* act in the ASI neurons to maintain *skn-1* expression and to mediate the DR-induced increase in lifespan in a *pmk-1*-independent manner.

sek-1 is known to be critical in resistance to multiple environmental stressors, such as heavy metals, oxidative damage, and pathogen infection, predominantly through

its action in the intestine⁴⁻⁶. The attenuation of cell-autonomous intestinal stress responses in *sek-1* animals likely accounts for their short basal lifespan. It is intriguing that, in contrast, the DR longevity response requires activity of the *sek-1* pathway primarily in two cells, promoting a cell-nonautonomous signal that extends lifespan.

We do not know the precise nature of the stimulus that activates *nsy-1* in the ASI neurons during DR. The mammalian homolog of *nsy-1*, ASK1, is primarily activated by cellular stress, mainly in the form of reactive oxygen species (ROS) and/or ER stress⁹. This suggests that DR may initially produce an increase in ROS, a more oxidizing cytoplasmic environment, and/or ER stress in the ASI neurons to promote longevity by initiating cell-nonautonomous signals via *skn-1*. Consistent with this idea, genomic transcriptional profiling of murine hypothalamic gene expression following fasting revealed that one of the ten most significantly induced transcripts encoded thioredoxin-interacting protein³², which activates ASK1 in mammalian cells by competitively binding the ASK1-inhibitory protein, thioredoxin^{9,33}. Interestingly, neuronal expression of the worm thioredoxin homologue, *trx-1*, is limited to the ASI and ASJ neuronal pairs³⁴.

The MAPK that acts downstream of *sek-1* to regulate *skn-1* in the ASI neurons remains elusive. However, the closest mammalian homologues of *sek-1*, MEK3 and MEK6, exclusively activate the p38 MAPKs², and *sek-1* is, similarly, an essential upstream activator of the p38 MAPK homologue *pmk-1*⁴. It is therefore reasonable to assume that *sek-1* acts on a p38 MAPK(s) to mediate DR longevity. The worm genome contains three p38 MAPK homologues, *pmk-1*, -2, and -3³⁰, though since neither deletion of *pmk-1* nor *pmk-3* can suppress DR longevity, the most likely candidate is *pmk-2*. Alternately, two or more MAPKs may mediate signaling from *sek-1* redundantly. The

ASI neurons likely respond to DR-induced cellular stress by releasing hormonal cues that adapt the worm's metabolism to the restricted diet. By analogy, mammalian p38 MAPKs are activated in the hypothalamus by fasting and deactivated by re-feeding^{35,36}, and can regulate secretion of certain pituitary hormones^{37,38}.

The notion that stress-responsive pathways might mediate DR longevity has been suggested before, as part of the "Hormesis Hypothesis" of DR longevity³⁹. Proponents of this hypothesis suggest that DR extends lifespan by inducing cell-autonomous general stress-response pathways throughout the body. The present results confirm the predicted importance of a stress resistance pathway in mediating DR longevity, but surprisingly, this pathway need function in only two cells, the ASI neurons, to promote longevity of the whole animal.

We have identified a genetic pathway, homologous to a stress-responsive MAPK pathway in humans, that mediates DR longevity by acting in two neurons of *C. elegans*. There is ample evidence that cellular stress-responsive genes and pathways are activated in many tissues during DR in mammals³⁹. An interesting theme that is beginning to emerge from the identification of genes mediating DR longevity in *C. elegans* is that genes known to be important for cell-autonomous stress resistance in peripheral tissues are proving also to be important in DR longevity, but their critical actions lie in just a few brain neurons. In specialized neurons that control organismal metabolism, such as the ASIs and hypothalamic neurons, stress response pathways that generally induce cytoprotective functions may instead be coupled to hormonal signaling. Further work will be needed to confirm this hypothesis. Given the wealth of pharmacologic modifiers of MAPK pathways already available, however, MAPK pathways in hypothalamic

neurons represent an exciting possible target for future therapeutics to extend healthy lifespan in humans.

Methods

Strains

We used the following strains: the wild-type N2, KU4 *sek-1(km4)*, AU1 *sek-1(ag1)*, LG320 *sek-1(km4);Ex(sek-1)* #1, LG311 *nsy-1(ky397)*, CB1370 *daf-2(e1370)*, GR1307 *daf-16(mgDf50)*, CB1124 *che-3(e1124)*, PR813 *osm-5(p813)*, LG231 *sir-2.1(ok434)*, DR20 *daf-12(m20)*, AA111 *daf-9(rh50)*, SS149 *mes-1(bn7)*, LG330 *gels7[sek-1::gfp]*, the *Is007[skn-1::gfp]* strain²⁷, LG318 *sek-(km4);Is007*, KU25 *pmk-1(km25)*, LG316 *pmk-1(km25);Is007*, LG344 *gels8[gpa-4p::skn-1b::gfp]*, LG346 *sek-1(km4);gels8*, LG351 *sek-1(km4);Ex(gpa-4p::sek-1::rfp)*, LG353 *sek-1(km4);Ex(ges-1p::sek-1::gfp)* #1, LG352 *sek-1;Ex(ges-1p::sek-1::gfp)* #2, LG374 *sek-1;Ex(gpa-4p::sek-1::gfp)* #1, LG375 *sek-1;Ex(gpa-4p::sek-1::gfp)* #2, LG325 *daf-2(e1370);sek-1(km4)*, MT2605 *unc-43(e1186)*, VC36 *unc-5(gk29) pmk-2(gk21)/nT1* and BS3383 *pmk-3(ok169)*.

Transgenic Strain Construction

Extrachromosomal array-carrying transgenic strains were generated using standard microinjection methods. The 10 kb *sek-1* rescue transgene was derived from a

PCR product containing the *sek-1* coding region, 5.6 kb of 5' promoter sequence, and 1.0 kb of 3' sequence, amplified from cosmid C38G3 using primers 5'-GGCATATGGCTTTTCTAAGAAGTGAATGTGAAAGCA-3' and 5'-CCGGTACCATCCCAATCAAGTCGTAGTGTG-3', and was injected at 5 ng/μL with 50 ng/μL pRF4 as a co-injection marker.

To generate the integrated *sek-1::gfp* reporter strain *gels7*, plasmid pNB82 *sek-1::gfp::sek-1 3'UTR* was constructed as follows. PCR fragment A, consisting of a portion of the last intron of *sek-1* and the last exon of *sek-1* fused to GFP, was amplified from the plasmid "pPD95.75-*sek-1*pSEK-1+GFP fusion"³ primers 5'-CTGAATTCATTCATTGCAGATTCTCG-ACACTGTTTGGCGACGATG-3' and 5'-CCGATATCCTATTTGTATAGTTCAT-CCATGCCATGTGTAATCCCA-3'. Fragment A was then digested with EcoRI and EcoRV. Fragment B was produced by first digesting pNB65, an 8kb genomic subclone of the *sek-1* locus containing the entire coding region plus 3.6 kb of 5' sequence and 1.0 kb of 3' sequence, with EcoRV/EcoRI and gel purifying the 2.2 kb fragment, then digesting this 2.2 kb fragment with MluI and gel purifying the resultant 1.6 kb fragment. Finally, a separate sample of pNB65 was digested with BsaBI and MluI, and the 9.1 kb vector fragment was gel purified to yield fragment C. Fragments A, B, and C were trimolecularly ligated to yield plasmid pNB82. This plasmid was injected at 50 ng/μL to generate an extrachromosomal array-carrying line, from which four independent integrants, *gels4-7*, were isolated from a standard γ-ray integration screen, and were backcrossed three times to N2 prior to analysis. All four integrants showed a similar expression pattern.

To generate the *sek-1;Ex(ges-1p::sek-1::gfp)* strain, first a 1.3 kb fragment of the *ges-1* promoter was generated by amplifying N2 genomic DNA with primers 5'-AATCTAGAATCTGAATTCAAAGATAAGATATGTAATAGATTTTTGAAG-3' and 5'-CTCATAACATCATTGTCAAGTGACG-3', then digesting with HindIII/XbaI. This *ges-1* promoter fragment was inserted into HindIII/XbaI-cut plasmid "sek-1p sek-1KN+GFP fusion"³, which contains a kinase-dead point mutant *sek-1* cDNA/GFP fusion, to yield pNB73, a translational fusion of the *ges-1* promoter to kinase-dead *sek-1::gfp*. The kinase-dead mutation was restored to wild-type by the insertion of wild-type *sek-1* cDNA sequence to yield pNB74 *ges-1p::sek-1::gfp*. This plasmid proved to drive only very mosaic intestinal expression when injected into worms, however, so the *ges-1* promoter was extended from 1.3 kb to 2.5 kb as follows. 2.5 kb of the *ges-1* promoter was amplified from cosmid C29B10 using primers 5'-AAGCATGCGACCCAATGGAAACTGCAAAAATCT-3' and 5'-AAGGTACCCTGAATTCAAAGATAAGATATGTAATAGATTTTTGAAGCC-3', and the resultant product cut with SphI/KpnI and ligated into SphI/KpnI cut pPD95.75 to yield pNB123 *ges-1p::gfp*. pNB123 was cut with XhoI/Bgl2 and inserted into XhoI/Bgl2-cut pNB74 to yield pBR1 *ges-1p::sek-1::gfp*, the version of the construct used in this report (this ligation performed by B. Redding, for which we are grateful). pBR1 was injected at 50 ng/μL along with 50 ng/μL pRF4, into *sek-1(km4)* animals to yield *sek-1(km4);Ex(ges-1p::sek-1::gfp)*, and the transformed worms exhibited robust intestinal expression.

To generate the *sek-1;Ex(gpa-4p::sek-1::rfp)* strain, a cDNA clone of *sek-1* was amplified from pNB74 using primers 5'-

AAGGATCCATGGAGCGAAAAGGACGTGA-3' and 5'-
CCTTTACTCATTCTTCTACCGGTACCCT-3' and digested with BamHI/KpnI to
yield fragment A. A plasmid derivative of pPD95.70 (a gift of H. Schwartz) in which the
GFP cassette had been replaced by cDNA encoding the red-fluorescent mStrawberry²⁸
was digested with KpnI/SpeI to excise the RFP region, fragment B. Fragments A and B
were trimolecularly ligated into BamHI/SpeI cut pNB121 *gpa-4p::skn-1b::gfp* (see
Chapter 2) to yield pNB130 *gpa-4p::sek-1::rfp*. pNB130 was injected at 50 ng/μL, along
with 50 ng/μL pRF4, into *sek-1(km4)* animals to yield *sek-1(km4);Ex(gpa-4p::sek-
1::rfp)*.

To generate the *sek-1;Ex(gpa-4p::sek-1::gfp)* strain, the *gfp* cassette from
pPD95.75 was swapped in for the *rfp* cassette in pNB130 by digestion with KpnI/SpeI to
generate pNB137 *gpa-4p::sek-1::gfp*. pNB137 was injected at 50 ng/μL, along with 50
ng/μL pRF4, into *sek-1(km4)* animals to yield *sek-1(km4);Ex(gpa-4p::sek-1::gfp)*.

Dietary Restriction Protocol

Dietary restriction was performed as described in Chapter 2. Briefly, lifespan
assays were performed in the outer four wells of 6-well tissue culture plates, with each
well containing 2.5 ml DR Bottom Medium and 2.5 ml DR Top Medium. DR Bottom
Medium is composed of standard NGM medium⁴⁰, supplemented with 1 mg/ml
erythromycin to prevent bacterial division, 12.5 μg/ml fluorodeoxyuridine to inhibit
progeny hatching, 50 μg/ml ampicillin, and 1 mM IPTG; DR Top Medium is identical to
DR Bottom Medium, excluding the agar. Ampicillin-resistant bacteria were added from a

concentrated stock to the desired concentration, and concentration was monitored spectrophotometrically. Worms were grown to the L4/young adult stage on NGM plates seeded with OP50 bacteria, then transferred individually into the wells and maintained at 20°C with gentle gyrotory shaking at 80 rpm.

Lifespan Assay

Lifespan assays were performed as described in Chapter 2.

Respiration Assay

Respiration assay was performed as described in Chapter 2. Briefly, mass plate cultures of synchronized worms were grown on OP50 plates to the L4 stage, then transferred to Erlenmeyer flasks containing AL or DR levels of bacteria. After three days of culture, animals were collected by centrifugation and washed free of bacteria in S buffer. Respiration rate was measured at 25°C using a Clark-type oxygen electrode (Microelectrodes Inc.). Protein concentration in each sample was measured and oxygen consumption rates were normalized to protein content.

DiI Staining

Young adult worms were incubated for 2 hours at room temperature in M9 buffer⁴⁰ supplemented with 10 µg/mL DiI (Molecular Probes). Worms were transferred

to NGM plates seeded with OP50 bacteria for 1 hour, and then visualized by Nomarski microscopy with a FITC filter.

Fluorescence Intensity Quantification

Fluorescent images were collected at 1000x magnification (Zeiss) from worms subjected to 5 days of AL or DR as described above. Fluorescence brightness in the ASI was quantified using NIH ImageJ software.

Sudan Black Fat Staining

Day 3 adults cultured on plates, in AL conditions, and in DR conditions were stained as described in Chapter 2.

Acknowledgements

We thank H.R. Horvitz for generously allowing use of essential equipment, and members of the Guarente and Horvitz labs for advice and useful discussions. We thank B.R. Redding and D.H. Kim for the gift of a plasmid. Many of the strains used in this work were provided by the Caenorhabditis Genetics Center. This work was supported by a grant from the National Institutes of Health.

References

1. Koubova, J. & Guarente, L. How does calorie restriction work? *Genes Dev* **17**, 313-21(2003).
2. Roux, P. P. & Blenis, J. ERK and p38 MAPK-activated protein kinases: a family of protein kinases with diverse biological functions. *Microbiol Mol Biol Rev* **68**, 320-44 (2004).
3. Tanaka-Hino, M., Sagasti, A., Hisamoto, N., Kawasaki, M., Nakano, S., Ninomiya-Tsuji, J., Bargmann, C. I. & Matsumoto, K. SEK-1 MAPKK mediates Ca²⁺ signaling to determine neuronal asymmetric development in *Caenorhabditis elegans*. *EMBO Rep* **3**, 56-62 (2002).
4. Kim, D. H., Feinbaum, R., Alloing, G., Emerson, F. E., Garsin, D. A., Inoue, H., Tanaka-Hino, M., Hisamoto, N., Matsumoto, K., Tan, M. W. & Ausubel, F. M. A conserved p38 MAP kinase pathway in *Caenorhabditis elegans* innate immunity. *Science* **297**, 623-6 (2002).
5. Kondo, M., Yanase, S., Ishii, T., Hartman, P. S., Matsumoto, K. & Ishii, N. The p38 signal transduction pathway participates in the oxidative stress-mediated translocation of DAF-16 to *Caenorhabditis elegans* nuclei. *Mech Ageing Dev* **126**, 642-7 (2005).
6. Inoue, H., Hisamoto, N., An, J. H., Oliveira, R. P., Nishida, E., Blackwell, T. K. & Matsumoto, K. The *C. elegans* p38 MAPK pathway regulates nuclear localization of the transcription factor SKN-1 in oxidative stress response. *Genes Dev* **19**, 2278-83 (2005).
7. Salinas, L. S., Maldonado, E. & Navarro, R. E. Stress-induced germ cell apoptosis by a p53 independent pathway in *Caenorhabditis elegans*. *Cell Death Differ* **13**, 2129-39 (2006).
8. Solomon, A., Bandhakavi, S., Jabbar, S., Shah, R., Beitel, G. J. & Morimoto, R. I. *Caenorhabditis elegans* OSR-1 regulates behavioral and physiological responses to hyperosmotic environments. *Genetics* **167**, 161-70 (2004).
9. Hayakawa, T., Matsuzawa, A., Noguchi, T., Takeda, K. & Ichijo, H. The ASK1-MAP kinase pathways in immune and stress responses. *Microbes Infect* **8**, 1098-107 (2006).
10. Sagasti, A., Hisamoto, N., Hyodo, J., Tanaka-Hino, M., Matsumoto, K. & Bargmann, C. I. The CaMKII UNC-43 activates the MAPKKK NSY-1 to execute a lateral signaling decision required for asymmetric olfactory neuron fates. *Cell* **105**, 221-32 (2001).
11. Kenyon, C. The plasticity of aging: insights from long-lived mutants. *Cell* **120**, 449-60 (2005).

12. Gems, D., Pletcher, S. & Partridge, L. Interpreting interactions between treatments that slow aging. *Aging Cell* **1**, 1-9 (2002).
13. Apfeld, J. & Kenyon, C. Regulation of lifespan by sensory perception in *Caenorhabditis elegans*. *Nature* **402**, 804-9 (1999).
14. Arantes-Oliveira, N., Apfeld, J., Dillin, A. & Kenyon, C. Regulation of life-span by germ-line stem cells in *Caenorhabditis elegans*. *Science* **295**, 502-5 (2002).
15. Hsin, H. & Kenyon, C. Signals from the reproductive system regulate the lifespan of *C. elegans*. *Nature* **399**, 362-6 (1999).
16. Gerisch, B., Weitzel, C., Kober-Eisermann, C., Rottiers, V. & Antebi, A. A hormonal signaling pathway influencing *C. elegans* metabolism, reproductive development, and life span. *Dev Cell* **1**, 841-51 (2001).
17. Partridge, L., Gems, D. & Withers, D. J. Sex and death: what is the connection? *Cell* **120**, 461-72 (2005).
18. Lin, S. J., Defossez, P. A. & Guarente, L. Requirement of NAD and SIR2 for life-span extension by calorie restriction in *Saccharomyces cerevisiae*. *Science* **289**, 2126-8 (2000).
19. Rogina, B. & Helfand, S. L. Sir2 mediates longevity in the fly through a pathway related to calorie restriction. *Proc Natl Acad Sci USA* **101**, 15998-6003 (2004).
20. Viswanathan, M., Kim, S. K., Berdichevsky, A. & Guarente, L. A role for SIR-2.1 regulation of ER stress response genes in determining *C. elegans* life span. *Dev Cell* **9**, 605-15 (2005).
21. Troemel, E. R., Chu, S. W., Reinke, V., Lee, S. S., Ausubel, F. M. & Kim, D. H. p38 MAPK regulates expression of immune response genes and contributes to longevity in *C. elegans*. *PLoS Genet* **2**, e183 (2006).
22. Lin, S. J., Kaeberlein, M., Andalis, A. A., Sturtz, L. A., Defossez, P. A., Culotta, V. C., Fink, G. R. & Guarente, L. Calorie restriction extends *Saccharomyces cerevisiae* lifespan by increasing respiration. *Nature* **418**, 344-8 (2002).
23. Houthoofd, K., Braeckman, B. P., Lenaerts, I., Brys, K., De Vreese, A., Van Eygen, S. & Vanfleteren, J. R. Axenic growth up-regulates mass-specific metabolic rate, stress resistance, and extends life span in *Caenorhabditis elegans*. *Exp Gerontol* **37**, 1371-8 (2002).

24. Houthoofd, K., Braeckman, B. P., Lenaerts, I., Brys, K., De Vreese, A., Van Eygen, S. & Vanfleteren, J. R. No reduction of metabolic rate in food restricted *Caenorhabditis elegans*. *Exp Gerontol* **37**, 1359-69 (2002).
25. Nisoli, E., Tonello, C., Cardile, A., Cozzi, V., Bracale, R., Tedesco, L., Falcone, S., Valerio, A., Cantoni, O., Clementi, E., Moncada, S. & Carruba, M. O. Calorie restriction promotes mitochondrial biogenesis by inducing the expression of eNOS. *Science* **310**, 314-7 (2005).
26. Barzilai, N. & Gabriely, I. The role of fat depletion in the biological benefits of caloric restriction. *J Nutr* **131**, 903S-906S (2001).
27. An, J. H. & Blackwell, T. K. SKN-1 links *C. elegans* mesendodermal specification to a conserved oxidative stress response. *Genes Dev* **17**, 1882-93 (2003).
28. Shaner, N. C., Campbell, R. E., Steinbach, P. A., Giepmans, B. N., Palmer, A. E. & Tsien, R. Y. Improved monomeric red, orange and yellow fluorescent proteins derived from *Discosoma sp.* red fluorescent protein. *Nat Biotechnol* **22**, 1567-72 (2004).
29. Jansen, G., Thijssen, K. L., Werner, P., van der Horst, M., Hazendonk, E. & Plasterk, R. H. The complete family of genes encoding G proteins of *Caenorhabditis elegans*. *Nat Genet* **21**, 414-9 (1999).
30. Berman, K., McKay, J., Avery, L. & Cobb, M. Isolation and characterization of *pmk-1-3*: three p38 homologs in *Caenorhabditis elegans*. *Mol Cell Biol Res Commun* **4**, 337-44 (2001).
31. Libina, N., Berman, J. R. & Kenyon, C. Tissue-specific activities of *C. elegans* DAF-16 in the regulation of lifespan. *Cell* **115**, 489-502 (2003).
32. Mobbs, C. V., Yen, K., Mastaitis, J., Nguyen, H., Watson, E., Wurmbach, E., Sealfon, S. C., Brooks, A. & Salton, S. R. Mining microarrays for metabolic meaning: nutritional regulation of hypothalamic gene expression. *Neurochem Res* **29**, 1093-103 (2004).
33. Junn, E., Han, S. H., Im, J. Y., Yang, Y., Cho, E. W., Um, H. D., Kim, D. K., Lee, K. W., Han, P. L., Rhee, S. G. & Choi, I. Vitamin D3 up-regulated protein 1 mediates oxidative stress via suppressing the thioredoxin function. *J Immunol* **164**, 6287-95 (2000).
34. Jee, C., Vanoaica, L., Lee, J., Park, B. J. & Ahnn, J. Thioredoxin is related to life span regulation and oxidative stress response in *Caenorhabditis elegans*. *Genes Cells* **10**, 1203-10 (2005).

35. Morikawa, Y., Ueyama, E. & Senba, E. Fasting-induced activation of mitogen-activated protein kinases (ERK/p38) in the mouse hypothalamus. *J Neuroendocrinol* **16**, 105-12 (2004).
36. Ueyama, E., Morikawa, Y., Yasuda, T. & Senba, E. Attenuation of fasting-induced phosphorylation of mitogen-activated protein kinases (ERK/p38) in the mouse hypothalamus in response to refeeding. *Neurosci Lett* **371**, 40-4 (2004).
37. de Guise, C., Lacerte, A., Rafiei, S., Reynaud, R., Roy, M., Brue, T. & Lebrun, J. J. Activin inhibits the human Pit-1 gene promoter through the p38 kinase pathway in a Smad-independent manner. *Endocrinology* **147**, 4351-62 (2006).
38. Safwat, N., Ninomiya-Tsuji, J., Gore, A. J. & Miller, W. L. Transforming growth factor beta-activated kinase 1 is a key mediator of ovine follicle-stimulating hormone beta-subunit expression. *Endocrinology* **146**, 4814-24 (2005).
39. Sinclair, D. A. Toward a unified theory of caloric restriction and longevity regulation. *Mech Ageing Dev* **126**, 987-1002 (2005).
40. Brenner, S. The genetics of *Caenorhabditis elegans*. *Genetics* **77**, 71-94 (1974).

Table 1. Interaction of Known Lifespan Mutants with DR Longevity

Lifespan Pathway Affected	Strain and Condition	# Deaths/# Censored (# Trials)	Mean ± s.e.m.	P-value vs. AL Control
Wild type	N2 AL	563/23(11)	25.5 ± 0.2	
	N2 DR	513/15(10)	33.2 ± 0.2	P < 0.0001
Insulin	<i>daf-2(e1370)</i> AL ^a	23/22(1)	39.0 ± 2.11	
	<i>daf-2(e1370)</i> DR ^a	32/21(1)	60.0 ± 2.7	P < 0.0001
Insulin	<i>daf-16(mgDf50)</i> AL ^a	51/2(1)	20.7 ± 0.80	
	<i>daf-16(mgDf50)</i> DR ^a	53/1(1)	28.4 ± 0.37	P < 0.0001
Sensory Neuron	<i>che-3(e1124)</i> AL ^a	57/48(2)	31.6 ± 0.71	
	<i>che-3(e1124)</i> DR ^a	48/4(1)	38.5 ± 0.74	P < 0.0001
Sensory Neuron	<i>osm-5(p813)</i> AL ^a	68/38(2)	34.3 ± 0.81	
	<i>osm-5(p813)</i> DR ^a	47/6(1)	41.1 ± 0.98	P < 0.0001
Germline	<i>mes-1(bn7)</i> fertile AL	47/0(1)	25.5 ± 0.5	
	<i>mes-1(bn7)</i> fertile DR	49/3(1)	29.8 ± 0.7	P < 0.0001
	<i>mes-1(bn7)</i> sterile AL	26/12(1)	30.7 ± 1.1	
	<i>mes-1(bn7)</i> sterile DR	42/6(1)	34.9 ± 1.0	P = 0.0021
Germline	<i>daf-12(m20)</i> AL	59/1(1)	25.6 ± 0.8	
	<i>daf-12(m20)</i> DR	52/2(1)	36.7 ± 1.0	P < 0.0001
Germline	<i>daf-9(rh50)</i> AL	55/4(1)	25.1 ± 0.7	
	<i>daf-9(rh50)</i> DR	47/1(1)	29.9 ± 0.8	P < 0.0001
Sirtuin	<i>sir-2.1(ok434)</i> AL	36/1(1)	25.5 ± 0.6	
	<i>sir-2.1(ok434)</i> DR	52/2(1)	31.7 ± 0.5	P < 0.0001

All P-values are relative to AL control, unless otherwise noted.

^aData from Bishop and Guarente, 2007.

Table S1. Lifespan Data.

Strain and Condition	# Deaths/# Censored (# Trials)	Mean ± s.e.m	P-value vs. AL Control
N2 in 2.5x10 ⁸ cfu/ml ("AL")	563/23(11)	25.5 ± 0.2	
N2 in 1.7x10 ⁸ cfu/ml	22/31(1)	25.6 ± 1.0	
N2 in 8.5x10 ⁷ cfu/ml	25/27(1)	33.0 ± 1.0	
N2 in 5.7x10 ⁷ cfu/ml	51/1(1)	34.9 ± 0.7	
N2 in 2.5x10 ⁷ cfu/ml ("DR")	513/15(10)	33.2 ± 0.2	P < 0.0001
N2 in 2.5x10 ⁶ cfu/ml	56/0(1)	25.9 ± 0.6	
<i>sek-1(km4)</i> in 2.5x10 ⁸ cfu/ml ("AL")	290/13(6)	20.4 ± 0.2	
<i>sek-1(km4)</i> in 2.5x10 ⁷ cfu/ml ("DR")	259/10(5)	21.2 ± 0.3	P = 0.0185
<i>sek-1(km4)</i> in 2.5x10 ⁶ cfu/ml	39/5(1)	22.3 ± 1.0	
<i>sek-1(km4)</i> in 2.5x10 ⁵ cfu/ml	50/0(1)	20.5 ± 0.7	
<i>sek-1(ag1)</i> AL	48/4(1)	23.4 ± 0.7	
<i>sek-1(ag1)</i> DR	53/2(1)	25.4 ± 0.7	P = 0.0158
<i>sek-1(km4);Ex(sek-1) #1</i> AL	48/2(1)	24.6 ± 0.7	
<i>sek-1(km4);Ex(sek-1) #1</i> DR	51/0(1)	30.7 ± 0.8	P < 0.0001
<i>sek-1(km4);Ex(sek-1) #2</i> AL	51/2(1)	24.2 ± 0.5	
<i>sek-1(km4);Ex(sek-1) #2</i> DR	51/2(1)	33.0 ± 0.7	P < 0.0001
N2 on plates	152/4(3)	22.7 ± 0.4	
<i>daf-2(e1370)</i> on plates	47/3(1)	40.2 ± 1.1	P < 0.0001 ^b
<i>sek-1(km4)</i> on plates	138/10(3)	17.0 ± 0.2	
<i>sek-1(km4);daf-2(e1370)</i> on plates	43/4(1)	26.4 ± 1.5	P < 0.0001 ^b
<i>nsy-1(ky397)</i> AL	40/1(1)	22.3 ± 0.7	
<i>nsy-1(ky397)</i> CR	45/1(1)	21.8 ± 0.7	P = 0.6937
<i>unc-43(n1186)</i> AL ^a	52/1(1)	27.1 ± 0.5	
<i>unc-43(n1186)</i> DR ^a	51/2(1)	32.4 ± 0.7	P < 0.0001
<i>pmk-1(km25)</i> AL ^a	56/1(1)	21.7 ± 0.6	
<i>pmk-1(km25)</i> DR ^a	33/6(1)	28.0 ± 1.1	P < 0.0001
<i>pmk-3(ok169)</i> AL ^a	46/7(1)	23.7 ± 0.8	
<i>pmk-3(ok169)</i> DR ^a	48/6(1)	30.0 ± 0.9	P < 0.0001
<i>sek-1(km4);Ex(gpa-4p::sek-1::gfp) #1</i> AL	57/1(1)	22.0 ± 0.7	
<i>sek-1(km4);Ex(gpa-4p::sek-1::gfp) #1</i> DR	52/2(1)	29.3 ± 0.8	P < 0.0001
<i>sek-1(km4);Ex(gpa-4p::sek-1::gfp) #2</i> AL	52/2(1)	22.3 ± 0.5	
<i>sek-1(km4);Ex(gpa-4p::sek-1::gfp) #2</i> DR	55/0(1)	30.2 ± 0.9	P < 0.0001
<i>sek-1(km4);Ex(ges-1p::sek-1::gfp) #1</i> AL	49/1(1)	25.2 ± 0.6	
<i>sek-1(km4);Ex(ges-1p::sek-1::gfp) #1</i> DR	50/2(1)	26.6 ± 0.7	P = 0.0231
<i>sek-1(km4);Ex(ges-1p::sek-1::gfp) #2</i> AL	53/0(1)	24.2 ± 0.6	
<i>sek-1(km4);Ex(ges-1p::sek-1::gfp) #2</i> DR	54/1(1)	26.2 ± 0.7	P = 0.0064

Shaded bars indicate the conditions used for all subsequent AL and DR lifespans.

^aThis survival curve is not shown in the figures.

^bThis p-value is versus the strain that immediately precedes it.

Figure 1. Activity of the MAPKK *sek-1* is Required for Multiple Physiological Responses to DR

(A) Wild-type N2 animals exhibited an increased mean lifespan with a maximum at an optimal level of DR, but mean lifespan of *sek-1(km4)* was not modulated by food level. Errors are s.e.m. The lifespan results in this and all subsequent figures represent combined data from independent experiments as indicated in Supplementary Table S1. Complete lifespan data are presented in Supplementary Table S1.

(B) Two different *sek-1* alleles had severely impaired DR-induced longevity response.

(C) The lifespan defects of *sek-1(km4)* were rescued by an extrachromosomal transgene carrying 10 kb of the wild-type *sek-1* genomic region.

(D) A mutant in *nsy-1*, a MAPKKK that acts immediately upstream of *sek-1*, exhibited identical longevity defects to *sek-1(km4)*.

(E) Relative to the wild-type, day 3 adult *sek-1(km4)* animals had a reduced respiration rate under AL conditions and, unlike the wild-type, respiration rate was not increased under DR. Both of these defects were rescued by a wild-type *sek-1* transgene. Data shown was pooled from four independent trials for N2 and *sek-1*, and two independent trials for *sek-1;Ex(sek-1)*, with measurements made in triplicate in each trial. Error bars show s.e.m.

(F) High intestinal fat level in the wild-type is reduced by DR, but *sek-1(km4)* has a constitutively low level of fat that is not altered by DR. The graph shows quantification of individuals with any detectable intestinal fat on day 3 of AL or DR. Similar results were obtained on later days (not shown). Data is pooled from two independent trials with

more than 30 animals examined in each trial. Errors are s.e.m. Fat was detected by Sudan Black staining; see Figure S2 for photographs of representative stained animals.

FIGURE 1

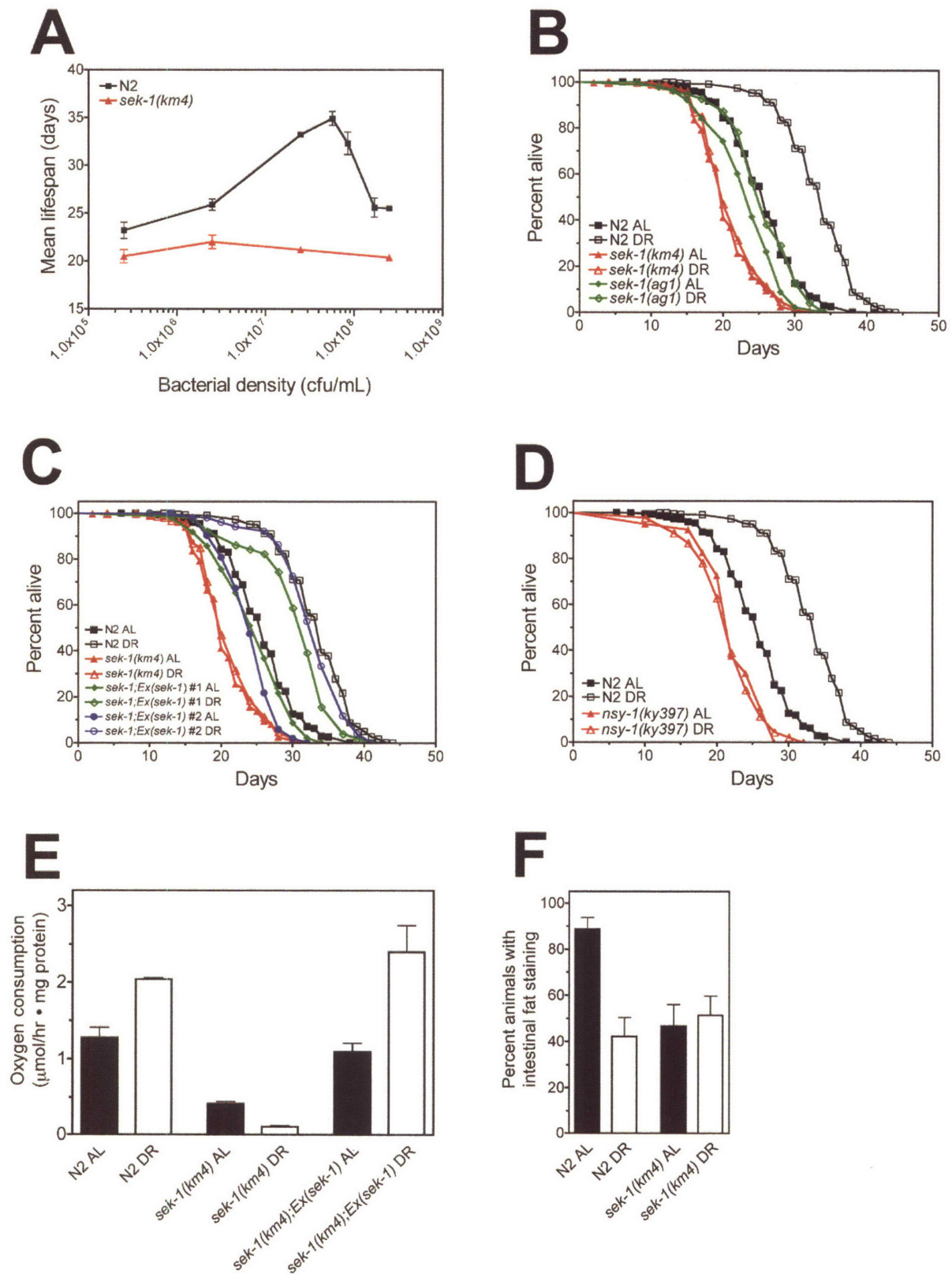


Figure 2. *sek-1* Regulates *skn-1* in the ASI Neurons

(A) The *sek-1* genomic locus is shown, with exons in pink and untranslated regions in grey. The location of the *ag1* mutation and the extent of the *km4* deletion are shown in red. The 10 kb genomic fragment contained in the transgene used for the rescue experiments in Figure 1 is shown in blue. *gels7[sek-1::gfp]* is indicated in green and comprises 7.6 kb of genomic DNA sequence, including *sek-1* and its promoter, translationally fused to the 5' end of a GFP cassette, the 3' end of which is fused to 1.0 kb of 3' *sek-1* sequence.

(B) The *gels7[sek-1::gfp]* reporter expressed in many, though not all, neurons, and in the intestine, spermathecae, and distal tip cells. Four independent integrants of this transgene were examined with similar results. Scale bar, 100 μm .

(C) The *gels7[sek-1::gfp]* reporter expressed SEK-1::GFP in the ASI neurons. Upper right shows animals with amphid neurons marked by uptake of the red fluorescent lipophilic dye DiI. Lower left shows green fluorescence from SEK-1::GFP. Lower right shows merged images, demonstrating double fluorescence in the ASI neuron. Scale bar, 10 μm .

(D) Expression of the integrated *skn-1::gfp* reporter *Is007* was present in most day 5 adult wild-type animals, but absent in most *sek-1* animals. This defect was rescued by an ASI-specific *gpa-4p::sek-1::rfp* transgene, and was independent of the MAPK *pmk-1*. Each graphed value represents pooled data from two independent trials of greater than 30 animals each. Errors are s.e.m.

(E) ASI fluorescence intensity was greatly reduced in day 5 adult *sek-1;Is007* animals, which express SKN-1::GFP from its native promoter, but not in *sek-1;geIs8* animals that express SKN-1::GFP from the *gpa-4* promoter. Each graphed value represents pooled data from two independent trials of greater than 25 animals each. Errors are s.e.m.

(F) SKN-1::GFP fluorescence intensity was increased by DR in the ASI neurons of *Is007* animals, but not *sek-1(km4);Is007* animals. Each graphed value represents pooled data from three independent trials for *Is007* and two independent trials for *sek-1;Is007*, with greater than 30 animals examined in each trial. Errors are s.e.m.

FIGURE 2

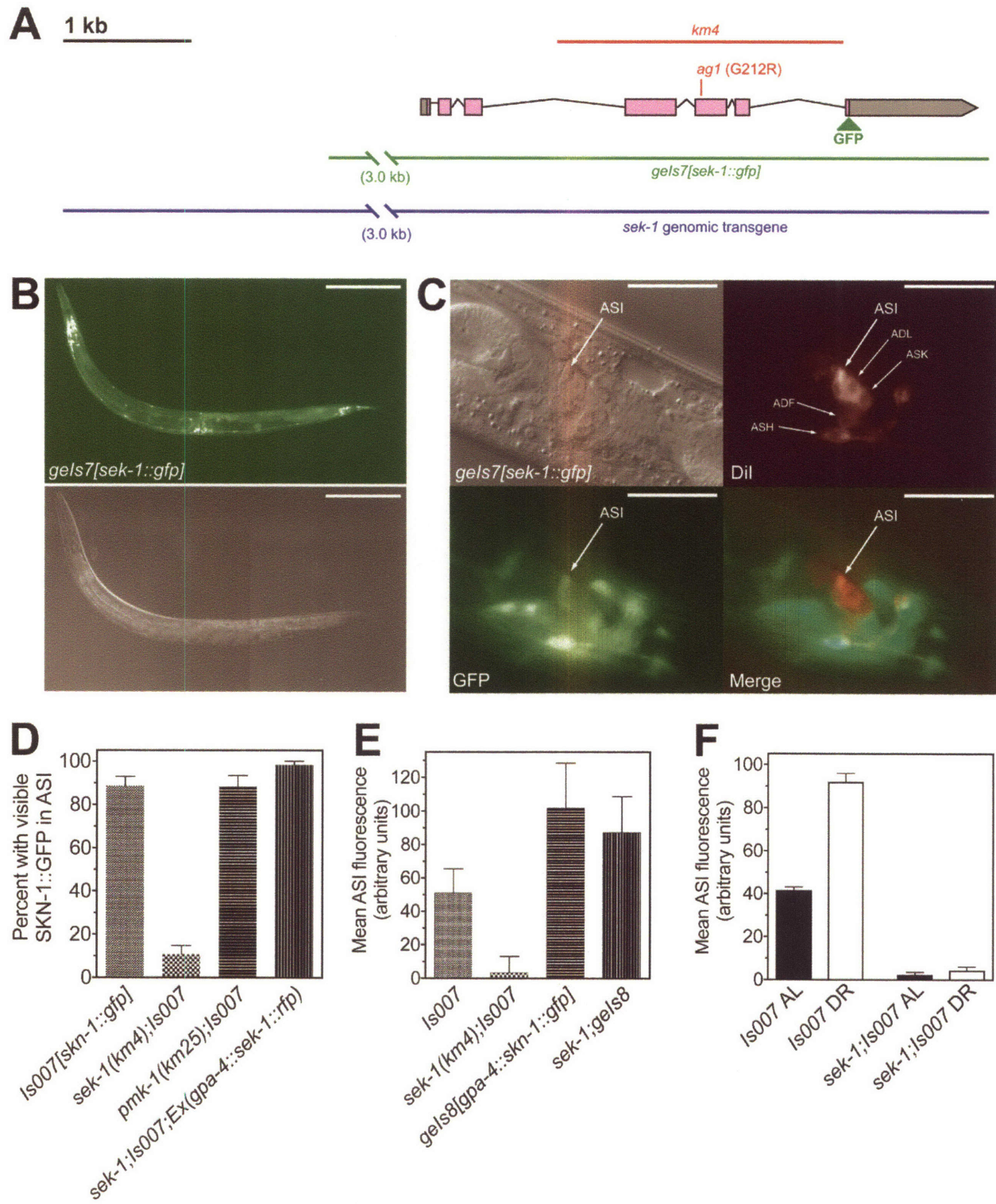
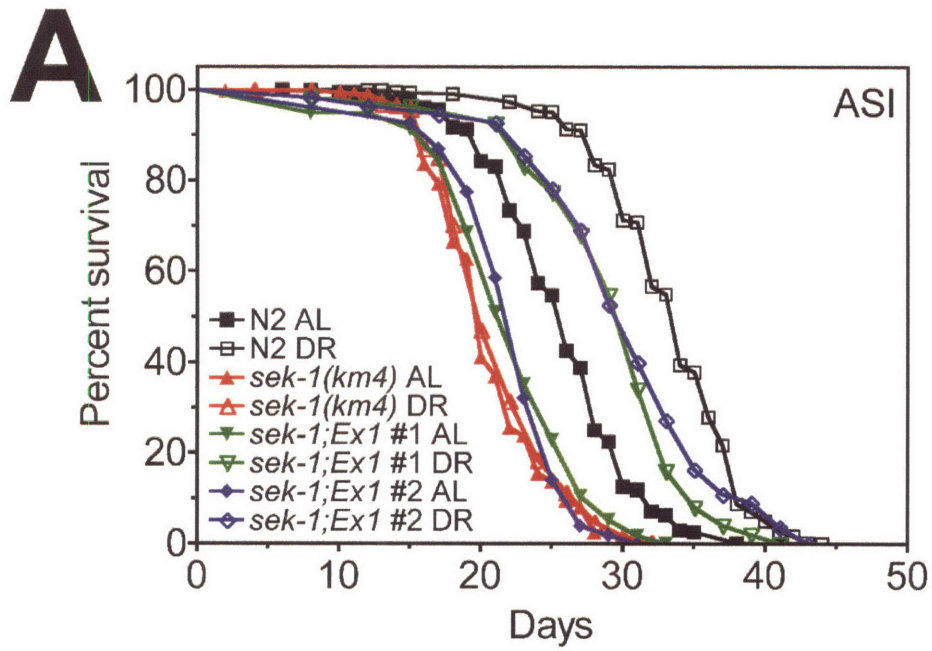


Figure 3. *sek-1* Acts in Two Separate Tissues to Affect Lifespan in Two Different Ways.

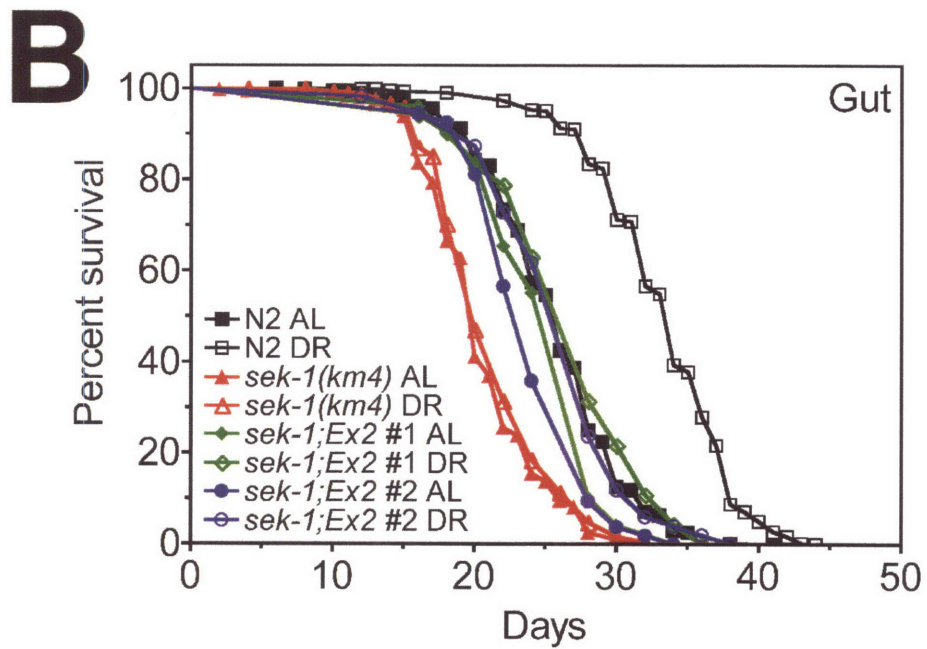
(A) Two independent transformed lines carrying the ASI-specific *gpa-4p::sek-1::gfp* transgene showed full rescue of the DR-induced longevity defect of *sek-1(km4)*, but the short basal lifespan was not rescued.

(B) Two independent transformed lines carrying the intestine-specific *ges-1p::sek-1::gfp* transgene showed rescue of the short basal lifespan defect of *sek-1(km4)*, but the DR longevity response defect was not rescued.

FIGURE 3



Ex1 = gpa-4p::sek-1::gfp



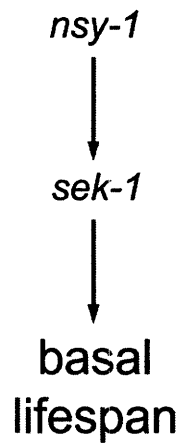
Ex2 = ges-1p::sek-1::gfp

Figure 4. Model: Separate effects of *sek-1* on Lifespan in the ASI Neurons and Intestine

sek-1 modulates lifespan in two separate tissues in two different ways. First, in the intestine, *sek-1* functions downstream of *nsy-1* to ensure normal basal longevity. Second, during DR, *nsy-1* and *sek-1* act in the ASI neurons to increase *skn-1* transcription, thereby activating the increased longevity response to DR. *sek-1* may directly mediate the effects of DR on *skn-1* expression, or DR may modulate *skn-1* expression in parallel to *sek-1*. Because elevated expression of *sek-1* or *skn-1* in the ASI neurons is not by itself sufficient to increase lifespan in the absence of DR (N.B. and L.G., unpublished observations), DR must activate an as yet unidentified genetic pathway(s) in the ASI neurons or other cells that act in parallel to *skn-1* to increase longevity.

FIGURE 4

Intestine



ASI

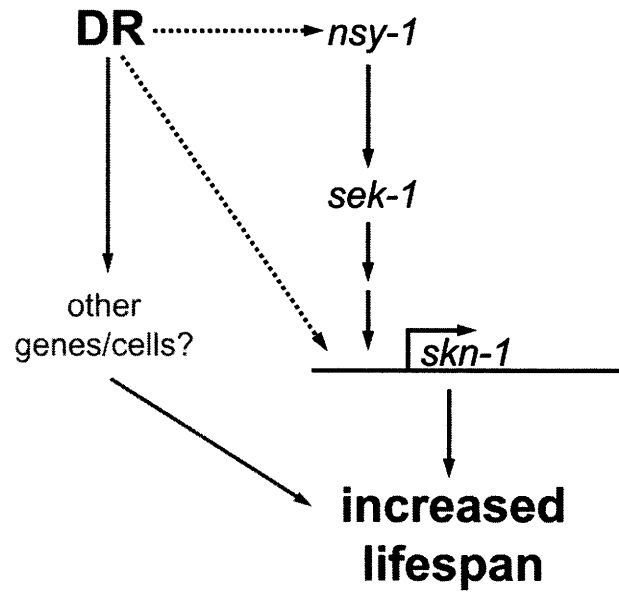


Figure S1. The *sek-1(km4)* Mutation Does Not Place an Upper Bound on Lifespan.

The lifespan of *sek-1(km4)* animals could be extended by introduction of the *daf-2(e1370)* mutation.

FIGURE S1

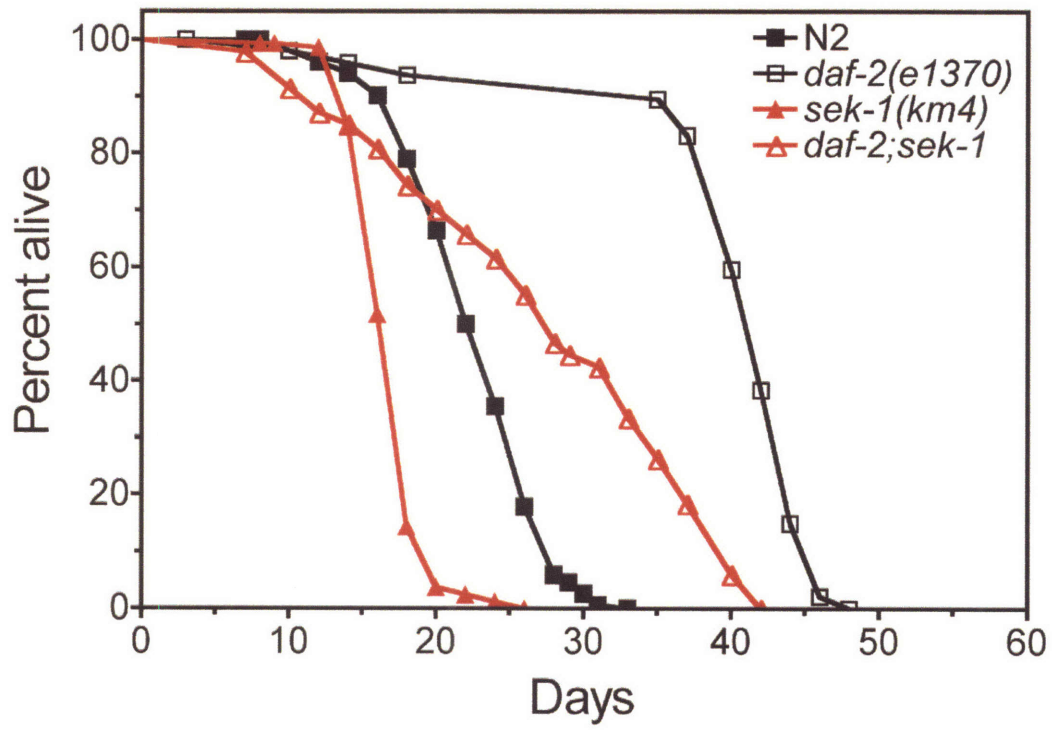


Figure S2. *sek-1(km4)* Uncouples Fat Storage From Dietary Conditions.

Representative day 3 adult animals cultured in AL or DR conditions, with fat stained by Sudan Black. Upper panels: Staining is observed in the anterior gut of AL wild-type animals (black arrows), but is reduced or invisible in DR wild-type animals (white arrowhead). Lower panels: *sek-1(km4)* mutants exhibit a low level of fat, comparable to DR wild-type worms, in both AL and DR conditions (white arrowheads; see Figure 1F for quantification). Staining is also visible in intrauterine eggs in all conditions. Scale bars, 100 μm .

FIGURE S2

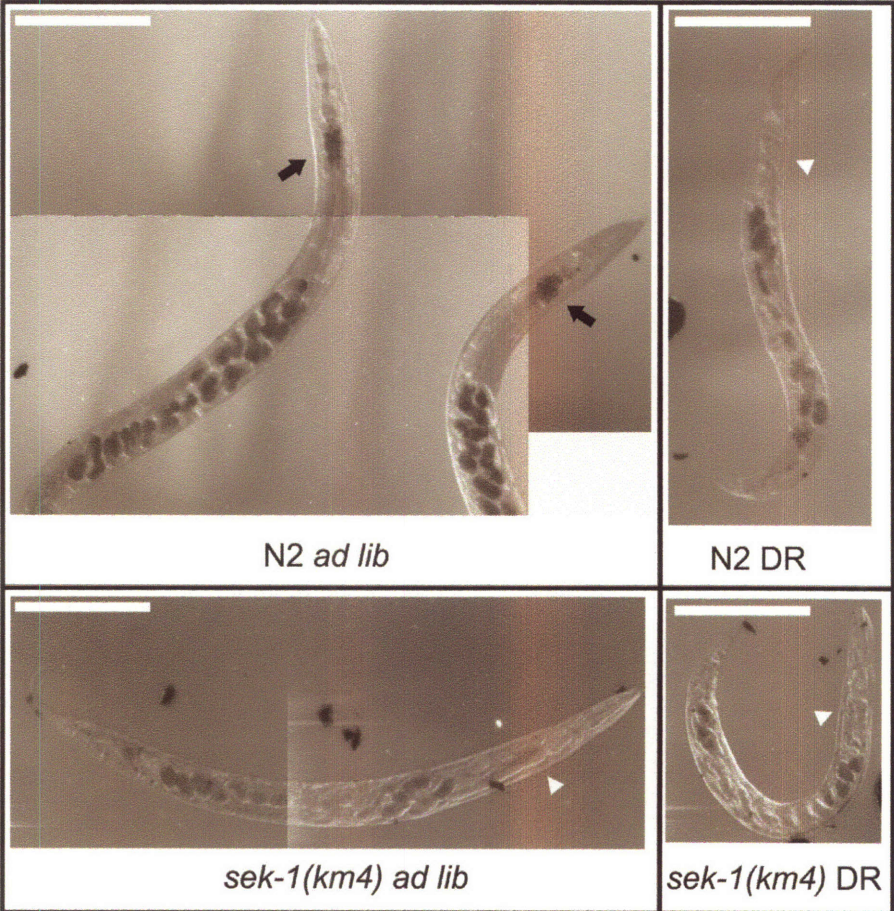
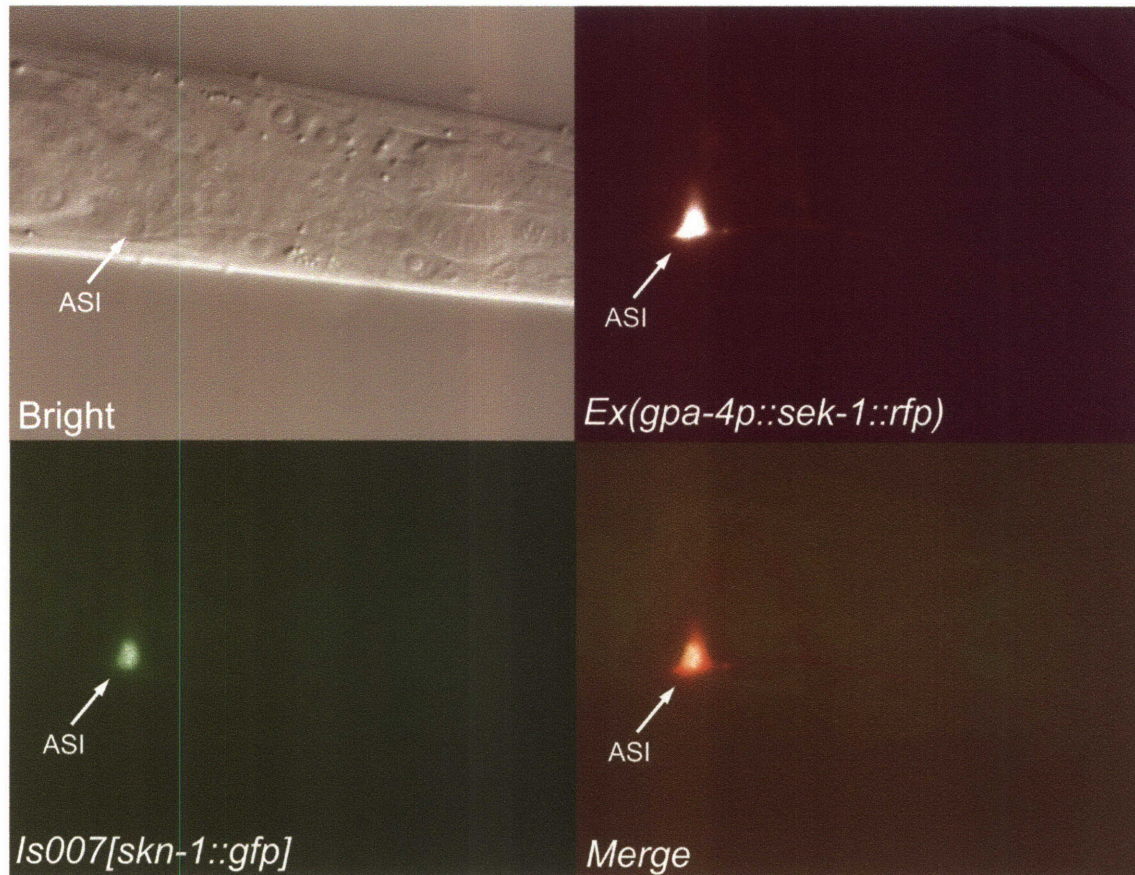


Figure S3. *Ex(gpa-4p::sek-1::rfp)* is Specifically Expressed in the ASI Neurons.

Upper left, Nomarski image of a *sek-1(km4);Is007[skn-1::gfp];Ex(gpa-4p::sek-1::rfp)* animal. Upper right, red channel shows SEK-1::RFP expression in the ASI neuron only. Lower left, green channel confirms identity of ASI neuron via nuclear SKN-1::GFP expression. Lower right, merged red and green channels. Scale bars, 10 μ m.

FIGURE S3



CHAPTER 4

Conclusions and Future Directions

Summary of Results

The overall conclusions of this work are diagrammed in **Figure 1**. The ASI neurons integrate as-yet-unidentified signals of organismal energy status to detect DR. These signals include some sort of intrinsic cues, either detection of intracellular energy status within the ASI, or afferent hormonal signals of peripheral energy status, or both. These intrinsic signals may be integrated with sensory perception of available food in the environment to ultimately permit detection of restricted organismal energy availability by the ASI neurons. Following detection of the DR state, *skn-1* is activated in the ASI neurons. This activation depends on the *nsy-1/sek-1* signaling cascade in the ASI neurons, though it remains undetermined whether *nsy-1* and *sek-1* act downstream of or in parallel to DR in regulating *skn-1*. Upon activation during DR, *skn-1* mediates appropriate cell-nonautonomous signals from the ASI neurons to peripheral tissues to promote increased respiration and longer lifespan. These signals are likely hormonal in nature, given the established endocrine functions of the ASI neurons. Because ASI-specific overexpression of *skn-1* is insufficient to increase lifespan by itself, another genetic pathway(s) must be required to act in parallel to *skn-1* to mediate the DR longevity response. This additional pathway may function in the ASIs or in other neuron(s).

Future Research Directions

Inspection of Figure 1 will reveal that many unanswered questions have been raised in the course of this work. Here, I will attempt to identify some of the more

important directions for future research on the control of DR longevity by *skn-1* and the ASI neurons.

What are the signals of energy status integrated by the ASI neurons?

An analogy to mammalian studies suggests that there are three general categories of cues that can modulate neuronal energy status detection (see also Chapter 1): environmental sensory perception, afferent hormonal signals from the periphery, and intracellular energy status monitoring. We have little information thus far as to the nature of the signals influencing the ASI neurons to adopt the DR response.

Chemosensory perception of the external environment is not required for a normal response to DR, since two different cilia-defective mutants that lack all chemosensory capability, *che-3* and *osm-5*, increased lifespan normally during DR (Chapter 2). However, *che-3* mutation does downregulate a *skn-1::gfp* reporter in the ASI neurons in certain environments (Figure 2). Therefore, the possibility exists that sensory perception, though not required for DR longevity, may be capable of suppressing it in some environments, as has been observed in flies¹. One potential means of addressing the modulatory capability of sensory perception during DR would be to combine the bacterial density control method developed in this work with pharyngeal pumping-deficient mutants such as *eat-2* to separate environmental and intrinsic energy restriction.

The intrinsic pathways affecting DR detection in the ASI neurons might be best identified by generating ASI-specific RNAi knockdown strains composed of an shRNA against the target of interest driven by an ASI-specific promoter and injected into an

RNAi spreading-defective mutant such as *sid-1*. Crucial metabolic enzymes involved in cell-intrinsic energy sensing in mammals, such as mTOR, AMPK, and acetyl-CoA carboxylase could be targeted to examine the effects of cellular energy sensing in the ASIs on basal and DR longevity. Similarly, RNAi against candidate hormone receptors in the ASIs could be used to screen for important afferent hormonal factors.

An additional possible type of initiating event in DR perception by the ASI is suggested by the particular genes this work has identified. *nsy-1* and *sek-1* are homologous to mammalian ASK1 and MEK6, respectively, and both the worm and mammalian homologues are known to be important in stress responses, such as ER stress, reactive oxygen species (ROS), and signaling from receptors that use ROS as a second messenger². Similarly, both worm *skn-1* and the homologous mammalian Nrf proteins are known to be involved in stress response and xenobiotic detoxification, and Nrf2 is a crucial mediator of the ER stress response^{3,4}. Therefore, it may be that one of the inputs initiating *skn-1*-mediated DR perception in the ASI neurons is some sort of stress signal caused by low energy availability, such as, for instance, unfolded proteins in the ER. In other words, DR may be detected by activation of general stress-responsive pathways in response to nutrient limitation. This hypothesis warrants further investigation.

What genes act downstream of sek-1 and skn-1 to mediate DR longevity?

Since the MAPKK *sek-1* appears to regulate *skn-1* at the transcriptional level, there is presumably a MAPK(s) and a transcription factor(s) connecting *sek-1* and *skn-1*. These remain to be identified. Since the mammalian homologue of *sek-1* exclusively

activates p38 MAPKs⁵, the most likely candidates are the worm p38 MAPK homologues, *pmk-1*, *-2*, and *-3*⁶. In fact, *sek-1* is known to be a critical regulator of *pmk-1* in the intestine⁷. However, deletion alleles of *pmk-1* or *pmk-3* failed to reproduce the ASI *skn-1::gfp* expression defect of *sek-1* (Chapter 3). Therefore, *pmk-2* is a strong candidate, but could not be tested because the only available deletion strain arrests during larval development. Alternately, more than one MAPK might act redundantly to regulate *skn-1*. Future availability of additional deletion alleles may permit identification of the genes connecting *sek-1* and *skn-1* in the ASI neurons.

An important goal of future work will be to identify the crucial genes regulated by *skn-1* in the ASIs to mediate DR longevity, and the cell nonautonomous signals released by the ASIs during DR. Possible clues as to the identity of these genes were provided by a computerized scan for *skn-1* consensus binding sites in the promoter regions of all predicted genes in the *C. elegans* genome (the promoter-scanning Perl script, written by the author, is available upon request). The 168 genes with eight or more predicted binding sites are presented in **Figure 3** (representing < 1% of genes in the genome; the full list is available from the author on request). Because of the degenerate nature of the *skn-1* consensus site, this list will necessarily contain many false positives. However, the *bona fide skn-1* target *dod-24* was identified using this scan (Chapter 2), validating the presence of true positives in the list. Strikingly, of the 97 genes that could be assigned a predicted function based on homology to proteins of known function, 33 (34%) are likely to function in regulation of energy balance, either in neuronal perception of food availability, production of hormones or neuropeptides, or response to hormones or neuropeptides. In particular, the scan predicts *skn-1* regulation of several genes whose

mammalian homologues are known to be critical in regulation of feeding and energy balance, including receptors for hypocretin, neuropeptide FF, thyrotropin, somatostatin, ghrelin, and progesterin, as well as the nuclear hormone receptor hepatocyte nuclear factor-4 and glucocorticoid modulatory element binding protein. These predicted *skn-1* targets provide a good starting point for experimental validation of crucial *skn-1*-dependent genes, and suggest that *skn-1* may broadly modulate endocrine properties of the ASI neurons during DR.

Interestingly, a mammalian master regulator of xenobiotic detoxification enzymes, CAR, which is expressed in liver, intestine, and brain, is induced by fasting in mice and is required for normal neuroendocrine adaptation to DR⁸. This suggests a possible conserved role of certain xenobiotic detoxification genes in regulation of endocrine responses to DR. The significance of such a functional overlap is unclear, but certainly intriguing.

What hormone(s) mediate the DR longevity response?

To identify hormones mediating the DR response, I would suggest using the metabolic alteration of peripheral tissues as a proxy phenotype in lieu of lifespan analysis of screening purposes. Direct measurement of oxygen consumption is prohibitively time- and labor-intensive, but some sort of visible reporter indicating peripheral mitochondrial respiration could be developed. For example, a fluorescent electron-transport chain subunit might serve⁹. This reporter should indicate a *skn-1*-dependent respiration increase in response to DR. Then, a mutant screen for animals that fail to increase respiration

during DR, followed by a secondary test of lifespan response, might permit identification of critical hormonal signals. Alternately, many hormonal expression patterns have been determined, including many expressed in the ASI neurons. ASI-specific RNAi of candidate hormones (as described above) might identify those essential for DR. It is worth noting that DR seems to extend lifespan more effectively in a *daf-2* mutant background, and less effectively in a *daf-9* mutant background, possibly implicating insulin-like and steroidal hormones as negative and positive regulators of DR longevity, respectively.

What other genetic pathways are required for DR longevity?

Overexpression of *skn-1* in the ASI neurons does not extend lifespan by itself, so another genetic pathway(s) is apparently required to act in parallel to *skn-1* to induce the DR longevity response. Various approaches could be employed to try and identify these. Ablation of neurons other than the ASIs might reveal additional neurons that are required for a normal DR longevity response, providing a good starting point for further analysis. Alternately, mutant screens in a strain overexpressing *skn-1* in the ASIs might uncover genes acting in parallel to increase respiration and lifespan.

Conclusions

The discovery that central neuroendocrine cells, known to be critical in integrating organismal energy status, coordinate metabolic and lifespan responses to DR

by cell-nonautonomous signaling is an important conceptual advance in the mechanistic understanding of DR longevity in metazoans. Prior to this work, essentially the only model system in which the mechanism of DR was understood at the genetic level was the unicellular yeast¹⁰. Therefore, though it has been known for many years that DR produces dramatic alterations in neuroendocrine signaling in mammals¹¹, no causative role of any cell-nonautonomous signal in coordinating the response to DR had been demonstrated. In fact, until recent years, the most popular theories to explain DR longevity tended to suggest that the phenomenon was an essentially passive byproduct of altered metabolism during DR, resultant from, for example, reduced ROS production, rather than being an actively regulated longevity response in times of low nutrition¹². The demonstration that DR longevity results from increased activity of specific effectors in yeast has brought most of the field around to the idea that DR longevity is a coordinated response to low nutrition, but most contemporary theories still regard it as a basically cell-autonomous phenomenon, brought on by changes in cellular metabolism¹². The discovery in the present work that a single pair of neurons plays a critical role in sensing DR and coordinating organismal metabolic and lifespan responses strongly argues that DR longevity is an active survival program that is engaged in times of low nutrient availability, rather than some mere accident of altered peripheral metabolism.

The recent demonstration that *Drosophila* olfaction is sufficient to partially suppress DR longevity provides further evidence for the critical role of neurons in DR, and suggests that neuronal control of DR longevity is evolutionarily conserved¹. This notion has important implications for mammalian aging biology, since DR is the most robust lifespan-increasing intervention known in mammals. Quite a lot is known about

how the hypothalamus reflexively controls organismal energy balance, and the hypothalamus is also a critical center of lifespan control in the mammal (Chapter 1 and references therein). It will be interesting to see whether future work can connect these two areas of knowledge, hypothalamic energy sensing and hypothalamic lifespan control, to show that the hypothalamus coordinates mammalian responses to DR. It may be hoped that one day, pharmacological activators of these putative hypothalamic DR longevity pathways might be developed, permitting longer, more disease-free life for humankind.

References

1. Libert, S., Zwiener, J., Chu, X., Vanvoorhies, W., Roman, G. & Pletcher, S. D. Regulation of *Drosophila* life span by olfaction and food-derived odors. *Science* **315**, 1133-7 (2007).
2. Hayakawa, T., Matsuzawa, A., Noguchi, T., Takeda, K. & Ichijo, H. The ASK1-MAP kinase pathways in immune and stress responses. *Microbes Infect* **8**, 1098-107 (2006).
3. An, J.H. & Blackwell, T.K. SKN-1 links *C. elegans* mesendodermal specification to a conserved oxidative stress response. *Genes Dev* **17**, 1882-93 (2003).
4. Motohashi, H. & Yamamoto, M. Nrf2-Keap1 defines a physiologically important stress response mechanism. *Trends Mol Med* **10**, 549-57 (2004).
5. Roux, P.P. & Blenis, J. ERK and p38 MAPK-activated protein kinases: a family of protein kinases with diverse biological functions. *Microbiol Mol Biol Rev* **68**, 320-44 (2004).
6. Berman, K., McKay, J., Avery, L. & Cobb, M. Isolation and characterization of *pmk-(1-3)*: three p38 homologs in *Caenorhabditis elegans*. *Mol Cell Biol Res Commun* **4**, 337-44 (2001).
7. Inoue, H., Hisamoto, N., An, J. H., Oliveira, R. P., Nishida, E., Blackwell, T. K. & Matsumoto, K. The *C. elegans* p38 MAPK pathway regulates nuclear localization of the transcription factor SKN-1 in oxidative stress response. *Genes Dev* **19**, 2278-83 (2005).
8. Maglich, J.M., Watson, J., McMillen, P. J., Goodwin, B., Willson, T. M. & Moore, J. T. The nuclear receptor CAR is a regulator of thyroid hormone metabolism during caloric restriction. *J Biol Chem* **279**, 19832-8 (2004).
9. Kayser, E.B., Morgan, P.G., Hoppel, C.L. & Sedensky, M.M. Mitochondrial expression and function of GAS-1 in *Caenorhabditis elegans*. *J Biol Chem* **276**, 20551-8 (2001).
10. Dilova, I., Easlson, E. & Lin, S.J. Calorie restriction and the nutrient sensing signaling pathways. *Cell Mol Life Sci* **64**, 752-67 (2007).
11. Mobbs, C.V., Bray, G. A., Atkinson, R. L., Bartke, A., Finch, C. E., Maratos-Flier, E., Crawley, J. N. & Nelson, J. F. Neuroendocrine and pharmacological manipulations to assess how caloric restriction increases life span. *J Gerontol A Biol Sci Med Sci* **56** Spec No 1, 34-44 (2001).
12. Sinclair, D.A. Toward a unified theory of caloric restriction and longevity regulation. *Mech Ageing Dev* **126**, 987-1002 (2005).

Figure 1. Model of ASI neuronal function during DR.

DR is sensed by integration in the ASI neurons of intrinsic signals related to energy status, which may include intracellular energy sensing and/or afferent hormonal signals from the periphery. Sensory perception of food in the environment may also influence the DR decision. Following the detection of an energy-restricted organismal state, *skn-1* is activated in the ASIs. Activation of *skn-1* depends on cell-autonomous activity of the *nsy-1/sek-1* MAPKK signaling module, which may function downstream of or in parallel to DR. Active *skn-1* then promotes a cell non-autonomous signal to peripheral tissues that increases respiration rate and extends lifespan. At least one additional genetic pathway, which has not yet been identified, is likely to function in the ASIs and/or other neurons in parallel to the *skn-1* pathway to promote DR longevity.

FIGURE 1

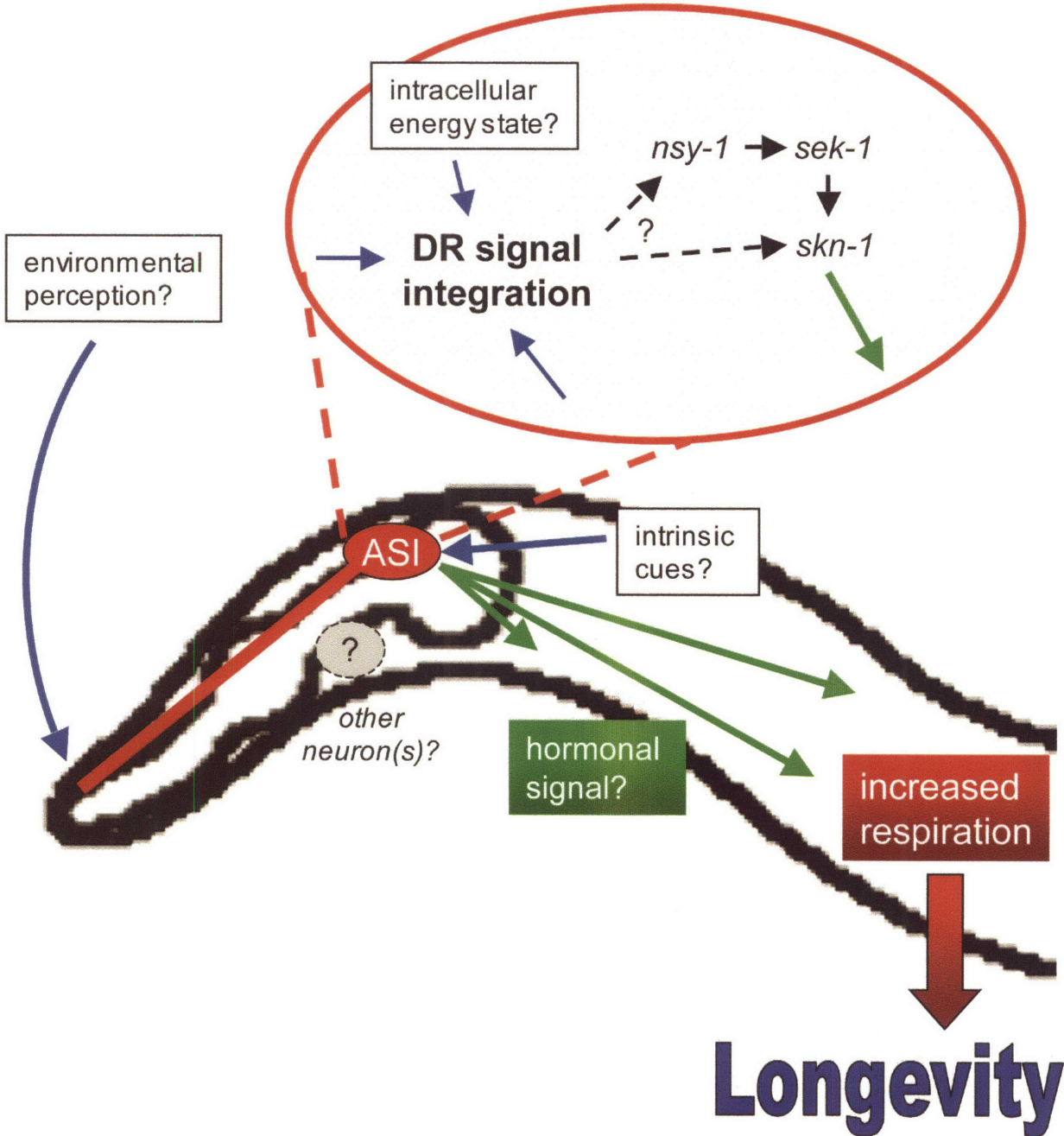


Figure 2. Sensory cilia defective mutant *che-3(e1124)* disrupts normal *skn-1::gfp* expression in the ASI neurons under certain environmental conditions.

skn-1::gfp expression is substantially reduced by *che-3* mutation under standard plate conditions, but not under the AL or DR liquid culture conditions. Animals were assayed on day 5 of adulthood. Each graphed value represents the mean of two trials; errors are s.e.m. *n* in trial 1, 2: *Is007* plate: 36, 31; *che-3;Is007* plate: 33, 37; *Is007* AL: 21, 26; *che-3;Is007*: 20, 36; *Is007* DR: 21, 29; *che-3;Is007* DR: 19, 28.

FIGURE 2

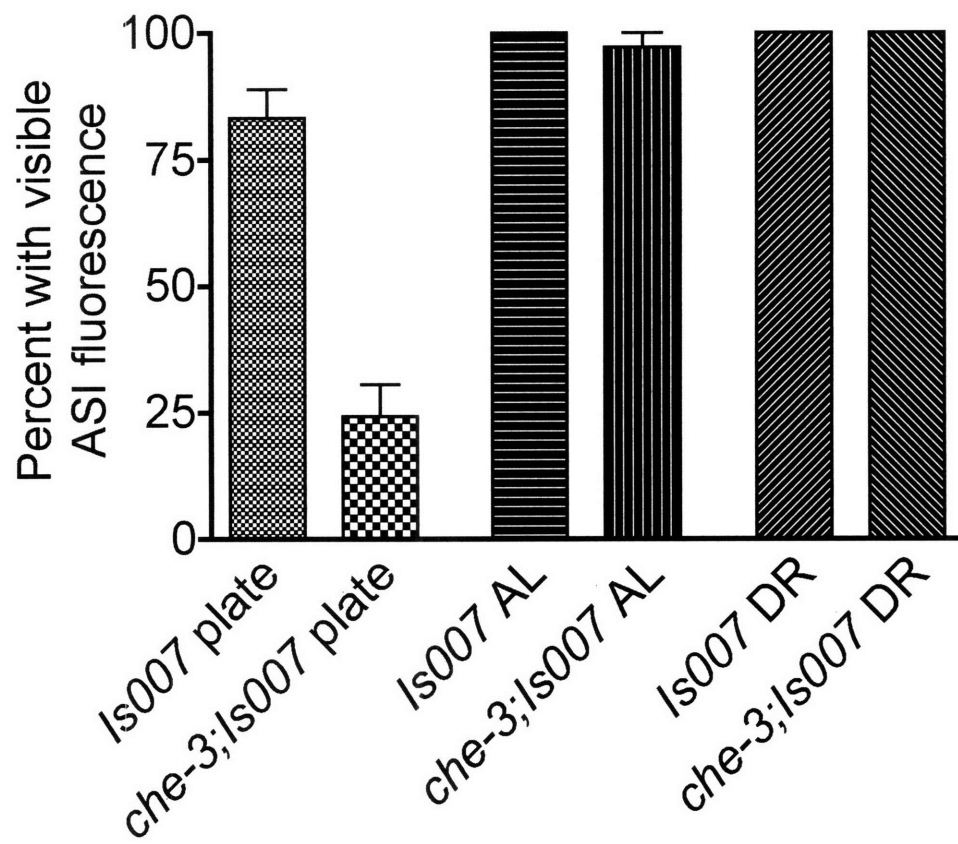
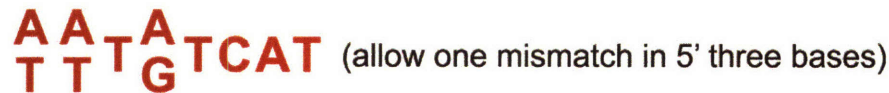


Figure 3. Predicted *skn-1* transcriptional target genes.

Both strands of the 5' 1000 bp of each predicted gene in the *C. elegans* genome (Wormbase) was scanned for the *skn-1* consensus binding site WWTRTCAT, where W = T or A and R = G or A (see ref. 3). One mismatch was permitted in the first three bases. All genes with eight or more predicted binding sites are listed, with functional annotations, where possible, principally based on homology to mammalian genes with known function. Shaded rows indicate genes likely to be involved in neuronal perception of food availability, production of hormones or neuropeptides, or response to hormones or neuropeptides. One predicted gene, *dod-24* (dashed box) has been experimentally confirmed to be a *bona fide skn-1* target. The others have not been experimentally tested.

FIGURE 3

skn-1 binding site:



CDS	Name	# <i>skn1</i> Sites	Predicted Function
ZC395.2	<i>clk-1</i>	16	ubiquinone synthesis
F58E6.8		13	unknown
C33G6.1	<i>srw-127</i>	12	hypocretin receptor-like
Y69H2.8	<i>nhr-241</i>	12	nuclear hormone receptor (HNF-4-like)
B0331.1	<i>cyp-29A4</i>	11	cytochrome P450
Y71F9AL.6		11	unknown
Y71G12B.33		11	unknown
C32H11.12	<i>dod-24</i>	11	unknown
F58E6.7		10	unknown
Y37H2C.3		10	unknown
F17A2.6	<i>srd-41</i>	10	chemoreceptor
C50F7.1b	<i>C50F7.1</i>	10	neuropeptide FF receptor-2-like
Y59H11AR.4		10	amino acid transporter
K04C2.7		10	unknown
Y43F4A.3		10	Zn finger
Y50D7A.2		10	transcription initiation factor subunit-like
C17G10.5	<i>lys-8</i>	10	lysozyme
K01A2.6		10	unknown
Y17G7B.12		10	RNA 3' to 5' exonuclease
C06H2.8	<i>mir-268</i>	9	microRNA
C27A7.9		9	unknown
C51F7.1	<i>frm-7</i>	9	membrane-associated tyrosine phosphatase
F26F12.6b	<i>srh-76</i>	9	olfactory GPCR
K03B8.2	<i>nas-17</i>	9	protease
Y58A7A.3		9	unknown
Y59A8B.6		9	pre-mRNA processing factor 6-like
ZC116.1		9	unknown
F11C7.5		9	unknown
F29G6.3a		9	unknown
F29G6.3b		9	unknown
F29G6.3c.1		9	unknown
F29G6.3c.2		9	unknown
F48C5.1		9	neuregulin-3-like
F49H12.4		9	unknown
R04D3.14		9	tRNA (Tyr)
T02C5.5d.1	<i>unc-2</i>	9	voltage-gated calcium channel
ZC13.2		9	unknown
W03G9.7		9	unknown
Y47H9C.4a	<i>ced-1</i>	9	LDL receptor paralogous; cell engulfment
Y47H9C.4b	<i>ced-1</i>	9	LDL receptor paralogous; cell engulfment
Y47H9C.4c	<i>ced-1</i>	9	LDL receptor paralogous; cell engulfment
Y71F9B.16	<i>dni-30</i>	9	protein chaperone
C02F4.3		9	unknown
C33H5.13		9	unknown
F01D4.8		9	cystathione synthase
T04A11.7a	<i>sru-20</i>	9	7TM receptor
T04A11.7b	<i>sru-20</i>	9	7TM receptor
Y41D4B.21	<i>nhr-274</i>	9	nuclear hormone receptor (HNF-4-like)
B0361.2b		9	cell cycle control protein CWF19
T16H12.5a	<i>bath-43</i>	9	speckle-type POZ protein
Y22D7AL.12		9	unknown
C30G12.3		9	unknown
C41C4.5.1	<i>unc-105</i>	9	ion-channel (degenerin)
DH11.5b		9	unknown
M05D6.10		9	pseudogene
Y38E10A.15		9	unknown
C06B8.11		8	unknown
C06B8.9	<i>srw-21</i>	8	7TM receptor (cysteinyl leukotriene receptor-like)
C09H5.8	<i>str-128</i>	8	7TM receptor
C29F3.7		8	unknown
C49G7.10		8	unknown
C50H2.1	<i>fshr-1</i>	8	neuropeptide receptor (FSHR, LHR, TTR-like)
F08E10.2	<i>srbc-61</i>	8	olfactory 7TM receptor
F10A3.15	<i>str-111</i>	8	olfactory 7TM receptor
F16E3.11		8	unknown
F19F10.3		8	unknown
F22B8.2		8	pseudogene
F37B4.9	<i>sre-24</i>	8	chemoreceptor
F38B7.7	<i>srx-86</i>	8	7TM receptor (purinoreceptor-like)
F40F9.2	<i>tag-120</i>	8	transmembrane protein
F44A2.4	<i>nhr-39</i>	8	nuclear hormone receptor (ER-like)
F54E2.1		8	unknown
F55A11.8		8	unknown
F55C10.2	<i>col-154</i>	8	collagen
F67A8.4		8	7TM receptor (somatostatin receptor 2-like)
F58H1.3		8	enolase-phosphatase E1-like
H39E23.3		8	neurofilament heavy protein
K01D12.9		8	unknown
R08H2.8		8	unknown
T06E6.6	<i>srh-257</i>	8	olfactory GPCR
T20D4.19		8	unknown
T21C9.8		8	unknown
T21H3.5		8	unknown
W02D7.2		8	lectin

CDS	Name	# <i>skn1</i> Sites	Predicted Function
Y37H2A.5		8	unknown
Y38C9B.3		8	unknown
Y59A8B.5	<i>srh-307</i>	8	pseudogene
ZK997.12	<i>srw-102</i>	8	growth hormone secretagogue/ghrelin receptor-like
C02C6.2a		8	unknown
C03F11.4		8	unknown
C04F6.2		8	unknown
C34E11.3	<i>tag-241</i>	8	unknown
F17A2.8	<i>srd-44</i>	8	7TM chemoreceptor (opioid receptor kappa 1-like)
F31F6.6	<i>nac-1</i>	8	Na-coupled dicarboxylate transporter (drosophila INDY-like)
F35C8.5		8	cholesterol 25-hydroxylase-like
F40B5.3		8	neprilysin (peptide hormone regulation)
F42G10.1.1		8	neprilysin (peptide hormone regulation)
F44A6.5		8	unknown
F52G3.4		8	DNA helicase
F52H2.5		8	unknown
K02G10.3		8	unknown
K08A8.3	<i>coh-1</i>	8	DNA repair (RAD21-like)
R03E9.3b	<i>abts-4</i>	8	anion/bicarbonate exchange transporter
R03G8.1		8	unknown
R04D3.1	<i>cyp-14A4</i>	8	cytochrome P450
R07E3.1.1		8	cysteine protease cathepsin F
R07E3.1.2		8	cysteine protease cathepsin F
W03H1.2	<i>elc-2</i>	8	transcription elongation factor B subunit-like
C32E12.6	<i>mir-88</i>	8	microRNA
C53D5.3		8	unknown
F17B5.3		8	lectin
F21C3.6		8	unknown
F28C12.4	<i>sra-20</i>	8	olfactory 7TM receptor
F32H2.10		8	unknown
F36F2.4	<i>syn-13</i>	8	syntaxin
F39H2.1	<i>ftp-22</i>	8	neuropeptide
Y105E8A.24a		8	guanine nucleotide exchange factor
Y105E8A.24b		8	guanine nucleotide exchange factor
ZC247.1		8	unknown
C02F4.2b	<i>tax-6</i>	8	calcineurin
C18H7.9		8	unknown
C23H5.6		8	pseudogene
C28D4.11		8	pseudogene
C32H11.13		8	unknown
C35D6.4		8	Zn-finger
F30B5.4		8	unknown
F38E11.6a		8	adenylate kinase (purine metabolism)
F38E11.6b		8	adenylate kinase (purine metabolism)
H20E11.3a		8	unknown
K02B2.3		8	unknown
K03H6.5		8	unknown
Y37A1B.7		8	unknown
Y43C5A.4		8	unknown
Y46C8AL.9a	<i>clec-75</i>	8	lectin
Y46C8AL.9b	<i>clec-75</i>	8	lectin
Y67A10A.8		8	progesterin receptor family 3-like
Y73B6BL.14		8	DNA ligase III
Y73B6BL.5d		8	unknown
Y9C9A.8		8	unknown
C23G10.5		8	unknown
C44F1.2		8	glucocorticoid modulatory element binding protein-like
F42A10.7.1		8	unknown
F42A10.7.2		8	unknown
M01F1.7		8	phosphatidylinositol transfer protein
T16H12.5b.1	<i>bath-43</i>	8	speckle-type POZ protein
Y39A1B.1		8	lectin
Y42G9A.4c		8	mevalonate kinase (sterol synthesis)
ZK688.6a.2	<i>tag-282</i>	8	Prolycarboxypeptidase
C06A8.3		8	hypodermal antigen OV17
C08B11.1	<i>zyg-11</i>	8	serine/threonine protein kinase
C08H9.7		8	chitinase
C41C4.5.2	<i>unc-105</i>	8	ion-channel (degenerin)
C52A11.3		8	POZ domain protein
DH11.5a		8	unknown
EEEE8.2		8	unknown
F10G7.2	<i>tsn-1</i>	8	transcriptional coactivator p100
F11G11.3	<i>gst-6</i>	8	glutathione S-transferase
F15A4.7	<i>srg-17</i>	8	G-protein coupled receptor
F49E12.11	<i>mir-85</i>	8	microRNA
H43E16.1		8	unknown
K02E7.10		8	cysteine protease cathepsin L
R07G3.7a		8	unknown
R07G3.7b		8	unknown
R09D1.11		8	chitinase
T01H3.2		8	unknown
Y48B8A.4	<i>eal-2</i>	8	acetylcholine receptor (pharyngeal pumping rate)
ZK622.3d.3	<i>pmt-1</i>	8	phosphoethanolamine methyltransferase

APPENDIX 1

Additional Mutants Tested for a Role in DR Longevity

This chapter consists of a table listing some additional mutants that were tested for a role in DR longevity and that do not appear elsewhere in this thesis.

Table 1. Additional mutants tested for a role in DR longevity.

Strain and Condition	# Deaths/# Censored (# Trials)	Mean ± s.e.m	P-value vs. AL Control
N2 AL	832/50(17)	25.7 ± 0.1	
N2 DR	792/60(16)	32.8 ± 0.2	P < 0.0001
<i>sra-13(zh13)</i> AL	49/3(1)	24.9 ± 0.6	
<i>sra-13(zh13)</i> DR	47/5(1)	35.0 ± 0.9	P < 0.0001
<i>geIn3[sir-2.1;rol-6(su1006)]</i> AL	48/6(1)	30.1 ± 1.0	
<i>geIn3[sir-2.1;rol-6(su1006)]</i> DR	52/4(1)	36.7 ± 0.7	P < 0.0001
<i>jkk-1(km2)</i> AL	46/4(1)	21.8 ± 0.6	
<i>jkk-1(km2)</i> DR	40/5(1)	26.4 ± 0.6	P < 0.0001
<i>mek-1(ks54)</i> AL ^a	26/23(1)	~10 ^a	
<i>mek-1(ks54)</i> DR ^a	17/27(1)	~10 ^a	P = 0.3625
<i>sir-2.1(pk1640::Tc1)</i> AL	100/3(2)	25.8 ± 0.5	
<i>sir-2.1(pk1640::Tc1)</i> DR	100/5(2)	28.0 ± 0.5	P < 0.0001
<i>crh-1(n3315)</i> AL	50/5(1)	23.6 ± 0.8	
<i>crh-1(n3315)</i> DR	38/2(1)	30.3 ± 0.9	P < 0.0001
<i>isp-1(qm150)</i> AL	54/1(1)	23.2 ± 0.8	
<i>isp-1(qm150)</i> DR	49/5(1)	27.8 ± 0.7	P < 0.0001
<i>unc-43(n498sd)</i> AL	48/4(1)	22.7 ± 0.8	
<i>unc-43(n498sd)</i> DR	51/1(1)	26.4 ± 0.6	P = 0.0033
<i>ctb-1(qm189)</i> AL ^b	23/28(1)	~27 ^b	
<i>ctb-1(qm189)</i> DR ^b	3/49(1)	>>27 ^b	P < 0.0001
<i>isp-1(qm150);ctb-1(qm189)</i> AL ^b	23/28(1)	~27 ^b	
<i>isp-1(qm150);ctb-1(qm189)</i> DR ^b	3/49(1)	>>27 ^b	P < 0.0001
<i>aak-2(ok524)</i> AL ^c	32/24(1)	~20 ^c	
<i>aak-2(ok524)</i> DR ^c	7/46(1)	>>20 ^c	P < 0.0001
<i>kat-1(n4430)</i> AL	62/2(1)	24.4 ± 0.5	
<i>kat-1(n4430)</i> DR	44/12(1)	28.4 ± 0.9	P < 0.0001
<i>daf-28(sa191)</i> AL	46/0(1)	25.6 ± 0.6	
<i>daf-28(sa191)</i> DR	52/0(1)	31.0 ± 0.8	P < 0.0001
<i>daf-7(e1372)</i> AL	52/0(1)	24.1 ± 0.7	
<i>daf-7(e1372)</i> DR	50/0(1)	32.6 ± 0.6	P < 0.0001
<i>daf-7(m62)</i> AL	43/0(1)	23.4 ± 0.5	
<i>daf-7(m62)</i> DR	47/4(1)	30.7 ± 0.5	P < 0.0001

^aLifespan only followed to day 10; mean is an approximation.

^bLifespan only followed to day 27; mean is an approximation.

^cLifespan only followed to day 20; mean is an approximation.

BIOGRAPHICAL NOTE

Nicholas A. Bishop

Education:

- 8/99 – 6/07 **Massachusetts Institute of Technology** Cambridge, MA
Ph.D. Biology.
- 8/95 – 5/99 **Rice University** Houston, TX
B.A. Biochemistry, *cum laude*.

Awards and Fellowships:

Sigma Xi Scientific Research Society, 2007
Anna Fuller Graduate Cancer Research Fellowship, 2002
Golden Key National Honor Society, 1999
Phi Lambda Upsilon National Honorary Chemical Society, 1999

Research and Professional Experience:

- 6/00 – 6/07 **MIT, Department of Biology** Cambridge, MA
Thesis Advisor: Dr. Leonard Guarente
- 6/01 – 6/04 **Consultant, *Science* magazine** Cambridge, MA
- 8/98 – 5/99 **Rice University, Department of Biology** Houston, TX
Undergraduate research advisor: Dr. Kate Beckingham
- 5/98 – 8/98 **National Institute on Aging** Baltimore, MD
Undergraduate research advisor: Dr. Yusen Liu
- 4/97 – 5/98 **Rice University, Department of Biology/HHMI** Houston, TX
Undergraduate research advisor: Dr. Richard Gomer
- 6/95 – 5/99 **Los Alamos National Laboratory** Los Alamos, NM
Undergraduate research advisor: Dr. Jill Trehwella

Teaching Experience:

- 7/02 – 8/02 **Woods Hole Marine Biological Laboratory** Woods Hole, MA
Course Assistant, Molecular Biology of Aging Course
- 7/02 – 6/03 **MIT, Department of Biology** Cambridge, MA
Mentor to Undergraduate Student Researcher
- 8/02 – 12/02 Human Physiology, Teaching Assistant
- 8/00 – 12/00 Microbial Genetics Project Lab, Teaching Assistant

Publications:

Nicholas A. Bishop and Leonard Guarente. (2007) "Two neurons mediate diet-restriction-induced longevity in *C. elegans*." *Nature*, in press.

Nicholas A. Bishop and Leonard Guarente. (2007) "A Conserved MAPK Signaling Pathway Mediates Dietary Restriction-Induced Longevity in *C. elegans*." In preparation.

Joanna K. Krueger, **Nicholas A. Bishop**, Donald K. Blumenthal, Gang Zhi, Kate Beckingham, James T. Stull and Jill Trehwella. (1998) "Calmodulin Binding to Myosin Light Chain Kinase Begins at Substoichiometric Ca²⁺ Concentrations: A Small-Angle Scattering Study of Binding and of Conformational Transitions." *Biochemistry*, 37(51):17810-17817.

Krueger, J. K., **Bishop, N. A.**, Trehwella, J., Zhi, G. Stull, J. T., Beckingham, K., and Blumenthal, D. (1998) "Solution Studies Reveal Mechanism for Ca²⁺/Calmodulin Regulation of Myosin Light Chain Kinase". *Prot Sci* 7(suppl.1): 133 (466-T).

Krueger, J. K., **Bishop, N. A.**, Blumenthal, D. K., Zhi, G., Stull, J., and Trehwella, J. (1998) "Small-angle Scattering Studies of the Ca²⁺-dependence of Calmodulin-Myosin Light Chain Kinase Interactions". *Biophys J* 74(2): A349.

Krueger, J. K., Gu, W., Olah, G. A., **Bishop, N.**, Zhi, G., Stull, J. T. and Trehwella, J. (1996) "Small-Angle Scattering and Modeling Studies of Myosin Light Chain Kinase with and without Ca²⁺-Calmodulin". *Biophys J* 70(2): A49.

Invited Oral Conference Presentations:

Nicholas A. Bishop and Leonard Guarente. "*skn-1* acts in two neurons to mediate calorie restriction-induced longevity in *C. elegans*." Molecular Biology of Aging, at Cold Spring Harbor Laboratory, Cold Spring Harbor, NY, October 2006.

Nicholas A. Bishop and Leonard Guarente. "The *C. elegans* apoptosis-promoting caspase CED-3 also limits organismal lifespan." Molecular Biology of Aging, at Cold Spring Harbor Laboratory, Cold Spring Harbor, NY, October 2002.

Other Abstracts Presented at Conferences:

Nicholas A. Bishop and Leonard Guarente. "Conserved MAPKK *sek-1* is required for calorie-restricted longevity in *C. elegans*." Molecular Biology of Aging, at Cold Spring Harbor Laboratory, Cold Spring Harbor, NY, October 2004.

Nicholas A. Bishop and Leonard Guarente. "Conserved MAPKK *sek-1* is required for calorie-restricted longevity in *C. elegans*." East Coast *C. elegans* Meeting, Yale University, New Haven, CT, June 2004.